OFFSHORE RENEWABLES JOINT INDUSTRY PROGRAMME (ORJIP) FOR OFFSHORE WIND

Range dependent nature of impulsive noise (RaDIN)

Final report

May 2024

working to accelerate offshore consenting

ORJIP Offshore Wind

The Offshore Renewables Joint Industry Programme (ORJIP) for Offshore Wind is a collaborative initiative that aims to:

- Fund research to improve our understanding of the effects of offshore wind on the marine environment.
- Reduce the risk of not getting, or delaying consent for, offshore wind developments.
- Reduce the risk of getting consent with conditions that reduce viability of the project.

The programme pools resources from the private sector and public sector bodies to fund projects that provide empirical data to support consenting authorities in evaluating the environmental risk of offshore wind. Projects are prioritised and informed by the ORJIP Advisory Network which includes key stakeholders, including statutory nature conservation bodies, academics, non-governmental organisations and others.

The current stage is a collaboration between the Carbon Trust, EDF Energy Renewables Limited, Ocean Winds UK Limited, Equinor ASA, Ørsted Power (UK) Limited, RWE Offshore Wind GmbH, Shell Global Solutions International B.V., SSE Renewables Services (UK) Limited, TotalEnergies OneTech, Crown Estate Scotland, Scottish Government (acting through the Offshore Wind Directorate and the Marine Directorate) and The Crown Estate Commissioners.

For further information regarding the ORJIP Offshore Wind programme, please refer to the Carbon Trust website, or contact Ivan Savitsky (ivan.savitsky@carbontrust.com) and Žilvinas Valantiejus (zilvinas.valantiejus@carbontrust.com).

Acknowledgements

This document was produced on behalf of ORJIP Offshore Wind by SMRU Consulting and itap. The report was authored by Madalina Matei, Magda Chudzińska, Patrick Remmers, Michael Bellman, Aimee Kate Darias-O'Hara, Ursula Verfuss, Jason Wood, Natasha Hardy, Faith Wilder, Cormac Booth.

On behalf of the authors of the report, we would like to acknowledge all offshore wind farm developers who provided data to be used in this project. This project used data from a UXO clearance acoustics study funded by the UK Department for Energy Security and Net Zero's Offshore Energy Strategic Environmental Assessment research programme.

We would like to acknowledge Dr. Dorian Houser, Dr. Darlene Ketten, and Dr. Colleen Reichmuth for the provided support, including studies and feedback on the list of studies reviewed. We would also like to acknowledge Dr. Lindesay Scott-Hayward for the provided statistical support, and thank Dr. Brandon Southall and Dr. Gordon Hastie for their support and guidance during the selection of the acoustic metrics of impulsiveness and for their feedback throughout this project.

The project was advised by the ORJIP Offshore Wind Steering Group and the RaDIN Project Expert Panel. We would like to thank the following organisations for their advice and support of the project via participation on the Project Expert Panel:

- Joint Nature Conservation Committee (JNCC)
- Natural England
- Natural Resources Wales
- NatureScot
- Scottish Government's Marine Directorate

This report was sponsored by the ORJIP Offshore Wind programme. For the avoidance of doubt, this report expresses the independent views of the authors.

Who we are

Our mission is to accelerate the move to a decarbonised future.

We have been climate pioneers for more than 20 years, partnering with leading businesses, governments and financial institutions globally. From strategic planning and target setting to activation and communication - we are your expert guide to turn your climate ambition into impact.

We are one global network of 400 experts with offices in the UK, the Netherlands, Germany, South Africa, Singapore and Mexico. To date, we have helped set 200+ science-based targets and guided 3,000+ organisations in 70 countries on their route to Net Zero.

Contents

List of tables

List of figures

Abbreviations

Term	Description
EIA	Environmental Impact Assessment
IBI	Inter-blow interval – time between subsequent pile strikes
LF	Low frequency cetaceans – functional hearing group from Southall et al. (2019)
HF	High frequency cetaceans – functional hearing group from Southall et al. (2019)
VHF	Very high frequency cetaceans – functional hearing group from Southall et al. (2019)
PCW	Phocids in water – functional hearing group from Southall et al. (2019)
OWF	Offshore wind farm
PTS	Permanent threshold shift
SEL	Sound exposure level
SEL_{ss}	Single strike sound exposure level
SEL_{cum}	Cumulative sound exposure level
SNR	Signal-to-noise ratio
SPL	Sound pressure level
L_{peak}	Peak sound pressure level
TTS	Temporary threshold shift
UXO	Unexploded ordnance
WP	Work package

Executive summary

Multiple studies across various animal taxa have concluded that, at comparable sound levels, impulsive noise is generally more hazardous for animal hearing than non-impulsive noise. However, as impulsive noise travels further away from the source, its energy is manipulated and it is absorbed by the environment. This energy dissipation and the way signals travel and get reflected off the seabed and sea surface lead to a loss of impulsive characteristics as a function of distance from the sound source.

The objective of this study was to improve our understanding of how the impulsiveness of sounds produced during pile driving and unexploded ordnance clearances changes with increasing distance from the source, and to help refine the estimation of auditory injury impact ranges for marine mammals during noise impact assessments.

A literature review was conducted to identify metrics that characterise signal impulsiveness. The identified metrics were then extracted from field acoustic recordings collected during unabated impact pile driving activities and unexploded ordnance clearance. The resulting dataset for impact pile driving activities was supplemented by metadata which included pile characteristics (pile type and diameter), hammer energy, environmental variables (bathymetry and sediment type), as well as spatial and temporal attributes (distance from the pile and time since the first pile strike, respectively). The dataset for unexploded ordnance was accompanied by metadata concerning the placement of the acoustic recorders and charge weight.

Four metrics of impulsiveness collected from the pile driving dataset (kurtosis, crest factor, peak sound pressure level, and high frequency content) were modelled to investigate changes with range and other variables and to assess at what distance impulsive sounds transition to being non-impulsive, based on thresholds from the scientific literature. **This study has shown a decrease in impulsiveness as sounds travel further away from the source.** Although a marked decrease was noted in all metrics of impulsiveness within the first five kilometres from the piling location, there is still insufficient evidence to establish a range of distances from which these sounds are no longer impulsive. This is driven by limitations in the available data on auditory impacts from signals with intermediary levels of impulsiveness.

In parallel to the assessment of field data, a framework (software tool) was developed for estimating permanent hearing damage impact ranges from impact pile driving by considering a variety of factors. The framework allows the user flexibility to test different scenarios by varying: how the soundscape is modelled (by changing the source level and transmission loss, as well as the time interval between pile strikes), how animals react to piling (by changing the fleeing speed), and the assumed distance threshold at which sound becomes non-impulsive. Simulations involving standardised fleeing speed, transmission loss and source level indicated that when the transition from impulsiveness to non-impulsiveness occurred at 5 km from the piling source, the permanent hearing damage impact ranges were equal to those from instances where this transition occurred at 50 km. **Scenarios where this transition occurred at ranges less than 5 km from the piling source resulted in reduced impact ranges**.

Additionally, simulated scenarios using piling sequences from 44 representative hammer logs (out of over 200 provided from offshore wind developments) suggest that the **assumptions assessed in noise**

impact assessments may result in an overestimation of the auditory injury impact ranges (a median percentage reduction in PTS impact area of 57%). The time between subsequent pile strikes in the first 45 minutes of piling was found to have the largest effect on hearing damage onset ranges (for a standardised source level, transmission loss, and animal swim speed) compared to characteristics like the total duration of piling. The simulations involving real hammer logs with longer periods between subsequent pile strikes in the first 45 minutes of piling produced smaller impact ranges. The framework developed here could be used to help design installation blow temporal patterns to help minimise impacts at the design or pre-consent stage.

1 Introduction

1.1 Background

An area of concern during the consenting of foundation based offshore wind farms (OWFs) is the emission of anthropogenic noise emitted through impact pile driving, which is used to install both turbine and offshore substation foundations. In addition to this, the disposal of unexploded ordnance (UXOs) also emits high amplitude, impulsive anthropogenic noise into the surrounding marine environment. Exposure to these kinds of sounds can lead to a reduction in hearing sensitivity in a specific hearing band (i.e., a shift in hearing threshold (Ketten 2004a, Popper et al. 2014, Southall et al. 2019)). If this threshold shift is recovered over time, it is considered a temporary threshold shift (TTS). If the hearing threshold never returns to its pre-exposure level in the affected frequency band, it is considered a permanent threshold shift (PTS). The likelihood of these impacts occurring (and the number of animals predicted to experience them) is estimated in noise impact assessments.

Impacts on hearing caused by noise exposures have been evaluated using energy metrics such as sound exposure level or peak sound pressure level (Finneran 2015). Sound exposure level (SEL) quantifies the amount of sound energy experienced within an exposure window, which can either be the duration of a stimulus (e.g., impulse) or it can be set to a constant time window in the case of continuous noise. Peak sound pressure level records the highest sound pressure level within a measuring window and is often applied to transient signals such as impulses. These energy metrics can be further corrected by using auditory frequency weighting functions, which take into account the portions of the frequency spectrum where the exposed subject is particularly sensitive or less sensitive to noise (Southall et al. 2019).

Southall et al. (2019) provide noise exposure criteria for both impulsive and non-impulsive (continuous) noise. For non-impulsive noise, the auditory frequency weighted sound exposure level is used to assess hearing threshold shifts. For impulsive noise, dual criteria are used to assess these hearing threshold shifts: a single strike, unweighted peak sound pressure level criteria (L_{peak}) and a cumulative weighted sound exposure level criteria (SEL_{cum}, which includes the accumulated exposure of multiple pulses) for both TTS and PTS. These dual criteria are only employed when assessing impulsive noise and the criteria which generates the largest calculated range is typically used as the relevant impact range in impact assessment.

A critical consideration, which drives the need for this study, is that there are separate noise thresholds for the onset of TTS and PTS recommended for impulsive and non-impulsive noise sources (Southall

et al. 2019). This is because impulsive sound sources (e.g., impact pile driving and UXO clearance) require less acoustic energy to induce TTS or PTS, compared to non-impulsive noise (Henderson and Hamernik 1986, Dunn et al. 1991, Hamernik and Qiu 2001). As a result, noise exposures involving impulsive noise are expected to trigger TTS or PTS at lower noise levels compared to continuous noise exposures (Southall et al. 2019). Sound sources like explosive detonations, impact piling and seismic airguns are considered impulsive noise sources, whereas sources such as sonars, vibro piling, drilling and other continuous noises are considered non-impulsive. The Southall et al. (2019) criteria assume that impulsive signals retain their hazardous characteristics regardless of distance from the source, although the authors emphasise that this was a precautionary approach and that changes in impulsive characteristics with range need to be considered in impact assessments. A characterisation of impulsive features and how they relate to effects on hearing would provide a more realistic assessment of the hazardous nature of signals produced during anthropogenic activities at various distances from the source.

Impulsive sound sources demonstrate a loss in impulsive characteristics as a function of distance from the source, and could therefore be characterised as non-impulsive beyond a certain distance (Figure 1). As these sounds travel further away from the source, sharp, transient peaks become less prominent, generally resulting in noise exposures becoming less physiologically damaging (Southall et al. 2019). The exposure criteria for impulsive and non-impulsive noise should be applied with consideration to the signal features likely to be received by the receptor (i.e., marine mammal) rather than those emitted by the noise source itself.

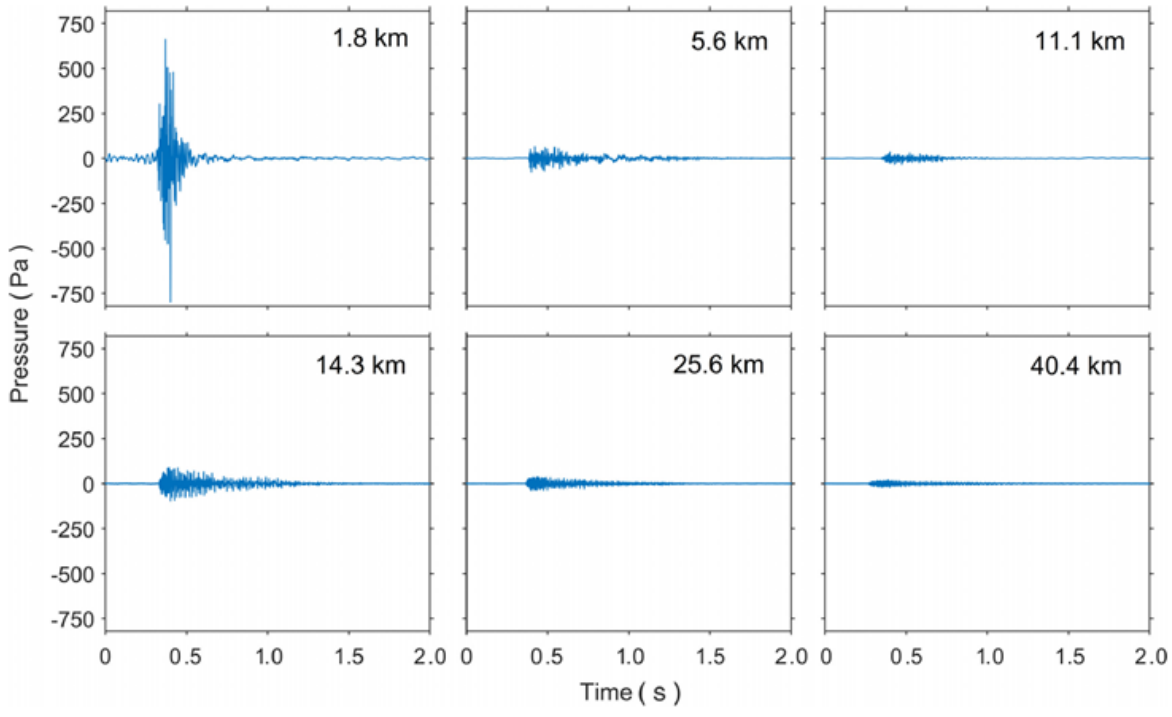

Figure 1. Waveform of pile driving sounds measured at different ranges from the source, from Hastie et al. (2019).

Whether or not a sound should be considered impulsive can make a large practical difference in impact assessment predictions. These assessments can affect decisions on required mitigation for offshore wind farm construction and, as such, carry potentially significant investment decisions. The offshore

wind industry has expanded and developed in recent years, both in terms of technology (e.g., larger foundations or novel ways of installing them) and geographical coverage (e.g., expansion into new regulatory jurisdictions). These developments will need to be taken into consideration during future impact assessments in order to identify suitable mitigation measures.

To date, the range at which impulsive sounds become non-impulsive, like those generated during pile driving, has only been investigated in a few studies. The draft National Marine Fisheries Service (2018) guidance (NOAA guidance) proposed four criteria to determine if a signal is to be considered impulsive, or non-impulsive. These include signal duration[1], rise time[2], crest factor[3] and peak pressure divided by the signal duration[4]. Hastie et al. (2019) utilised these criteria in estimating the transition from impulsive to non-impulsive characteristics of pile driving noise generated during the installation of OWF turbine foundations at two UK sites. This was done using noise recordings collected at increasing distances from the sound source, and the authors reported that each metric reached its respective non-impulsive threshold at variable distances from the source (Hastie et al. 2019). Other characteristics such as the high frequency content of signals (e.g., energy content above 10 kHz) have been proposed as proxies of impulsiveness, given that higher frequencies are associated with a shorter waveform phase and therefore a more pronounced rise time (Southall 2021).

Martin et al. (2020) also investigated the changes in impulsive characteristics of sounds as they move further away from the sound source, and emphasised that impulses maintain their hazardous features regardless of range as long as they are above the effective quiet threshold. This threshold represents the highest sound pressure level that neither induces a temporary threshold shift nor prevents the recovery from TTS caused by previous noise exposures (Ward et al. 1976). This concept is based on the fact that animals are constantly exposed to sound waves, but they only become harmful once they exceed this threshold.

Obtaining a better understanding of how impulsive sounds can be characterised, how these factors vary with range from the source (i.e., quantifying a reduction in impulsiveness), and the importance of this transition relative to other factors affecting PTS remain key gaps to be filled. Linking these characteristics of impulsiveness to the way receptors experience hearing loss will be particularly relevant when more hearing data become available from marine mammal studies.

The SEL_{cum} experienced by an animal is also assessed considering the sound exposure level received by an animal over the course of pile driving. This approach accounts for the accumulated exposure over the duration of a noise generating activity and does not assume that hearing recovery occurs between pile strikes. This SEL_{cum} criteria typically results in larger estimated PTS ranges than the L_{peak} criteria. Therefore an important consideration when assessing the risk of PTS using SEL_{cum} is that the temporal pattern of the exposure (i.e., the time between pile strikes) affects the resulting threshold shift (e.g.,

[1] Time interval between the arrival of 5% and 95% of total energy in the signal, with <1 s defined as impulsive.

[2] Measured time between the onset (defined as the 5th percentile of the cumulative pulse energy) and the peak pressure in the signal, with <25 ms defined as impulsive.

[3] The decibel difference between the peak sound pressure level (i.e., the peak pressure expressed in units of dB re: 1µPa) of the pulse and the RMS SPL calculate over the signal duration, with >15 dB defined as impulsive.

[4] Peak pressure defined as the greatest absolute instantaneous sound pressure within a specified time interval, and with >5000 Pa/s defined as impulsive.

Kastak et al. (2005), Mooney et al. (2009), Finneran et al. (2010), Finneran (2015)). As such, considering the temporal pattern of pile strikes may be of critical importance in determining the risk of PTS using SEL_{cum} and finding ways to improve the assessment of PTS impact ranges.

1.2 Report structure and intention

The objective of this study was to improve our understanding of how the impulsiveness of sounds produced during pile driving and UXO clearance changes with range from the source to help refine the estimation of auditory injury (PTS) impact ranges. This was assessed in parallel to the development of a framework (a software tool) for estimating PTS impact ranges considering other factors, such as sound propagation, animal swim speed, or temporal patterns of pile strikes. The goal was that this framework would allow an investigation of the precaution inbuilt into current assessments of the risk of auditory injury in marine mammals (N.B. behavioural response is not in the scope of this study). However, it is essential to note that this framework was not built as an alternative to the current methods for estimating PTS impact ranges, but rather as a means to explore how these ranges may be influenced by factors such as the swim speed of the animals, time between subsequent pile strikes, the impulsive-non-impulsive transition, and distance at which sounds transition from impulsive to non-impulsive. Therefore, this framework can act as a sensitivity analysis tool to evaluate how the above factors interact and drive the predicted PTS ranges.

To facilitate such development, this project was executed as a series of work packages. The following report loosely follows this work package structure which covered:

- An extensive review of literature on the impulsiveness of sound and its effect on the auditory system of mammals (section 2).
- The collation and analysis of noise monitoring data from UXO detonations and pile driving during offshore wind farm construction, considering the most appropriate impulsiveness metrics as revealed by the literature review (section 3).
- Statistical modelling to assess the influence of project and site-specific covariates quantitatively, investigated by means of a generalised additive model, to understand which covariates have a major influence on the impulsiveness of noise (section 4).
- The development and use of the framework to assess the importance of the impulsive-non-impulsive transition and the other factors (above) in the context of offshore wind farm construction (section 5).

This work is summarised and concludes with recommendations for how this work can be integrated into offshore wind consenting practices (involving a range of stakeholders), and how this topic area can be advanced to improve confidence in auditory injury assessments.

It is important to note that this project relies on empirical data provided by a number of offshore wind farm developers. In section 3 these data sources are stated to aid understanding of the industry data used to support this project's objective. Following this (sections 4 and 5), we have anonymised the data as the purpose of the project is not to identify specific projects (i.e., results are not linked to specific wind farms), but to help guide the industry more broadly.

This report is written as a detailed summary of the entire programme of work undertaken to address the project goals. To aid the readability of the main report but provide additional detail on work carried out, the report is supplemented by a series of detailed appendices.

2 Literature review of impulsive metrics

2.1 Outcomes of literature review

A literature review was conducted to identify available metrics of impulsiveness, and how the characteristics of impulsive sounds change with increasing distance from the source. Additional topics covered by this literature review included the mechanism of noise induced hearing loss in the mammalian ear, with a focus on the impulsiveness of noise, and the potential to transfer the knowledge obtained from studies on terrestrial mammals to marine mammals (see section 9 in the appendix for more details).

Measures of acoustic energy such as sound exposure level, peak sound pressure level, and frequency content have been extensively used in studies of hearing loss (e.g., Lucke et al. (2009), Mooney et al. (2009), Finneran (2015), Kastelein et al. (2017), Sills et al. (2020)). Metrics of impulsiveness, on the other hand, have had limited use in such studies. For instance, measurements of the discrepancy between average and peak sound pressure levels within a pulse (crest factor) or the time it takes for an impulse to reach its peak sound pressure level (rise time) have been suggested to be potential indicators of acoustic hazard to the mammalian ear (Henderson and Hamernik 1986, Starck and Pekkarinen 1987). Pekkarinen and Starck (1983) suggested that a signal should be considered impulsive if it has a crest factor greater than 15 decibels, however, neither this metric nor rise time have yet been studied in a systematic manner to assess their effect on hearing.

The only metric of impulsiveness that has been systematically adjusted to quantify the magnitude of hearing loss is kurtosis (Hamernik et al. 1993, Lei et al. 1994, Hamernik and Qiu 2001, Hamernik et al. 2003, Hamernik et al. 2007). This metric characterises the sharpness of the peak of a distribution (e.g., an acoustic waveform). A kurtosis value greater or equal to 40 has been used to describe “fully-impulsive” signals, whereas kurtosis values less or equal to 3 have been associated with non-impulsive (or Gaussian) noise (Hamernik et al. 2007). The kurtosis metric, combined with energy metrics such as sound pressure level and sound exposure level, has been found to be positively related to the magnitude of TTS and PTS in studies with both terrestrial mammals (Hamernik et al. 2007, Goley et al. 2011, Xie et al. 2016) and cetaceans held in captivity (von Benda-Beckmann et al. 2022).

When impulsive sounds were studied in the field using recorders deployed at various distances from the source, variable results were observed concerning the intensity of the relationship between the chosen metrics and the distance from the source (also referred to as range). For example, Hastie et al. (2019) reported a marked decrease in the peak sound pressure level of a pulse approximately five kilometres away from the sound source and an increase in pulse duration, but a relatively poor relationship between crest factor and range. Amaral et al. (2020) also reported a decrease in peak sound pressure level at greater distances from impact piling activities and an increase in pulse duration and rise time, indicating that the signals became less impulsive. Studies using kurtosis to quantify impulsiveness also reported a decrease in this metric with range (Martin et al. 2020, Guan et al. 2022), although there was a high degree of variability observed during acoustically complex activities like down-the-hole pile driving and drilling (Guan et al. 2022).

The findings of this review informed the analysis of impulsive sounds from pile driving and unexploded ordnance activities by facilitating the selection of metrics of impulsiveness based on the current

available scientific knowledge. This review also informed and provided scientific background to the development of a framework which facilitated the assessment of permanent threshold shift impact ranges.

The acoustic metrics selected to be extracted from pile driving pulses and UXO blasts are presented in Table 1. A subset of these metrics (kurtosis, crest factor, peak sound pressure level, and high frequency content) were subsequently used to model changes in signal characteristics with range. This subset of metrics was chosen based either on their use in hearing loss studies or because of previous investigations of how they change with increasing distance from the source. For example, the kurtosis metric has been used in multiple studies of hearing loss and its features at increasing distance from the source were investigated by Martin et al. (2020) and Guan et al. (2022). The variations in the crest factor metric were assessed by Hastie et al. (2019) from data collected during impact pile driving and seismic surveys, and this study aimed to provide a dataset for comparison. Peak sound pressure level was selected given its use as part of the Southall et al. (2019) impulsive noise exposure criteria and its inclusion in the set of metrics investigated by Hastie et al. (2019). Lastly, high frequency content was recommended by Southall (2021) as a proxy of impulsiveness for the other metrics, therefore it was included in the modelling subset to investigate the patterns in this metric at various distances from the source and the similarities to the other three modelled metrics.

Table 1. Definitions of acoustic metrics identified during the literature review which were extracted from pile driving pulses and UXO blast waves. Four of these metrics were chosen for further analysis and modelling.

Metric	Definition	Used in modelling
Unweighted peak sound pressure level	20 times the logarithm to the base ten of the ratio re: 1µPa of the maximum absolute value of the instantaneous unweighted sound pressure, as defined by Southall et al. (2019)	Yes
Signal duration	Time interval that contains 90% of the sound energy of an impulse, as defined by De Jong et al. (2011)	No
Frequency weighted sound exposure level	Level in decibels calculated as ten times the logarithm to the base ten of the ratio of the time integral of the squared instantaneous frequency weighted sound pressure, weighted with the frequency weighting functions proposed by Southall et al. (2019)	No
Kurtosis	Ratio of the fourth central moment divided by the square of the variance of the sound pressure time series over a specified time interval, where kurtosis of a Gaussian distribution is equal to 3, as defined by Müller et al. (2020)	Yes
Kurtosis corrected frequency weighted sound exposure level	Frequency weighted sound exposure level with an added kurtosis correction for impulsiveness from Goley et al. (2011)	No

Metric	Definition	Used in modelling
Rise time	The time taken for a signal to rise from onset (defined as in Hastie et al. (2019) as the 5th percentile of the cumulative pulse energy) to its maximum absolute value of sound pressure	No
Crest factor	Difference between the unweighted peak level and the root-mean-square level, as defined by Pekkarinen and Starck (1983)	Yes
High frequency content	The energetic sum of three filtered noise band levels measured from the third octave bands centred around 8, 10, and 12.5 kHz (novel metric, recommended by Southall (2021))	Yes

3 Collation and preparation of data

As part of the RaDIN project, field acoustic recordings were collated from several impact pile driving and unexploded ordnance disposal activities, which had been collected by passive acoustic monitoring (PAM) sensors deployed at various distances from each sound source. This section provides an overview of the projects from which data were obtained and the methods used to extract acoustic measurements from each impulse.

3.1 Sources of acoustic datasets

Permissions were obtained to use data collected during impact pile driving activities at eleven OWF projects and unexploded ordnance disposals within four OWF projects in the North Sea and the Danish Kattegat (Figure 2).

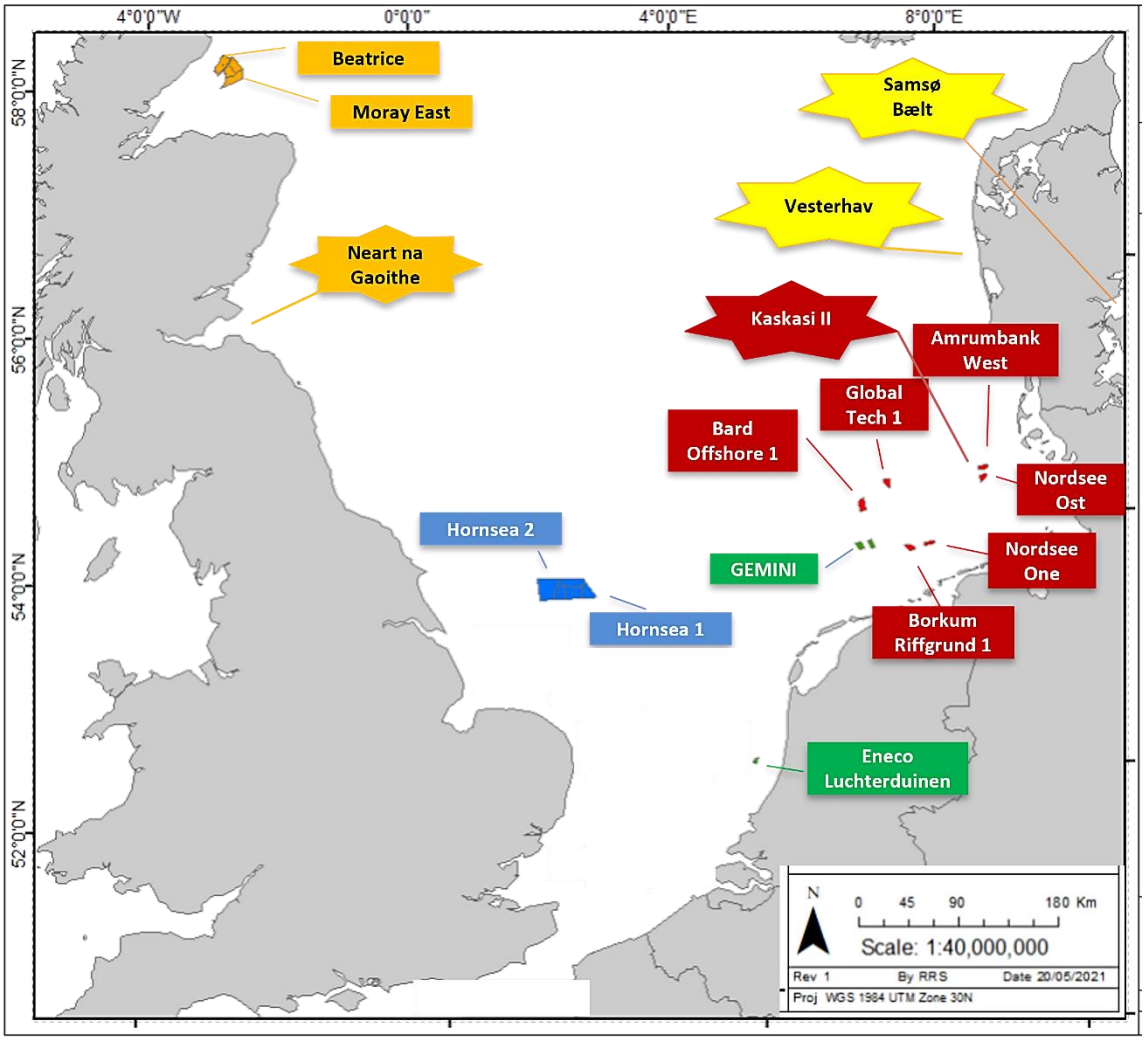

Figure 2. Location of the offshore wind farm projects for which underwater noise measurements are available for the RaDIN project. Rectangles are associated with impact pile driving datasets whereas star-shaped boxes are associated with unexploded ordnance datasets. The colours of the shapes are associated with different countries as follows: orange – Scotland, blue – England, green – Netherlands, red – Germany, yellow – Denmark.

3.1.1 Impact pile driving datasets

Raw acoustic recordings had already been collected as part of the ReCON project (Reducing uncertainty in underwater noise assessments) funded by ORJIP, which investigated the characteristics of sounds produced during unabated impact pile driving activities at different British, German, and Dutch offshore wind farms in the North Sea. The eleven OWF projects were chosen to cover a broad range of pile diameters and bathymetry conditions (Table 2), which were found to influence the characteristics of pile driving pulses during the ReCON project (Verfuss et al. 2023).

The two types of piles installed were monopiles and pin piles. The pile diameter ranged from 2.2 m to 9.5 m, and piling took place in water depths ranging between 21 m and 45 m, which is representative for OWF projects in the North Sea. The underwater noise measurements were carried out during the foundation installation campaigns between 2013 and 2020. The passive acoustic recorders deployed

to measure underwater noise levels were placed at distances between 243 m and 54 km from the respective piling location.

All underwater noise measurements were recorded by stand-alone recorders in the lower half of the water column (usually 2 m above seabed) in accordance with international standards (ISO 2017a) and comparable national measurement guidelines (BSH 2011, Robinson et al. 2014).

For all the listed OWF projects in Table 2, the raw acoustic data as well as the following supporting information were collated: (i) coordinates of the pile and the corresponding acoustic recording units, (ii) bathymetry at the pile location, and (iii) penetration depth and hammer energy used for each single strike as a function of time during installation.

All pile driving activities were performed without any noise abatement system such as Big Bubble Curtain (BBC) or Hydro Sound Damper (HSD). However, all OWF projects deployed a soft-start approach which involves a reduced hammer energy during the initial pile strikes followed by a ramp-up procedure. One site had some pin piles partially installed using vibro piling prior to using impact pile driving procedures, therefore these acoustic datasets were excluded from further analyses.

Table 2. Characteristics of the OWF projects within the North Sea used to investigate the acoustic properties of impact pile driving pulses.

OWF name	Country	Pile type (diameter [m])	Water depth (m)	Year	# of piles	# of acoustic recorders	Acoustic recording unit distances (min – max)
Amrumbank West	Germany	Monopile (6.0 m)	21	2014	1	4	0.75 km -1.5 km
Beatrice	Scotland	Pin pile (2.2 m)	49-52	2017	13	4	0.75 km – 11 km
Borkum Riffgrund 1	Germany	Monopile (5.9 m)	27	2014	1	13	0.25 km – 5 km
Gemini	Netherlands	Monopiles (6.6 m and 7.0 m)/ Pin-pile (2.2 m)	34-35	2015	3	8	0.75 km – 54 km
Global Tech I	Germany	Pin pile (2.48 m)	40	2012	1	3	0.75 km -1.5 km
Hornsea Project One	England	Monopile (8.1 m)	30-32	2018	6	14	0.75 km – 13.3 km
Hornsea Project Two	England	Monopiles (9.3 m and 9.5 m))/ Pin pile (2.44 m)	35-41	2020	5	24	0.75 km – 14.3 km

OWF name	Country	Pile type (diameter [m])	Water depth (m)	Year	# of piles	# of acoustic recorders	Acoustic recording unit distances (min – max)
Eneco Luchterduine	Netherlands	Monopile (5.0 m)	22	2014	2	6	0.75 km – 13 km
Moray East	Scotland	Pin pile (2.5 m)	40	2019	8	3	5 km – 7.6 km
Nordsee One	Germany	Monopile (6.1 m)	28	2015	2	8	0.75 km -1.5 km
Nordsee Ost	Germany	Pin pile (2.4 m)	25	2013	1	6	0.75 km -1.5 km

3.1.2 Unexploded ordnance datasets

Raw acoustic data were available from 39 UXO detonations within four OWF projects in the North Sea and Danish Kattegat (Table 3). The charge weights varied between 0.05 kg and 350 kg, although the proportion of the old explosive that detonated could not be confirmed. The detonations occurred between 2018 and 2022 and the acoustic recording units were located between 750 m and 28.7 km away from their respective UXO location.

All underwater acoustic measurements were collected by stand-alone recorders in the lower half of the water column (usually 2 m above the seabed), in accordance with international standards (ISO 2017a) and comparable national measurement guidelines (BSH 2011, Robinson et al. 2014).

Table 3. Characteristics of unexploded ordnances from the OWF projects within the North Sea and Danish Kattegat used to investigate the acoustic properties of UXO impulses.

OWF name	Country	Charge weight [kg]	Water depth (m)	Year of detonation	# of detonations	# of acoustic recording units	Acoustic recording unit distances (min – max)
Samsø Bælt	Denmark	10 -340	50	2022	5	9	1.79 km -22.4 km
Kaskasi II	Germany	Unknown	23	2021	2	9	0.75 km – 25.9 km
Neart na Gaoithe	Scotland	0.05 – 5	50	2020	30	4	1.71 km – 28.7 km
Vesterhav	Denmark	140 -325	50	2018	2	3	1.50 km – 6.1 km

3.2 Extraction of acoustic measurements from impulses

All underwater acoustic recordings were collected as single-channel time series, sampled at a frequency of at least 44.1 kHz (i.e., variable across OWF projects). The resulting time series were stored

in the MPEG1 Audio Layer 3 format or the PCM WAVE-file format. The variable sampling regimes have led to a restriction of the effective frequency range used for further analyses, which was 11.2 Hz to 17.8 kHz.

The acoustic metrics identified during this project (Table 1) were extracted from each single impulse from the time domain, following standards from ISO (2017a) and ISO (2017b). However, some of the metrics are not defined in these international standards, therefore they are described in section 10.1 of the appendix.

The pulses used for feature extraction were required to have a signal-to-noise ratio (SNR) of ≥6 dB in order to be detected, in accordance with the German measurement guideline (BSH 2011). This SNR threshold is different from that of 10 dB from ISO (2017b) and the reason for choosing a lower detection threshold is the long distance between some of the acoustic recording units and the sound source – these distances sometimes exceeded 20 km, which would have reduced the sample sizes at greater ranges.

Overall, acoustic metrics were extracted from 394,002 single impact pile driving strikes and 39 UXO detonations, measured at distances ranging between 0.23 – 31.82 km from the source. All data have been anonymised and are presented in section 10.2 of the appendix.

3.2.1 Auditory weighting functions

The frequency weighting functions used in this study are based on audiograms generalised from several functional hearing groups according to the recommendations from Southall et al. (2019). By using these hearing group-specific weighting functions, frequencies outside of the optimal hearing range are given less weight or contribution to the audibility of an acoustic event. Figure 3 shows the weighting functions provided by Southall et al. (2019) for very high frequency cetaceans (VHF, such as the harbour porpoise (*Phocoena phocoena*)), high frequency cetaceans (HF, including species like sperm whales (*Physeteridae*) and delphinids (*Delphinus*)), low frequency cetaceans (LF, e. g., minke whale (*Balaenoptera acutorostrata*)) and phocid carnivores in water (PCW, e. g., harbour seal (*Phoca vitulina*)).

The determined frequency weighted Sound Exposure Level ($SEL_{pcw,\ lf,\ hf,\ vhf}$) represents the received energy level specific to each functional hearing group from Southall et al. (2019).

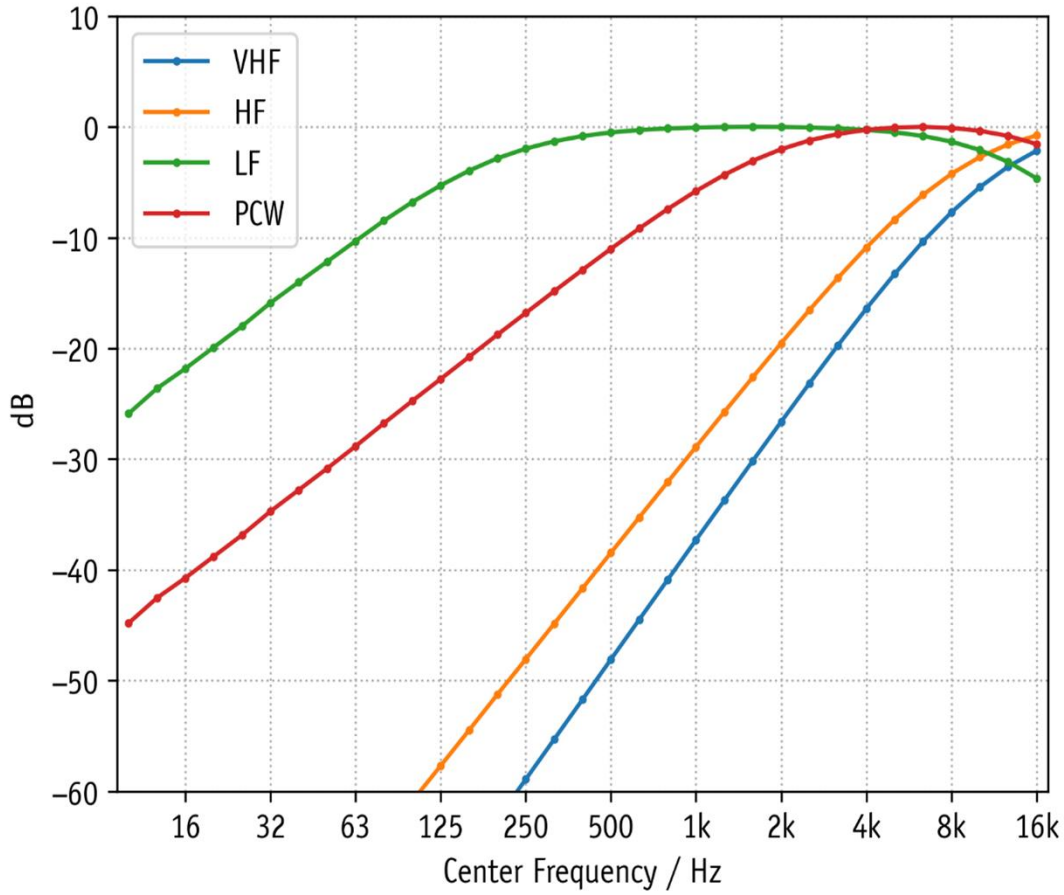

Figure 3: Auditory weighting functions for different functional hearing groups in frequency domain according to Southall et al. (2019).

3.3 Metrics of impulsiveness extracted from impact pile driving

All acoustic metrics extracted from individual pile strikes were calculated and anonymised in an internal database containing data from a total of 394,002 single strikes. The metrics of impulsiveness extracted from these strikes are presented in Figure 4. No attempts were made to normalise or harmonise some well-known factors that can influence the acoustic characteristics of pulses produced during impact pile driving such as pile diameter or hammer energy. This means that energy metrics such as sound exposure level (both unweighted (SEL_{ss}) and frequency weighted ($SEL_{pcw,\ lf,\ hf,\ vhf}$)), as well as zero-to-peak sound pressure level (L_{peak}), are likely to show a high degree of variance due to the differences in features like pile diameter, hammer energy, and site-specific bathymetry (Bellmann et al. 2020). However, the metrics meant to characterise the impulsiveness of signals (e.g., kurtosis, crest factor) are directly comparable across OWF projects.

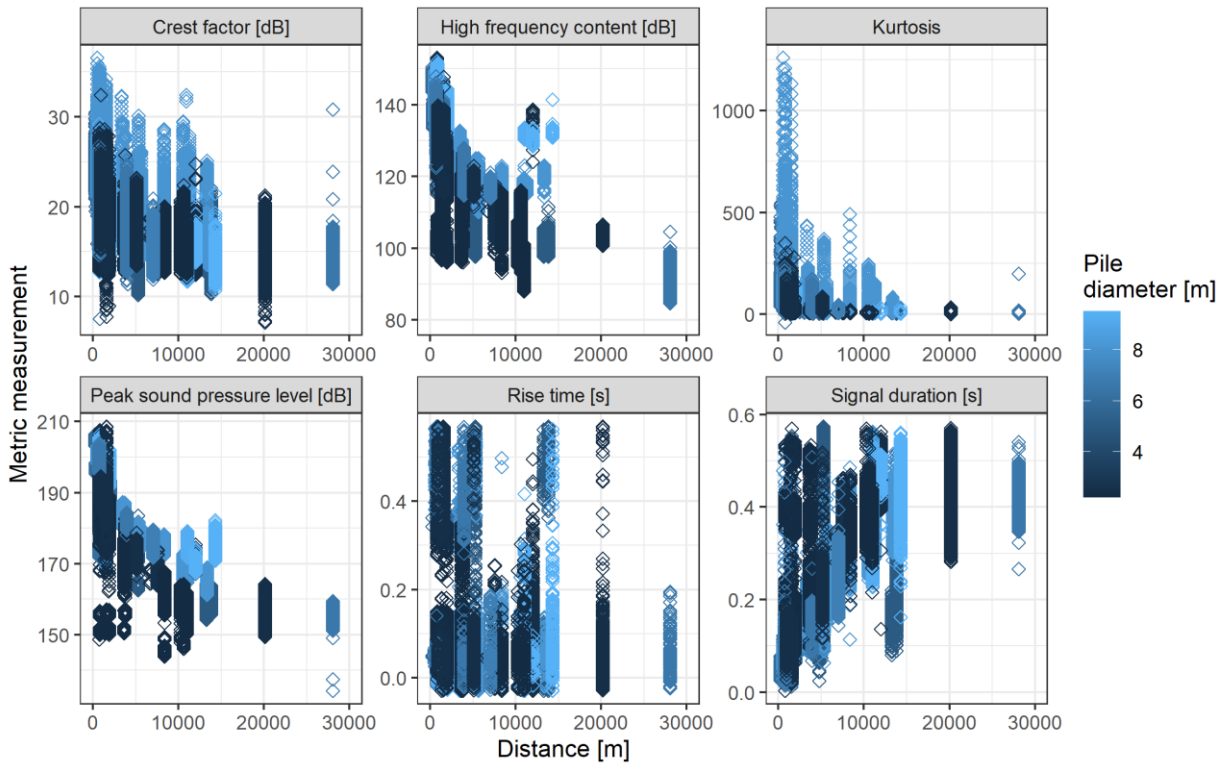

Figure 4. Metrics of impulsiveness extracted from sound waves produced during the installation of 43 piles of varying diameters.

3.4 Metrics of impulsiveness extracted from unexploded ordnance

The metrics of impulsiveness extracted from the detonation of 38 unexploded ordnance are presented in Figure 5 and Table 4. One of the detonation events was excluded from the plots due to erroneous measurements. The remaining detonation events suggest a decreasing trend in impulsiveness with increasing distance from the source, although strong impulsive characteristics were recorded at all distances. For example, estimates of crest factor and kurtosis were almost always above their corresponding thresholds of 15 dB and 40, respectively, with the exception of the minimum value (Table 4). These results suggest that the signals were still impulsive at the measured ranges. Therefore, this UXO dataset was not used to model the relationship between metrics of impulsiveness and range.

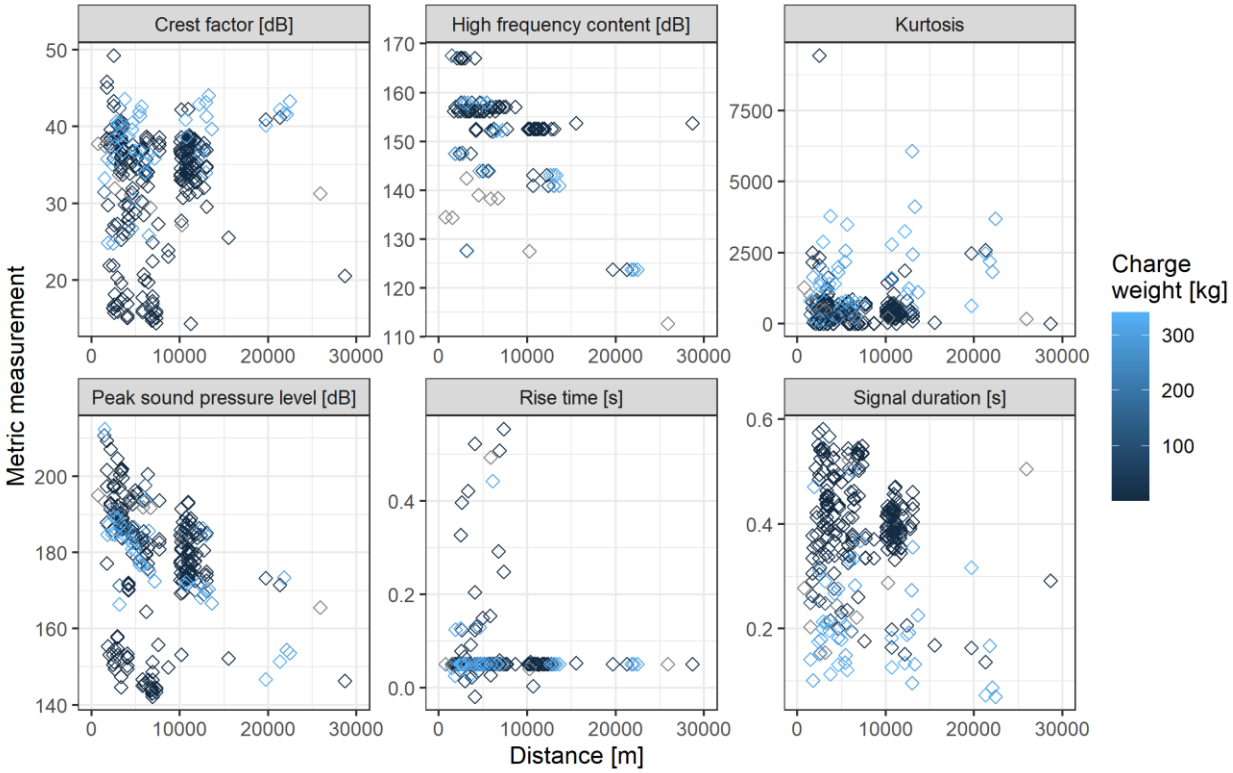

Figure 5. Metrics of impulsiveness extracted from sound waves produced during the detonation of 38 unexploded ordnances (received by 259 acoustic recording units deployed at various distances from their respective UXO sites).

Table 4. Summary statistics for six metrics of impulsiveness extracted from sound waves produced during the detonation of 38 unexploded ordnances (received by 259 acoustic recording units deployed at various distances from their respective UXO sites).

Metric [unit]	Minimum	1st quartile	Median	3rd quartile	Maximum
Cresf factor [dB]	14.4	29.8	35.1	37.9	49.2
High frequency content [dB]	112.7	152.5	152.5	156.2	167.5
Kurtosis	3.0	222.7	385.0	699.0	9432.9
Peak sound pressure level [dB]	142.1	171.4	180.8	188.1	212.4
Rise time [s]	0.003	0.05	0.05	0.4	0.6
Signal duration [s]	0.07	0.3	0.4	0.4	0.6

4 Modelling of pile driving data

4.1 Background and objectives

The RaDIN project has identified several acoustic metrics that have been used to describe changes in the impulsive nature of sound as described in section 2. The identified metrics were then extracted from acoustic recordings collected from the field as described in section 3.

In this section, we aim to understand how a subset of metrics of impulsiveness (kurtosis, crest factor, peak sound pressure level, and high frequency content) change with time and space. A range of other covariates which may influence these metrics was also investigated, including environmental variables (water depth, sediment type) and variables related to the sound source and piling characteristics such as piling duration, pile diameter, pile type, or hammer energy. These analyses focus on the pile driving datasets given the preliminary results for UXO shown in section 3.4.

The characteristics of the environment can influence the propagation of sound in the water column. For example, low frequency components of sounds propagate poorly in shallow waters (Forrest et al. 1993) and the depth or degree of stratification of the water column may affect how far sound waves can travel before their energy is absorbed by nearby particles or the sea floor. Additionally, sediment types such as rocky bottoms may act as effective sound reflectors whereas sandy or muddy sediments may absorb some acoustic energy as the sound waves travel through the water column. Lastly, high frequencies attenuate more rapidly compared to low frequencies, therefore broadband signals lose energy in the upper frequency range closer to the sound source.

The characteristics of the pile and the amount of energy transferred from the hammer into the pile may also influence the properties of the sounds produced during impact pile driving. For instance, piles with large diameters require greater levels of hammer energy and produce greater noise levels compared to smaller pin piles. Moreover, the amount of hammer energy used to drive a pile into the seabed has been positively correlated with greater measured single strike sound exposure levels (Verfuss et al. 2023).

4.2 Methods

The acoustic metrics used to measure the amplitude of noise exposures and the degree of impulsiveness of stimuli which were identified in the papers reviewed for this project are presented in Table 1. Out of the eleven metrics listed in this table, four were used for the analysis as response variables presented in this report: kurtosis, crest factor, unweighted peak sound pressure level (referred to as ‘peak pressure’) and high frequency content. These four metrics were identified as strong potential candidates from the initial processing of field acoustic data (described in section 10.2).

4.2.1 Data cleaning and filtering

Data were cleaned to remove potentially erroneous data points and subsets with data gaps. This included the exclusion of data points from wind farm sites where impact pile driving was preceded by vibro piling (1 site), sites for which explanatory variables were either not available or were not provided (2 sites) and sites/acoustic recorders where key location information was missing in the available data (1 site). Instances where one or more acoustic recorders associated with the same pile had no data

collected during the start of the piling event led to the removal of the data points for the corresponding pile. Lastly, each combination of an acoustic recording unit and its corresponding sound source (pile location) was given a unique name.

4.2.2 Explanatory variables

The list of explanatory variables considered in the modelling is given in Table 5.

Table 5. Explanatory variables considered in the modelling. Underlined explanatory variables are the variables considered in the final model fitting. See Results for further explanation.

Explanatory variable	Unit	Description	Source
Distance to the source	m	Distance between each acoustic recording station and piling location (source).	itap
Pile diameter	m	Diameter of individual piles.	itap
Pile type	-	Monopile or pin pile.	itap
Time since first blow	s	Time since the first blow of a given piling operation. The first blow was calculated as the time of the first record for a given piling operation.	itap
Water depth at the source	m	Water depth at the piling location (source).	itap
Sediment type	-	Percentage of sand, mud, and gravel as well as median grain size at the location of each pile.	Wilson et al. (2018)
Wind farm	-	Name of each of the wind farm.	itap
Hammer energy	kJ	Energy of each blow binned into 500 kJ intervals. Energies > 2000 kJ were binned into one category.	itap

4.2.3 Modelling approach

A Generalised Additive Model (GAM) was fitted to each of the four response variables using MRSea package (Scott-Hayward et al. 2017, Scott-Hayward et al. 2021) which uses Spatially Adaptive Local Smoothing Algorithm (SALSA) for automated knot selection procurement (Walker et al. 2011). Model fitting in MRSea was done in two stages.

Initial modelling included the response variable and either of the following: (1) only the intercept or (2) the intercept and factor explanatory variables (here, Wind farm). Three family distributions were considered: Gamma, Quasipoisson and Tweedie. The `tweedie.profile` function from the `tweedie` library (Dunn 2022) was used to calculate index of power variance (ξ) of the initial model. If this index was close to or equal to 2, a gamma distribution with the logit link function was used. If

this index was close or equal to 1, a quasipossion distribution with the logit link function was used. Values between 1 and 2 led to the use of Tweedie distribution (Dunn 2022).

Secondly, we added a set of explanatory variables to the initial model using the SALSA approach, where the minimum and maximum number of internal knots was set to 1 and 3 respectively. Quadratic B- and natural splines were tested for each smooth explanatory variable.

4.2.3.1 Accounting for autocorrelation

Given that the data consisted of observations (measurements at each acoustic recording station) collected close together in time and space, consecutive observations are likely to be correlated beyond the underlying processes included in the model, resulting in residual autocorrelation which violates a key assumption of GAMs. We used `runACF` function from the MRSea package to assess residual correlation. To account for spatial autocorrelation, distance to the source was always retained in the model. To account for temporal autocorrelation, we added a panel structure to the model fitting step. Each panel contained all recordings from a given acoustic recording station and a given piling operation.

The input data were ordered by wind farm, then by each acoustic recording station and within each acoustic recording station by the time of recordings.

4.2.3.2 Model selection

First, a model including all variables listed in Table 5 was fitted to assess collinearity between covariates and to investigate the extent to which the standard errors were inflated by the other variables in the model (Fox and Weisberg 2019). A `vif` function from the package `car` (Fox and Weisberg 2019) was used for the purpose of this assessment of collinearity, and we used a 'vif' score ≥ 5 as a threshold to remove collinear variables. This led to a list of explanatory variables which could be used for final modelling for each response variable.

We used the Bayesian Information Criterion (BIC) as a Goodness of Fit measure for choosing flexibility in each variable and a 10-fold cross-validation (CV) procedure to govern all model selection elements. The CV procedure attempts to balance the fit to data unseen by the model while minimising the number of parameters (parsimony) and was used to determine which terms to include in each model and the extent of the flexibility exhibited by each term for those selected. Note, this cross validation was predicated on preserving correlated panels (recording from a given acoustic recording station and a given piling operation) so that any residual autocorrelation present was not disrupted when choosing folds. This was considered necessary to ensure independent sampling units in this analysis.

We then used forward selection to choose the best model. An initial model with distance to the source and each remaining explanatory variable from the retained list after accounting for collinearity was fitted. BIC was then used to decide whether this additional explanatory variable should be kept and CVs to decide which combination of explanatory variables should be retained in the final model. Additionally, we calculated deviance explained by each of the explanatory variables retained in the final model.

4.2.3.3 Model diagnostics

We recalculated `vif` scores for the final model and assessed observed versus fitted values, and fitted versus scaled Pearson residual plots, using the function `runDiagnostics` in the package MRSea.

4.2.3.4 Predictions and calculating uncertainties

Predictions were made for distances to the source between 0 and 50 km and for the observed ranges of the explanatory variables retained in the final models. Confidence intervals (CI) around model predictions were obtained by performing 500 bootstrapping iterations using the function `do.bootstrap.cress.robust` from the package MRSea.

4.3 Results

4.3.1 Data overview

Data from 7 different wind farms and 19 piling operations occurring between 2014 and 2020 were included in the final modelling (Figure 6).

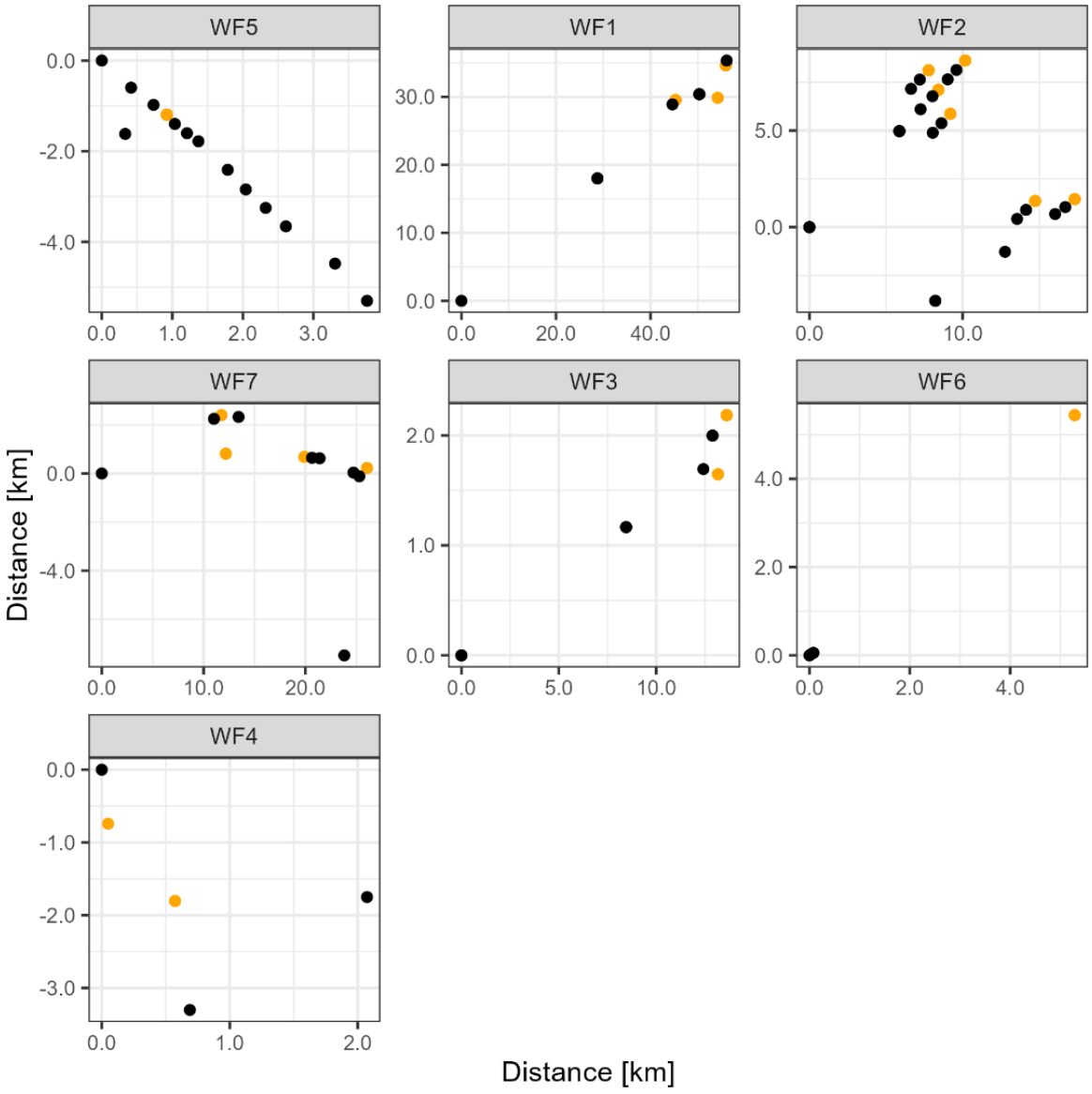

Figure 6. Location of the piles (orange dots) and acoustic recording stations (black dots) for seven wind farms (WF) used in the final modelling. X and y axes show the distance in kilometres between each pile and recording station by using the westernmost recording station for each of the seven wind farms as a reference point.

The resolution of sediments data was too low to account for potential differences between the sediments at the location of various piles. This explanatory variable was, therefore, not considered in further analysis. Pile type and pile diameter were strongly correlated and only the latter variable was

retained in the modelling (Figure 49 in section 11). The final list of the variables used in the modelling is shown as underlined variables in Table 6.

The distribution of all four metrics (kurtosis, crest factor, peak pressure, and high frequency content) with distance to the source is shown in Figure 7 and Figure 8. The majority of measurements were within the first 20 km from the source and no further than 50.4 km. All the measurements from distances > 20 km came from one wind farm (WF1 in Figure 6).

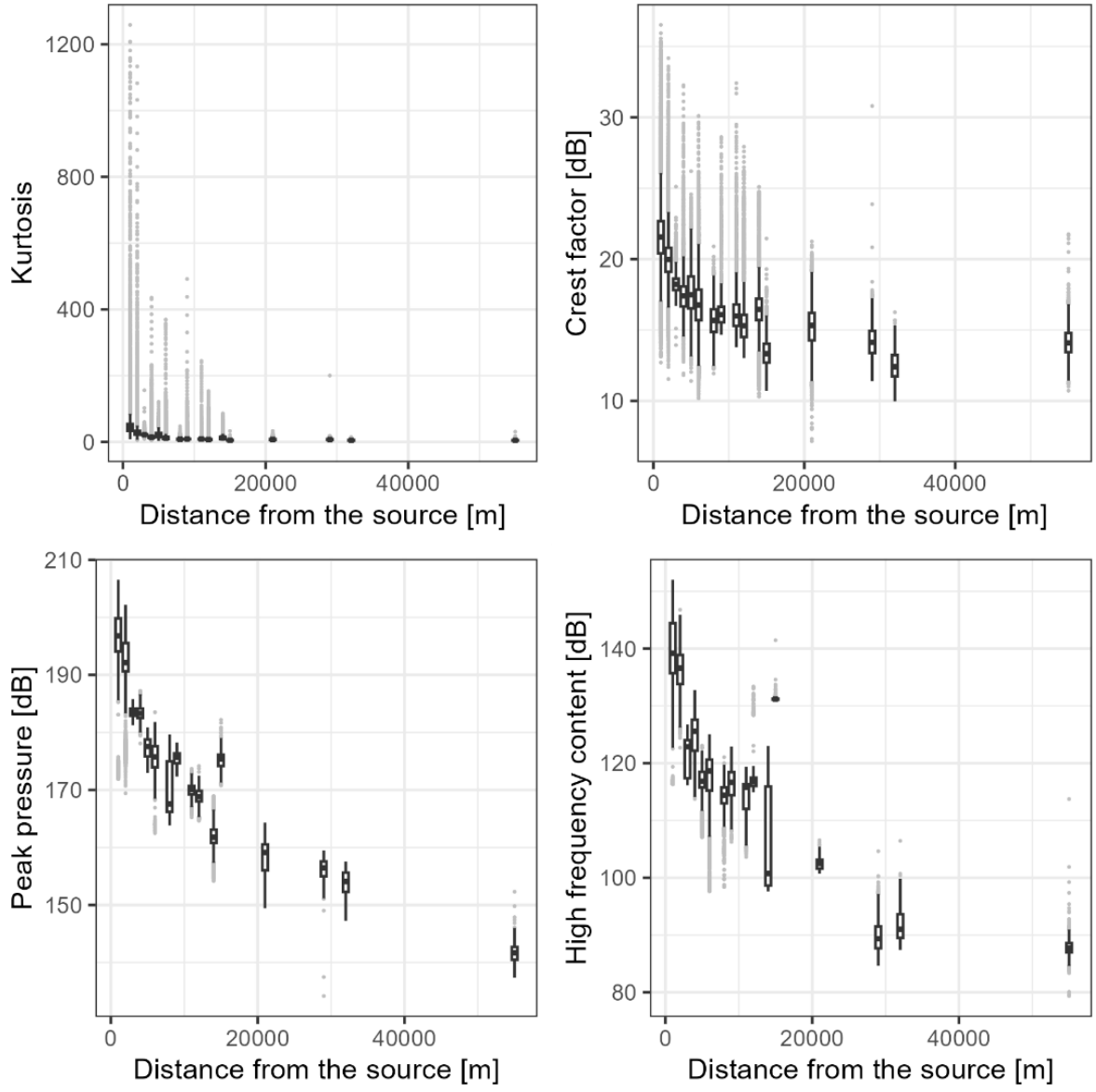

Figure 7. Four measured metrics plotted against distance from the source binned into 1000m bins. Horizontal lines within the box of the boxplot indicate median values, the lower and upper hinges correspond to the first and third quartiles (the 25th and 75th percentiles). The upper whisker extends from the hinge to the largest value no further than 1.5 * IQR from the hinge (where IQR is the inter-quartile range, or distance between the first and third quartiles). The lower whisker extends from the hinge to the smallest value at most 1.5 * IQR of the hinge. Data beyond the end of the whiskers are called "outlying" points and are plotted individually as dots.

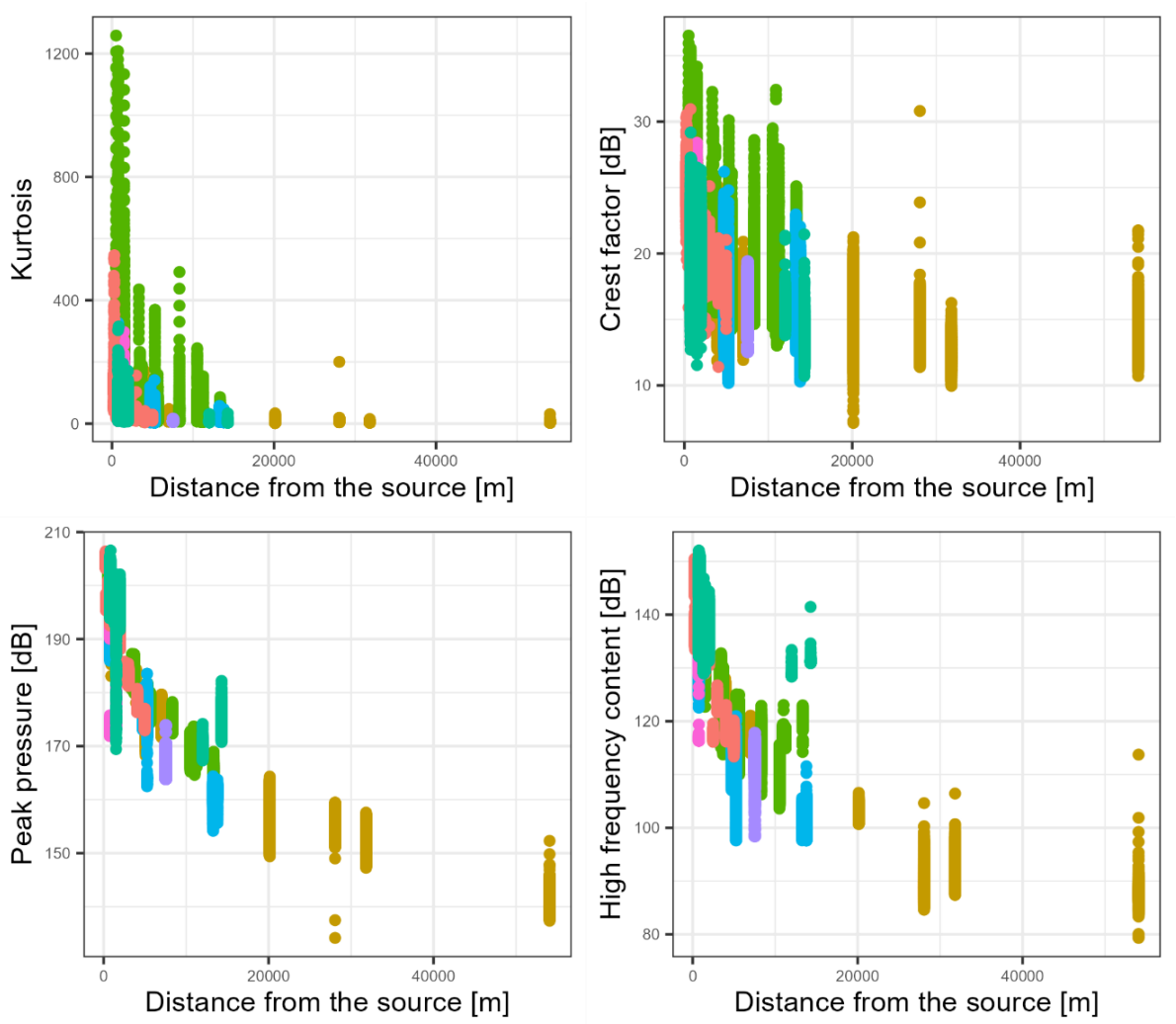

Figure 8. Four measured metrics of impulsiveness plotted against distance from the source colour-coded by the wind farm unique identifier.

4.3.2 Model fitting

A Gamma distribution with logit link function was chosen for modelling of all four metrics. The final list of covariates retained in the models is given in Table 6. A maximum of three explanatory variables were retained for each model. Wind farm was not retained for any of the models.

Table 6. List of explanatory variables retained in the final models for each metric.

Response	Explanatory variables retained in the final models
Kurtosis	Distance from the source Pile diameter Hammer energy

Crest factor	Distance from the source Time since the first blow
Peak pressure	Distance from the source Pile diameter Time since the first blow
High frequency content	Distance from the source Water depth Hammer energy

Distance to the source was the variable explaining the majority of the deviance in each model regardless of the response variable, with highest deviance explained for peak pressure (92.1 %) and lowest for kurtosis (61.3 %). The remaining explanatory variables explained additional deviance between 2 and 8.7 % (Table 7).

Table 7. Deviance explained (%) by each of the explanatory variable retained in the final model for the four metrics.

Response	Model	Deviance explained (%)
Kurtosis	Final: • Distance from the source • Pile diameter • Hammer energy	67.5
	• Distance from the source • Pile diameter	63.1
	• Distance from the source	61.3
Crest factor	Final: • Distance from the source • Time since the first blow	69.6
	• Distance from the source	67.6
Peak pressure	Final: • Distance from the source • Pile diameter • Time since first blow	96.2

Response	Model	Deviance explained (%)
	• Distance from the source • Pile diameter	95.4
	• Distance from the source	92.1
High frequency content	Final: • Distance from the source • Water depth • Hammer energy	92.4
	• Distance from the source • Water depth	85.6
	• Distance from the source	83.7

4.3.3 Model diagnostics

Model diagnostics for the models for all four metrics are shown in the section 11 (Figure 51 - Figure 62). All models show correlation in the residuals (see section 4.2.3.1 for the description of how autocorrelation was handled). Inspection of the observed versus fitted values and scaled Pearsons's residuals versus fitted values show good model fit to the data.

4.3.4 Model predictions

Most of the chosen metrics showed a rapid decrease in the first 5 km (see the details in each of the section below). The results from the model predictions for most of the metrics are therefore shown for the first 5 or 10 km. If the full predictions for the 50 km are not presented in this section, they are given in section 11.3.

4.3.4.1 Kurtosis

Kurtosis decreased very rapidly within the first 1 km from the source and this pattern was consistent with pile diameter and hammer blow energy (Figure 9, Figure 63). After 1 km, the values of kurtosis levelled off.

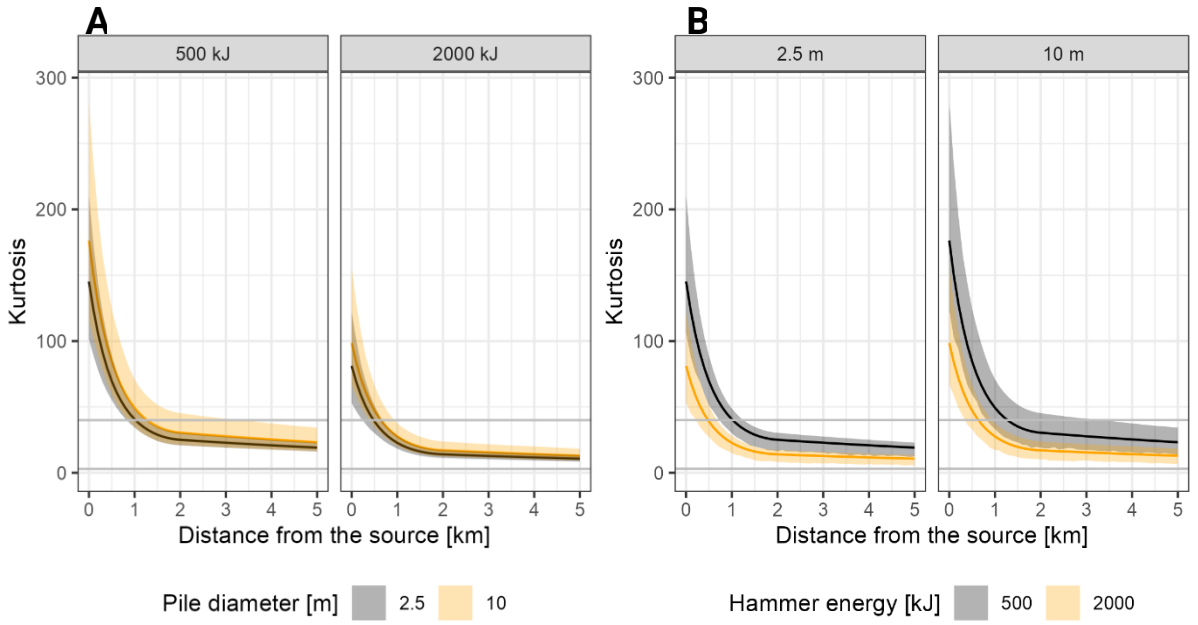

Figure 9. Changes in kurtosis with distance from the piling location for the first 5 km plotted for (A) the two pile diameters (2.5 and 10 m) and (B) two hammer blow energies (500 and 2,000 kJ). The horizontal grey lines indicate kurtosis values thresholds of 40 and 3 respectively. Shaded areas span between upper (95) and lower (5) confidence intervals.

If values of kurtosis ≥ 40 indicate the beginning of the transition from impulsive to non-impulsive sound (Hamernik et al. 2007), such a transition would happen within the first 0.6 to 3.3 km depending on the pile diameter and hammer energy (Figure 10). If values of kurtosis ≥ 3 indicate full non-impulsiveness of the soundscape, the distance at which sounds would become fully non-impulsive ranges between 13.5 and over 55 km depending on the pile diameter and hammer energy.

Note that these values consider the uncertainties in the model predictions and are based on ranges within confidence intervals and not only based on mean predictions.

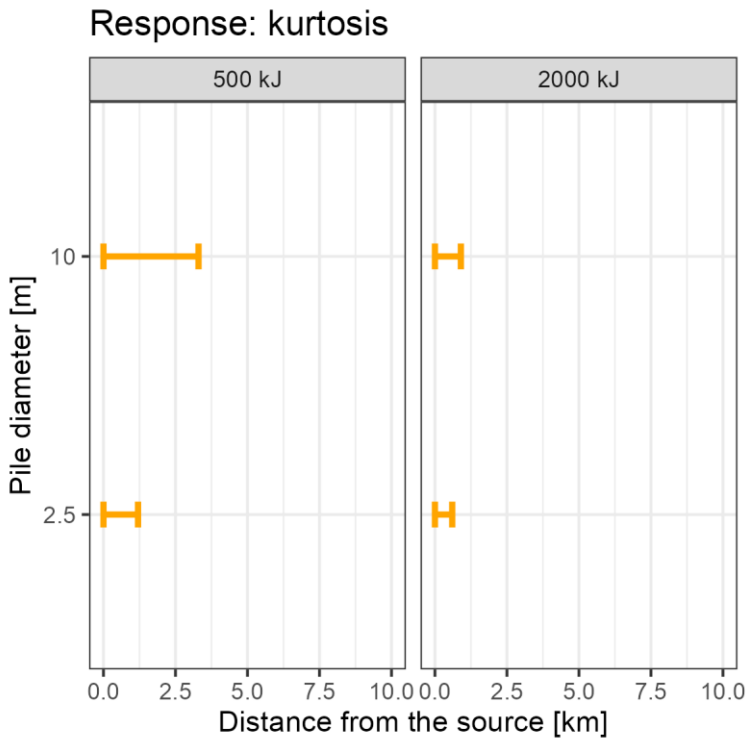

Figure 10. Range of distances from the source at which kurtosis is ≥ 40 for two hammer energies and two pile diameters. The range includes uncertainty in the model predictions.

4.3.4.2 Crest factor

Crest factor decreased very rapidly within the first 4 km from the source and then decreased steadily up to 40 km from the source. This pattern was consistent with time since piling started (Figure 11).

If values of crest factor ≥ 15 dB indicate the transition from impulsive to non-impulsive sound (Starck and Pekkarinen 1987), such a transition would happen within the first 0.4 – 55 km depending on the time since piling started (Figure 12).

Note that these values consider the uncertainties in the model predictions and are based on ranges within confidence intervals and are not only based on mean predictions.

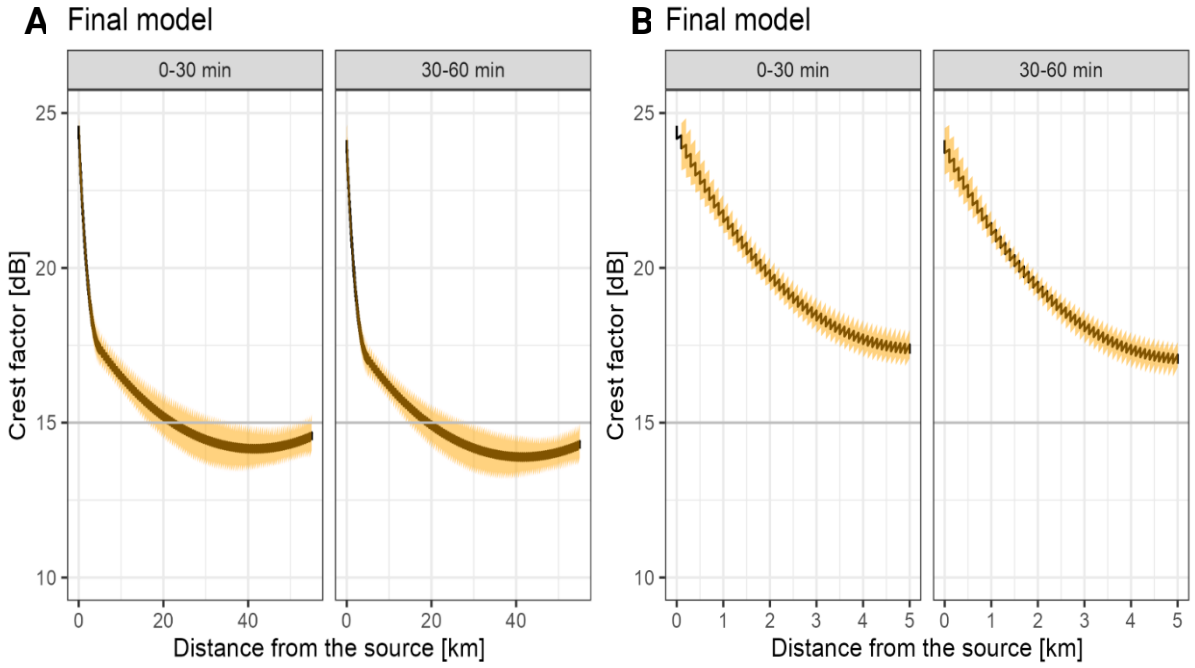

Figure 11. Changes in crest factor [dB] with distance from the piling location for (A) the first and second 30 min after piling operation started and for (B) the first and second 30 min after piling operation started for the first 5 km from the locations of the piling. The horizontal grey lines indicate crest factor = 15, a threshold indicting a non-impulsive nature of the soundscape (Starck and Pekkarinen 1987). Shaded areas span between upper (95) and lower (5) confidence intervals.

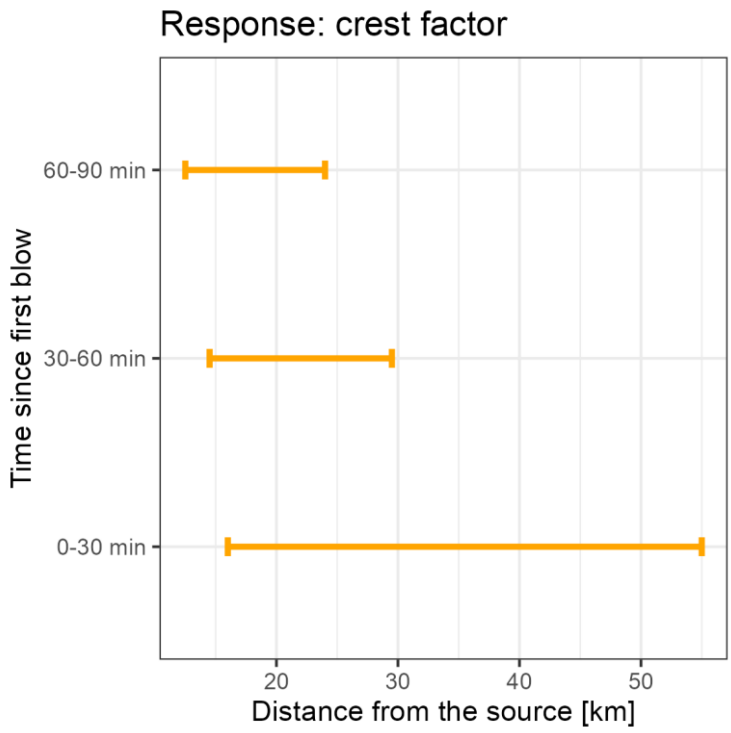

Figure 12. Range of distances from the source at which crest factor is ≥ 15 dB for the first, second and third 30 min of the piling operation. The range includes uncertainty in the model predictions.

4.3.4.3 Peak pressure

The peak pressure decreased rapidly for the first 1 km and continued decreasing until the maximum predicted distance of 55 km. This pattern was consistent for the range of modelled pile diameters (Figure 13). There was a large difference in the predicted distance at which peak sound pressure levels reached values below the PTS onset threshold for impulsive noise for the four functional hearing groups (Figure 14). Species from the high frequency group (e.g., dolphins) would most likely never experience impulsive sound if the pile diameter is ≥ 5 m. For larger diameters, animals from the remaining three hearing groups would experience impulsive sound within the first 3.5 km (Figure 14).

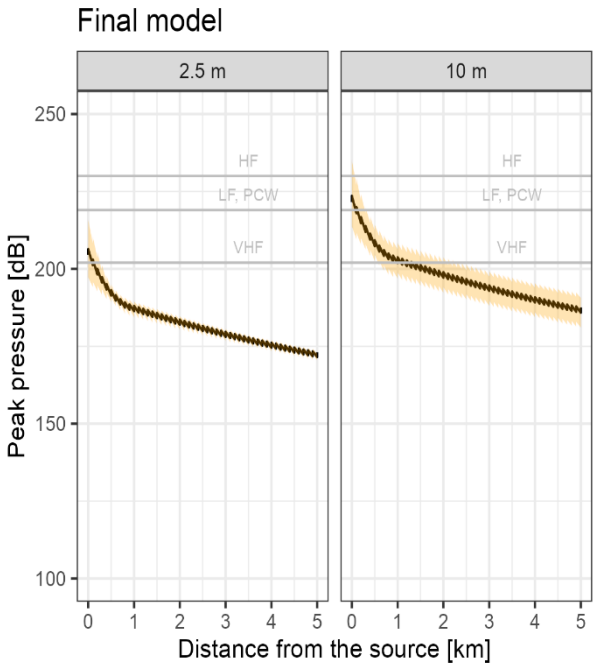

Figure 13. Changes in peak sound pressure level [dB] with distance from the piling location and in the first 30 min of piling for the two pile diameters for the first 5 km from the locations of the piling. The horizontal grey lines indicate onset thresholds for permanent threshold shifts following exposures to impulsive noise for four functional hearing groups of marine mammals: high frequency (HF), low frequency (LF), phocids in water (PCW) and very high frequency (VHF) as defined in Southall et al. (2019). Shaded areas span between upper (95) and lower (5) confidence intervals.

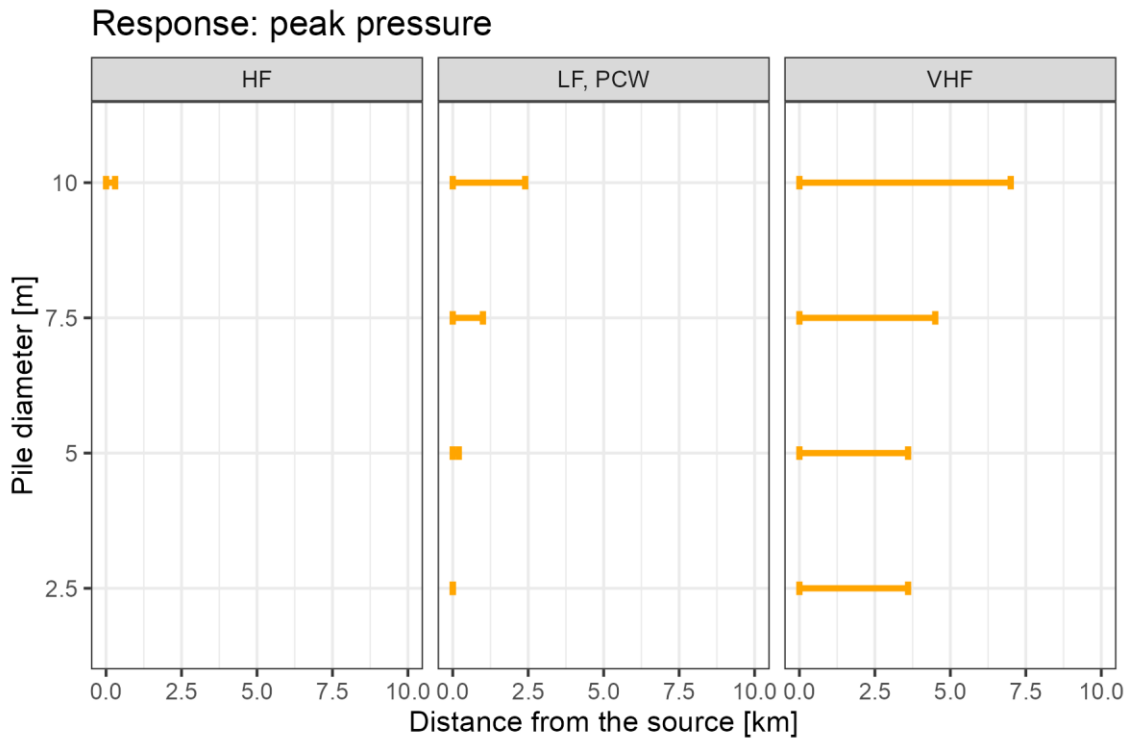

Figure 14. Range of distances from the source at which peak pressure falls below the thresholds for the four hearing groups of marine mammals defined by Southall et al. (2019), and for the four pile diameters. The range includes uncertainty in the model predictions.

4.3.4.4 High frequency content

High frequency content, like the other three metrics, decreased rapidly in the first 5 km (Figure 15). Currently there are no thresholds available in the scientific literature to mark the transition from impulsive to non-impulsive states for this metric, although Southall (2021) suggested that the absence of high frequency energy may act as a proxy for reduced impulsiveness for the other metrics.

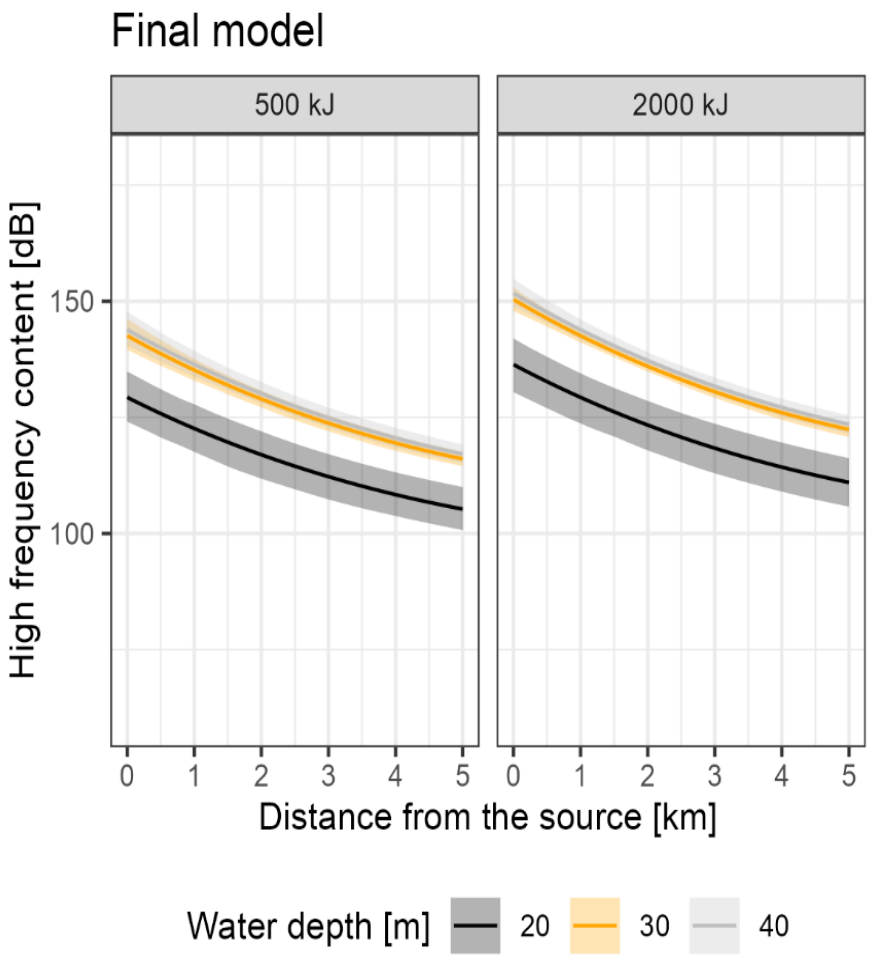

Figure 15. Changes in high frequency content [dB] with distance from the piling location for the two hammer blow energies for the first 5 km from the locations of the piling. Shaded areas span between upper (95) and lower (5) confidence intervals.

4.4 Summary of modelling of noise monitoring data

The modelling of pile driving data demonstrated declines in impulsive characteristics with increasing range from the source in all metrics. The final (i.e., best fitting) models included different explanatory variables between impulsive metrics but all resulted in range as a most important term.

In section 2 we detail the current state of knowledge on the limited values available to use as thresholds for impulsiveness (i.e., kurtosis of 3-40 dB, crest factor <15 dB). Using these values as thresholds highlights a variety of ranges from the source at which the modelled relationships fall below these (Figure 10, Figure 12, Figure 14, Table 8). These ranges indicate that the sound may become non-impulsive both very close to the source, as well as not at all within the predicted ranges of 55 km. This highlights the challenge of limited information characterising impulsiveness accurately (in the context of generating threshold shift).

Table 8. Summary of the ranges indicating the change from impulsive to non-impulsive sound based on four chosen explanatory variables. For the explanation of threshold used to estimate the range, please refer to previous sections.

Response	Range from source where impulses transition to non-impulsiveness
Kurtosis	0 – 4 km
Crest factor	0.4 – 55 km
Peak pressure	0 – 55 km
High frequency content	N/A

As with pile driving noise, the UXO detonation pulses also generally appeared to exhibit lower peak sound pressure levels and high frequency content with increasing range, although no clear pattern was observed in the other metrics (Figure 5). Additionally, the absolute values for these metrics were very high. This indicates the sounds generated during UXO detonations retained impulsive characteristics at all ranges monitored. These were not modelled further.

Given the challenges identified above, we explore how the PTS tool (section 5) can help identify the factors that are important in driving SEL_{cum} PTS ranges and consider how conservatism in range estimation can be improved.

5 PTS framework

5.1 Background and objectives

Given the challenges of characterising an impulsiveness threshold or range to be used in impact assessments (section 4 and 5), we investigated the importance of this transition point, relative to other factors, such as animal swim speed, sound source level and propagation, and the time between pile strikes.

PTS onset impact ranges represent the starting distances from the pile for animals to escape (i.e., move away from the sound source) and prevent them from receiving a dose higher than the PTS onset threshold. We define these as "PTS impact ranges". The aim of this work package is to develop a framework that will allow for the assessment of PTS impact ranges based on a fleeing animal model under different pile driving scenarios.

The purpose of this analysis was to determine the relative differences (i.e., increases or decreases in PTS onset ranges) between different scenarios. The absolute PTS ranges presented are only indicative.

In this section we describe an overview of the model and the analysis, as well as present the results from a range of scenarios. A detailed manual on how to use the model, and all the input files necessary to run it, are given in a public GitHub repository here https://github.com/SMRU-Consulting-Github/RADIN-framework-development. The detailed model description follows the updated ODD protocol (Overview, Design concepts, Details) suggested by Grimm et al. (2006), (2010), as a standard protocol for describing agent-based models is given in section 13.1.

5.2 Model overview

The model is a one-dimension (1D) agent-based model (ABM) simulating movement of animals (referred to as *animats*) moving through a soundscape (set with a constant source level and point transmission loss model) away from the source location in a straight line at a user defined speed. In reality, animals would be highly unlikely to move in a straight line away from the source. Therefore, we tested a range of speeds between 0.2 and 5 m/s. The lower speed values can account for the fact that animals may not move in a straight line away from the source and, in such cases, their average speed along the straight line could be close to the lowest value chosen. The pattern of blows from pile driving can be fixed to a specified blow rate or by using an input file (which provides the exact pattern of blows, for example, from a real pile installation log).

5.3 PTS onset range calculation

PTS onset ranges are calculated based on the noise exposure criteria from Southall et al. (2019). This analysis routine assumes that animats only accumulate SEL_{ss} following individual pile strikes. This assumption is based on the difference in amplitude between high amplitude pile strikes and other background sound sources, which are less likely to trigger hearing threshold shifts (Finneran 2015).

For each animat that accumulates enough SEL_{cum} to experience a TTS onset, this analysis routine continues to accumulate all additional measurements of SEL_{ss} until a 40 dB TTS is reached (i.e., the

animal accumulates enough threshold shift to reach the PTS onset). The 40 dB TTS is presumed to be a PTS onset level, as suggested by Southall et al. (2019).

The accumulation process that leads to PTS onset is performed by multiplying the cumulative experienced noise (SEL_{cum}) by a growth rate value which is distinct for continuous and impulsive noise (see Figure 16). For each decibel of impulsive noise experienced, the TTS is elevated by 2.3 dB whereas for non-impulsive sounds, the TTS is elevated by 1.6 dB. These growth rate multipliers are provided in the PTS onset criteria from Southall et al. (2019) and were established following noise exposure studies with chinchillas. The general patterns observed in these terrestrial mammal studies were subsequently supported by the data available from marine mammal studies (Finneran 2015).

When a TTS value of 40 dB is reached, the given animat is considered to have experienced PTS and their starting distance from the piling location (the first patch in the 1D simulation) is recorded.

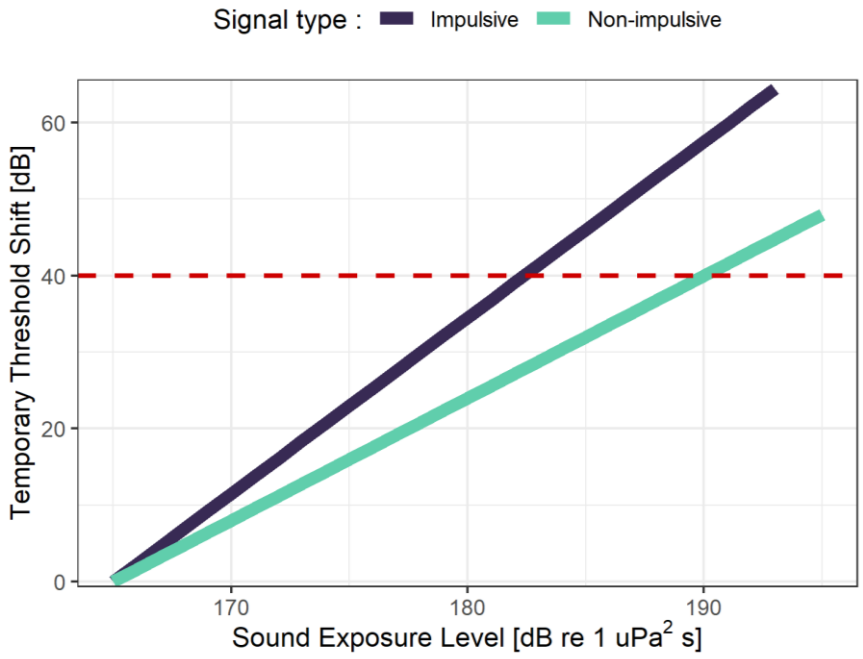

Figure 16. Visual representation of the auditory threshold shift growth rates for impulsive and non-impulsive sounds from Southall et al. (2019), with frequency weighted sound exposure level (SEL) on the x-axis and the magnitude of hearing threshold shift on the y-axis. A threshold shift of 40 dB is used as an indicator of the onset of PTS and is marked by the horizontal red dashed line.

The output of the tool is the maximum distance at which animats must be at the start of piling in order to experience PTS. These distances are calculated for four hearing groups: very high frequency (VHF), high frequency (HF), low frequency (LF), and phocids in water (PCW).

5.4 Assessing factors that affect PTS onset ranges

5.4.1 General patterns

Using the tool framework described above and in section 13.1 of the appendix, a range of parameter combinations were tested. These comprised different animal fleeing swim speeds (0.2, 0.5, 1.5, and 5

m/s) and transition points for impulsiveness (i.e., where the signal became non-impulsive at 1 km, 2km, 3km, 4km, and 50 km from the source). For this assessment, a constant blow rate of one blow every two seconds was used. These parameter combinations were assessed for each of the functional hearing groups (i.e., LF, HF, VHF cetaceans, and PCW). We assumed a source level of 220 dB re 1 µPa (matching future EIA chapter reviews) and transmission loss of $17*\log_{10}$(range). To ensure robust conclusions could be drawn from this analysis, different source level and transmission loss values were preliminarily tested (10, 15 and $16*\log_{10}$(range) source levels of 210 and 230 dB). The PTS onset ranges differed depending on the values used, but they did not change the relative patterns observed. A full sensitivity analysis of the framework was not the aim of this project. Additionally, we have considered a point source and cannot comment on if results would be the same with a match cone wavefront model.

5.4.2 Real world hammer logs

To understand how the temporal pattern of pile strikes from real world hammer logs affected PTS onset predictions, a total of 44 hammer logs from real pile installation events at the 11 studied wind farms were compiled to run simulations. Of these, 21 logs were provided by itap, which were generated by using the time into acoustic recordings of each detected pile driving impulse. The remaining 23 logs were selected from a larger set of 163 hammer logs provided by ORJIP. The patterns observed in the 163 logs were very similar, therefore 23 of these logs were semi-randomly selected as a representative subsample. Figure 17 shows all the piling sequences, covering the full duration of all piling installation activities (see Figure 18 for a zoomed in section of the first 45 minutes of piling activities). The duration of piling activities ranged from 30 minutes to 9.8 hours (mean and SD duration was 2 ± 1.7 hours). Across all piling events, the mean time between individual pile strikes (inter-blow interval, IBI) ranged from 1.2 to 19.6 seconds.

Additionally, the real offshore wind hammer logs were compared against an “EIA baseline” piling schedule which was constructed by emulating the proposed piling schedules for eight recent offshore wind farm applications. This review of recent offshore wind farm applications provided estimates of typical patterns of strike/blow rates that developers and their engineers are considering for future sites. The patterns of blows in three phases of piling (that occur sequentially) were mapped out and averaged across sites to create a “simulated baseline” against which the real world hammer logs (from already installed foundations) were compared. This simulated baseline comprised a hammer pattern of 11 blows per minute for the first 15 minutes, followed by 17 blows per minute for 17 minutes and then 34 blows per minute for 282 minutes. We focused on the VHF functional hearing group for these simulations due to the large number of simulations to be run. The relative patterns are expected to hold for each functional hearing group, although absolute ranges will differ.

For all simulations, including real hammer logs and simulated baseline we assumed a source level of 220 dB re 1µPa, a transmission loss of $17*\log_{10}$(range), and that animats moved at 0.2, 0.5, 1.5, or 5 m/s away from the source. The range of selected swim speeds aimed to capture realistic movement patterns of marine mammals (e.g., Blix and Folkow (1995) and Otani et al. (2000)), as well as account for instances where animals do not move away from a sound source in a straight line. We calculated PTS ranges for VHF cetacean hearing group only assuming thresholds when sound becomes non-impulsive at 1, 5, and 50 km from the source.

The intention of these simulations was not to determine the absolute PTS onset ranges, but instead to compare the relative differences between parameter values, with the aim of identifying sensitive parameters and possible means of improvement of the PTS impact assessment.

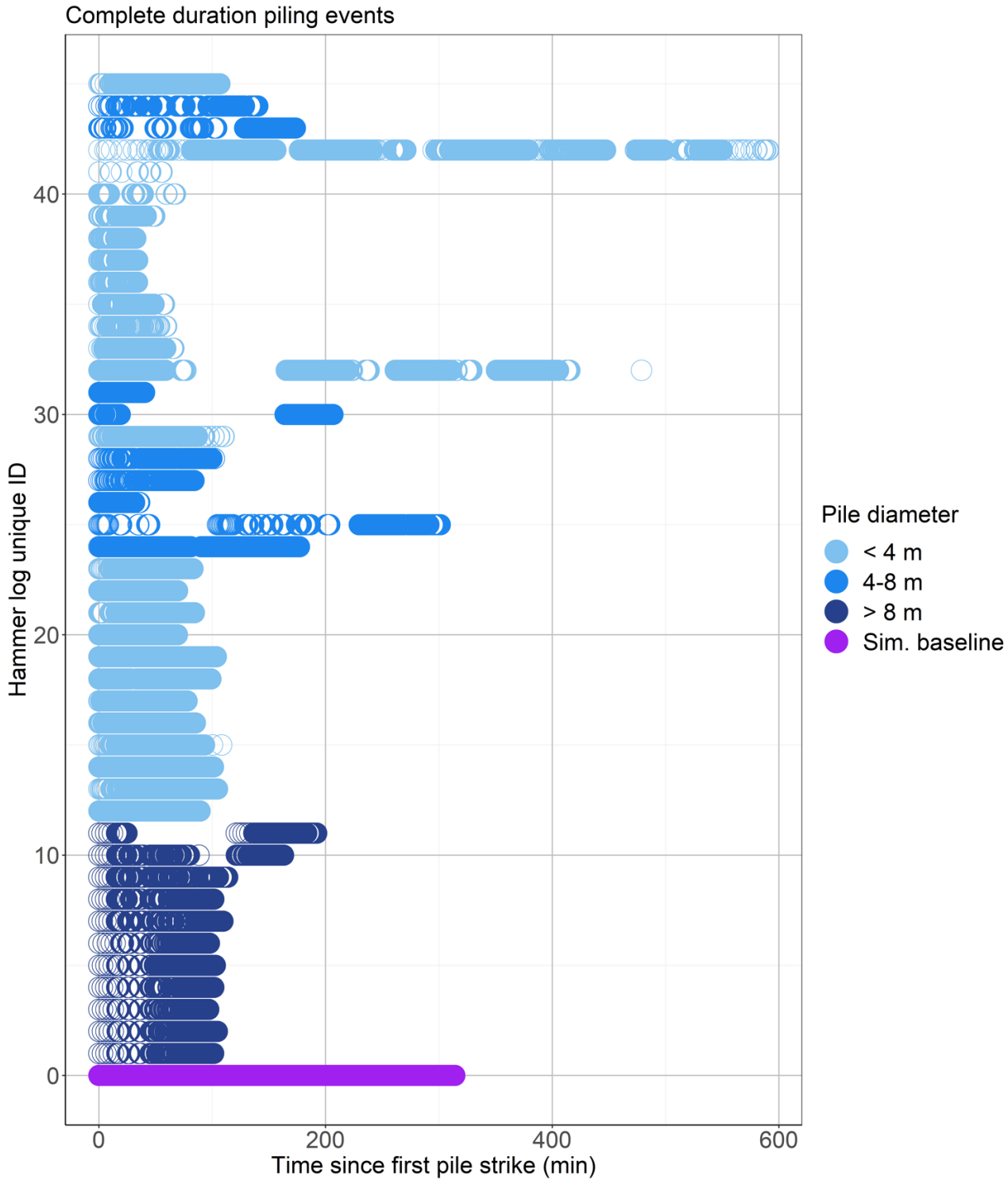

Figure 17. Graphical representation of the 44 real hammer logs and one simulated EIA baseline hammer log used in the simulations. Each dot represents the timing of one pile strike, and the logs are colour coded by the pile diameter being piled (except for the simulated EIA baseline log, for which pile diameter was not established).

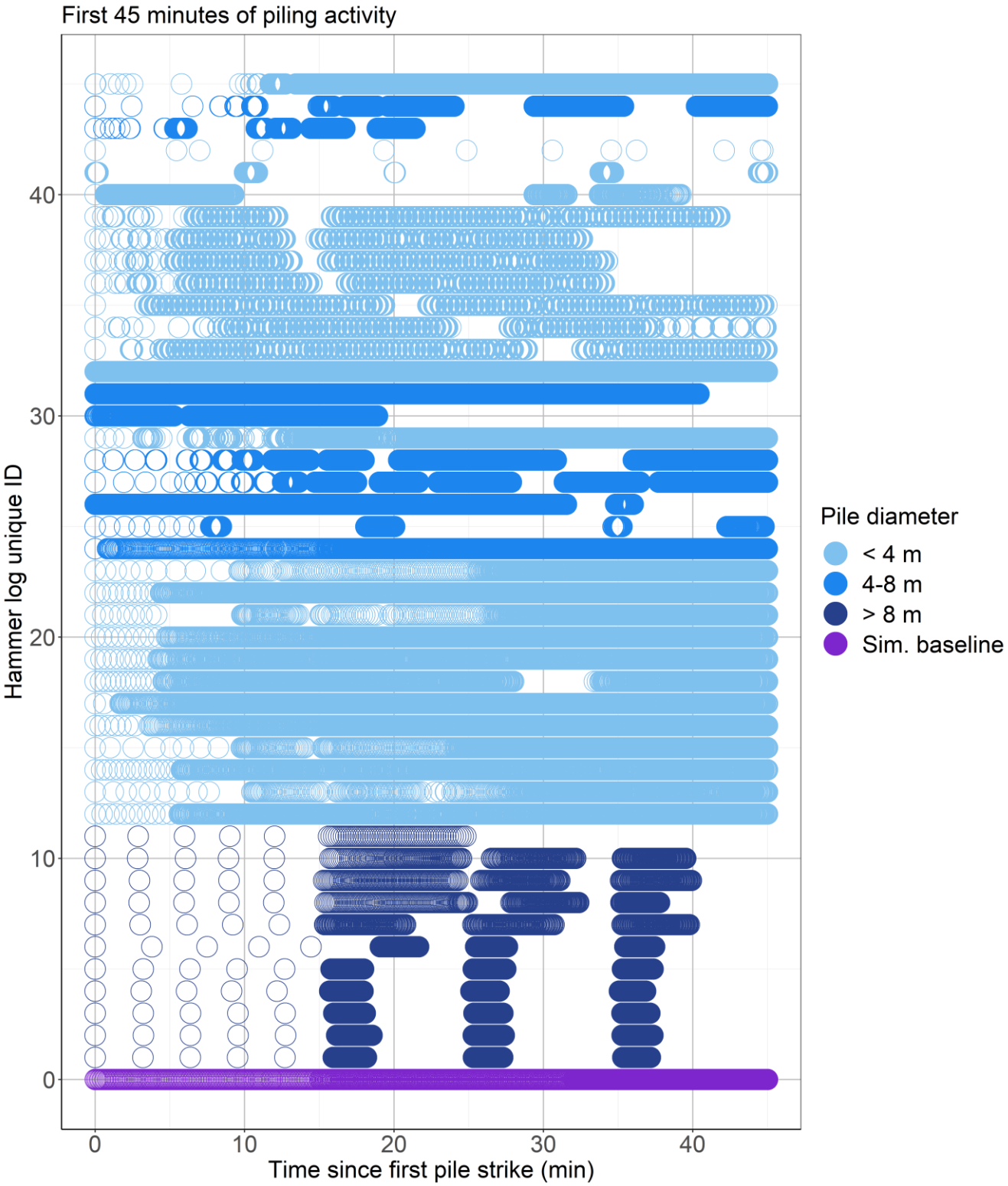

Figure 18. Graphical representation of the first 45 minutes of piling of 44 real hammer logs and one simulated EIA baseline hammer log used in the simulations. Each dot represents the timing of one pile strike, and the logs are colour coded by the pile diameter being piled (except for the simulated EIA baseline log, for which pile diameter was not established).

To assess the most important factors in PTS onset range predictions using real world hammer logs, we built a series of GAM models. PTS onset range was the response variable and candidate explanatory variables included mean IBI in the first 5, 10, 15, 45 min of piling (not all included in a single model due to collinearity), total duration of piling, and an interaction between mean IBIs in these four-time intervals and piling duration. All models were fitted assuming a gamma distribution. Results from the simulations assuming an animat swim speed of 0.5 m/s and the threshold between impulsive and non-impulsive sound occurring 5 km away from the source were used. We based model selection on the Akaike information criterion (AIC).

5.5 Results – Factors affecting PTS onset range predictions

5.5.1 General patterns

Here we are interested in understanding which factors are most important in explaining PTS onset ranges. We are focused on the relative differences (i.e., increases or decreases in PTS onset ranges) between different scenarios. The absolute PTS ranges presented are only indicative, given the constant source level and transmission loss assumptions.

Figure 19 shows the variations in PTS impact range, which is described as the maximum distance at which animats should be placed at the start of a simulation to experience a PTS onset. The results are split based on four functional hearing groups from Southall et al. (2019) and are plotted against swim speed. Distinct sets of PTS ranges are shown for each distance at which the transition from impulsiveness to non-impulsiveness is expected to occur.

For all the simulations based on the same transmission loss and source level, it was determined that for a given hearing group, the speed of the animals moving directly away from the piling location had a larger effect on the estimated PTS ranges than the distance of transition from impulsive to non-impulse sound (Figure 19). The most prominent reduction in impact range comes if the transition occurs within 1 and 2 km of the source for VHF and LF groups respectively (Figure 19). For the remaining two hearing groups, the results were comparable regardless of the transition distance.

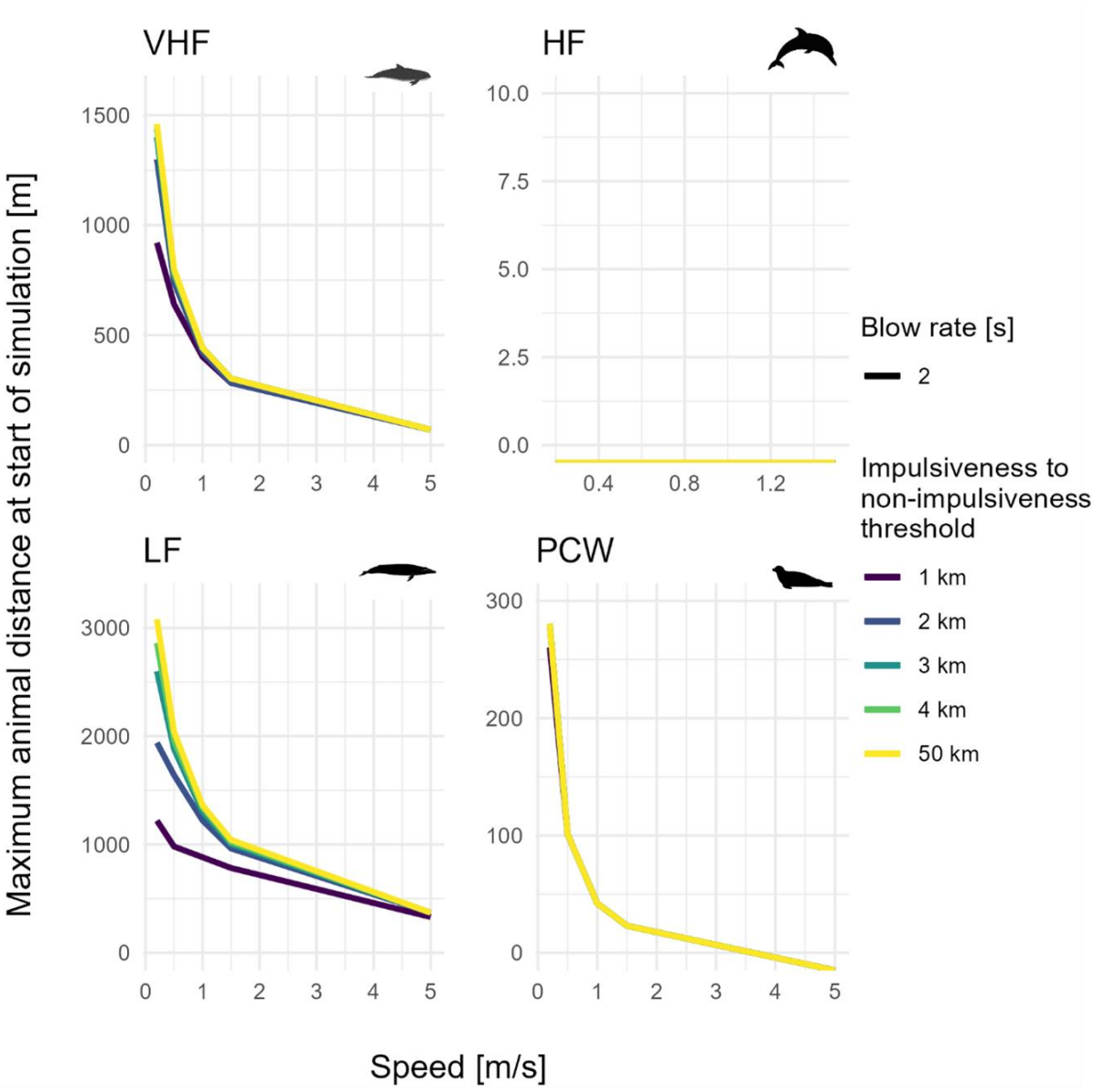

Figure 19. Changes in PTS onset ranges (expressed as maximum distance at which animals need to be at the start of piling to receive PTS during piling duration) with animal speed (x-axis) calculated following 6-hour simulated exposures to pile strikes every two seconds. Note: The focus was on relative differences between results, not on absolute PTS onset ranges.

5.5.2 Real world hammer logs

As with the general pattern, the swim speed of the fleeing animal was an important parameter affecting PTS ranges and this pattern applied to all simulated hammer logs and the simulated baseline. For example, assuming an animal moving away from the source at 0.2 m/s (akin to slow directed movement or variable heading resulting in slow speed over ground) resulted in 13 – 20 times larger PTS ranges than assuming an animal moving away at 5 m/s (Figure 20).

In general, using real world hammer logs resulted in markedly smaller impact ranges (when all other factors were standardised). Only one piling schedule (Piling ID 32, Figure 20) resulted in larger estimated PTS ranges than the simulated baseline schedule for all simulated animal fleeing speeds and the three assumed impulsiveness thresholds. Three other piling schedules (IDs 26 (Figure 71), 30, and 31 (Figure 72)) resulted in estimated PTS ranges larger than the simulated baseline for animals moving away from the source at ≥ 0.5 m/s. All the remaining 40 schedules resulted in lower estimated PTS ranges than the simulated baseline regardless of assumed animal fleeing speed and impulsiveness threshold (see section 13.2 of the appendix).

The real world hammer log simulations highlighted that the transition between non-impulsive and impulsive sound needed to occur < 5 km of the source in order to have a marked effect on PTS ranges (see Figure 20 and section 13.2 of the appendix). The simulations showed the same results whether this transition occurs at 5 or 50 km.

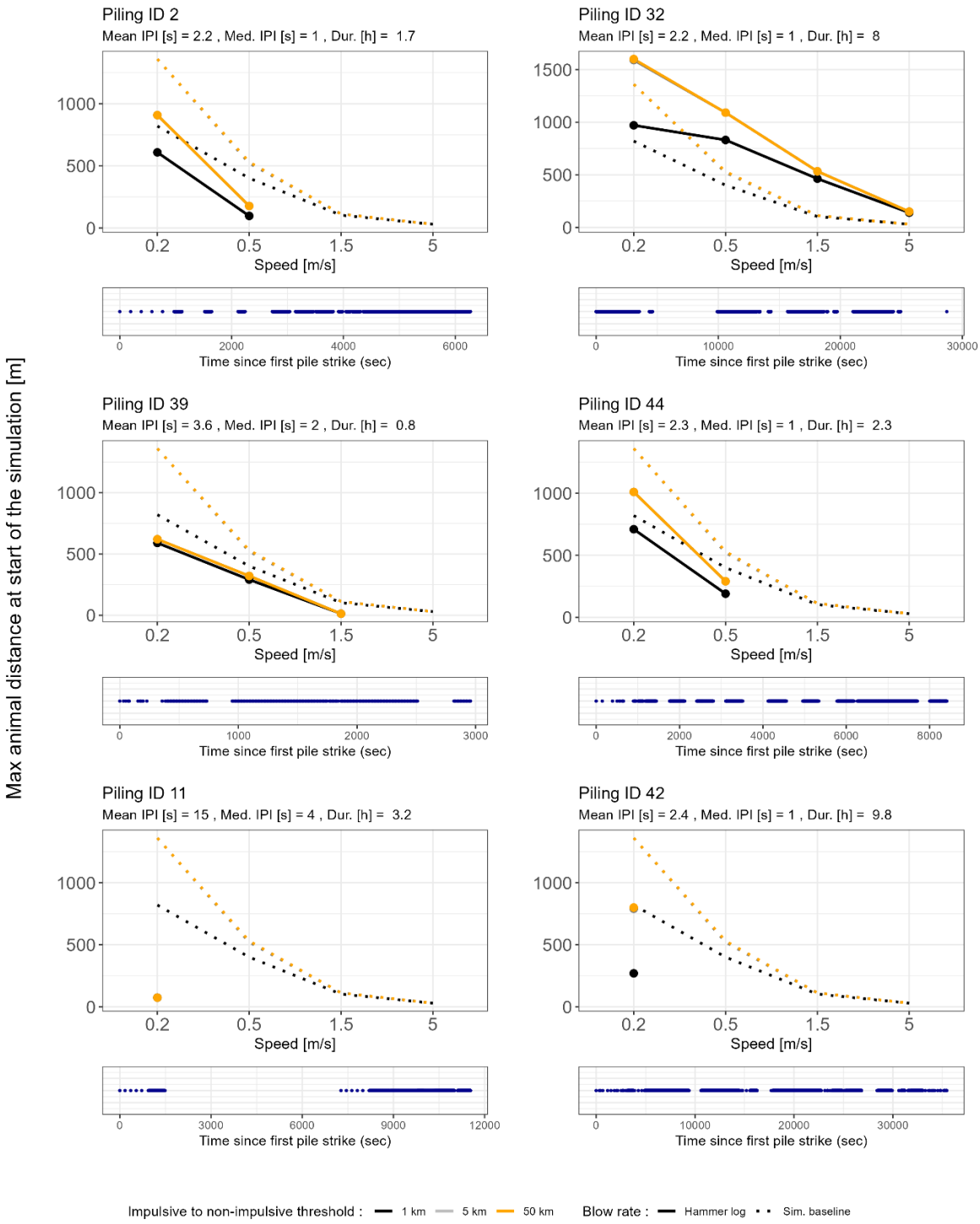

Figure 20. Changes in PTS ranges (expressed as maximum distance at which animals need to be at the start of piling to receive PTS during piling duration) with animal speed on the x-axis for 6 indicative real piling schedules out of 44 analysed schedules. The blow rate pattern is indicated by the line type: dotted lines show the results of a simulated baseline, and solid lines shows the results for a given hammer log. The distance from the source where sound is assumed to become non-impulsive is indicated by the colour of the lines. The chosen six simulations are piling events showing largest estimated PTS ranges (top four panels) and smallest estimates PTS ranges (lower two panels). Note that for all simulations grey and orange lines overlap. The title of each graph shows mean and median inter-pile strike interval (IPI)

and the total duration of piling. The lower panel depicts strike frequency and corresponds to the overview of the strike frequencies shown in Figure 17.

If the resulting PTS impact ranges were converted to impact areas (as circular surfaces), comparing the temporal patterns of pile strikes from real world hammer logs with that of the simulated baseline (where all simulations had the same animal swim speed of 0.2 m/s), we observed a large scale reduction in predicted PTS area (Table 9). The minimum percentage reduction in impacted area was a 16% reduction and the median was a 57% reduction. This means that half the scenarios showed at least a 57% reduction in area (compared to simulated baseline). It is important to note that in two cases the impacted area was larger. It was identified that these two scenarios had a very high blow rate immediately following the first pile strike.

Table 9. Percentage reductions in PTS impacted area across 44 real hammer logs compared to the simulated baseline hammer log.

Statistic	% reduction in PTS impact area
Minimum	16 %
Lower Quartile	43 %
Median	57 %
Upper Quartile	70 %
Maximum	99 %

5.5.3 Modelling of piling duration and inter-blow interval

When all other variables were standardised, the inter-blow interval (IBI) was the best predictor of a reduction in PTS impact range. Figure 21 shows the relationship between mean inter-blow interval (IBI) in seconds quantified during the first 45 minutes of piling operations against the maximum distance from the source (assuming an animal moves at 0.5 m/s away from the source and that the range where sound becomes non-impulsive is 5 km from the source). Mean IBI in the first 45 min of piling was retained in the final model and had a marked effect on PTS range. Specifically, the time between subsequent blows in the first 45 minutes of piling is the key parameter driving PTS ranges. This was more important overall than the total piling duration (in terms of drivers affecting PTS ranges with a fleeing receptor). PTS onset ranges were inversely proportionate to mean IBI. That means the real world hammer logs with longer periods between subsequent pile strikes (i.e., higher IBIs) in the first 45 minutes of piling had smaller impact ranges.

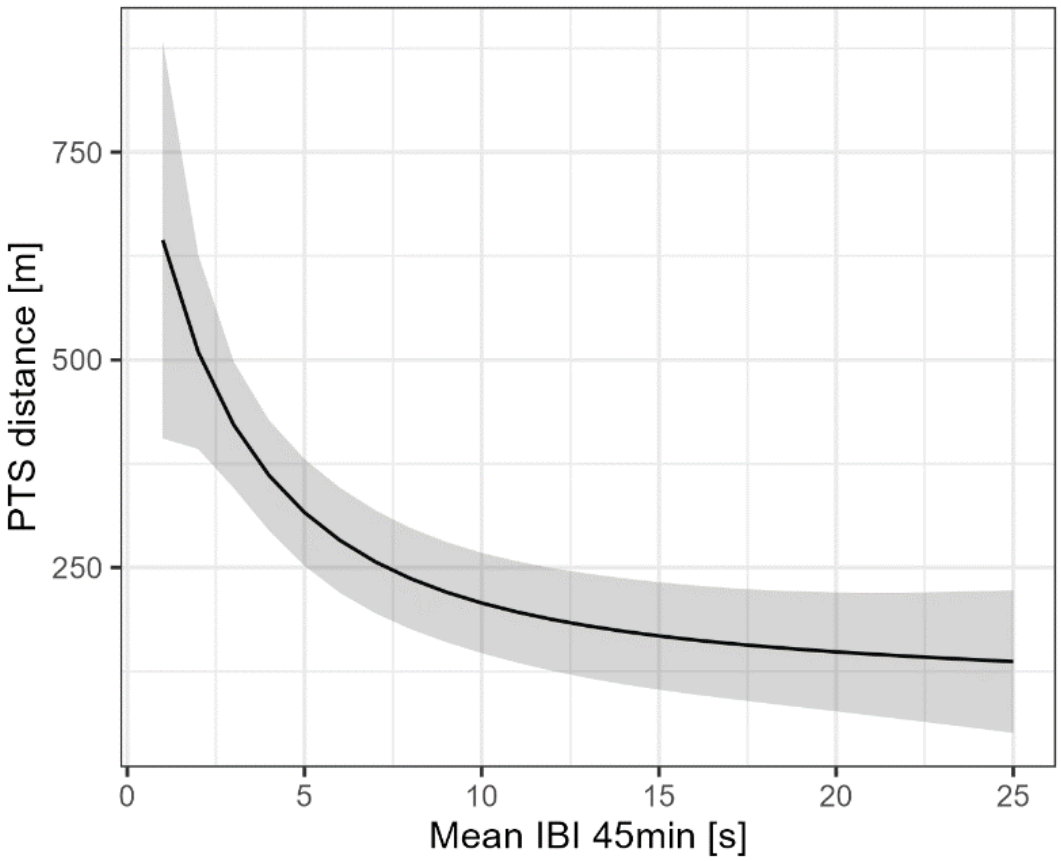

Figure 21. The relationship between mean inter-blow interval (IBI) in seconds quantified during the first 45 minutes of piling operations against the maximum distance from the source at which animal must be at the commence of piling in order to receive PTS. The model assumes that animals move at a speed of 0.5 m/s away from the source and that the range where sound becomes non-impulsive is 5 km from the source. Black line shows mean model predictions and grey ribbon confidence intervals.

5.6 PTS framework summary

Via the development of a PTS framework and assessing a variety of factors and their impact on PTS onset range predictions we have identified the following take-home messages:

PTS framework summary

- When many other factors are standardised, the transition from impulsiveness to non-impulsiveness must occur at distances <5 km from the source in order to have a meaningful impact on PTS onset ranges.
- The swim speed of the fleeing animal and the blow rate are generally more impactful parameters than the impulsive transition range (though a complete sensitivity analysis was outside the scope of the project).
- Real world hammer logs generally appear to predict smaller impacted areas than those predicted using the simulated baseline calculated from a review of wind farm applications for windfarms to be constructed in coming years.
- The pattern of blows in the first 45 minutes of piling had the largest effect on PTS onset ranges (for a standardised source level, transmission loss, and animal swim speed) – larger than the total duration of piling.

6 Discussion

This study has identified several factors that impact PTS onset range predictions and estimation of transition between impulsive and non-impulsive sound. Below we discuss these topics in more detail, highlighting assumptions and uncertainties, and suggest recommendations to help advance this field and support improved noise impact assessments.

6.1 Impulsive transition

The four chosen metrics (kurtosis, crest factor, peak pressure and high frequency content) used to assess impulsiveness from impact pile driving recordings showed rapid decreases in the first 1 to 5 km from the piling location, the rate of which varied between metrics. This sharp decrease showed very similar patterns between the four metrics even if other covariates were retained in the final model. Distance from the source had, therefore, the main explanatory power and as showed in Table 7 explained 60 – 95% of the deviance. Apart from distance from the source, there was no single explanatory variable that would be retained in the final models for all chosen metrics but pile diameter, hammer energy, and time since first blow were retained in two out of four chosen models. Wind farm site was not retained in any of the final models which indicates that there was a large overlap in the explanatory covariates between the piling operations for the analysed wind farms.

The best available current understanding of kurtosis is that values ≥ 40 indicate a beginning of the transition from impulsive to non-impulsive nature of the sound. Based on this assumption, and from the modelling results, we predict such a transition would happen within the first 0.6 km to 3.3 km depending on the pile diameter and hammer energy. If values of kurtosis ≥ 3 indicate full non-impulsiveness of the soundscape, the distance at which sounds would become fully non-impulsive ranges between 13.5 and > 55 km depending on the pile diameter and hammer energy. Currently, the only threshold for impulsiveness in the literature for crest factor is 15 dB. If crest a factor value ≥ 15 dB indicates that the nature of a given sound is non-impulsive, sounds produced by impact pile driving could meet this threshold within the first 0.4 – 55 km depending on the time since the start of piling. If peak sound pressure level were to be used to define the transition from impulsive to non-impulsive, the transition point would vary depending on the functional hearing groups of the marine mammals present and the diameter of the pile. Species from the HF cetaceans hearing group would most likely not experience sounds from impact pile driving as impulsive if the pile diameter was ≥ 5m. For larger pile diameters, animals from the remaining three functional hearing groups would be exposed to sounds characterised as impulsive within the first 3.5 km from the piling site.

These results highlight large differences in the estimated distance from the source where sound may be characterised as non-impulsive depending on the metrics used to characterise the nature of the sound. This finding is consistent with the results presented by Hastie et al. (2019), where the authors modelled the probability of the sound being non-impulsive with distance from the source using two of the metrics used in RaDIN (peak pressure and crest factor) and three additional ones: signal duration, rise time, peak pressure - signal duration ratio. Their results showed that a probability exceeding 50% of signal being non-impulsive occurred at 0.5 – 55 km from the source, depending on the metrics considered.

On the assumption that the limited impulsiveness thresholds available are fit for purpose, each impulsiveness metric indicated a different range from the source at which pile driving sounds become non-impulsive. However, it is clear that there is a great level of uncertainty over what thresholds should be considered for each metric to distinguish impulsive and non-impulsive sounds (in terms of their ability to harm the auditory system). For example, the use of a threshold of kurtosis of 3 for sounds to be considered fully non-impulsive is most likely very conservative. This kurtosis value is synonymous with Gaussian noise, which is not often characteristic of underwater soundscapes, given the vast variety of naturally occurring sound sources, both abiotic (e.g., wind, raindrops, anthropogenic noise) and biotic (e.g., snapping shrimps, fish choruses, vocalising marine mammals). During this study, metrics of kurtosis were computed for time periods outside of impact pile driving pulses but while other construction activities were ongoing. A broader set of underwater noise conditions (e.g., during periods without construction activities) would be required to identify possible ranges of kurtosis values for periods without impulsive sounds.

During the feature extraction process from individual pulses, the presence of additional sound sources making up the ambient noise needs to be considered, especially in the case of metrics such as high frequency content. For instance, known sound sources co-occurring with the pile driving pulses, such as dynamic positioning systems or depth scanners, should be filtered out, if possible, by using custom sound processing filters matching the characteristics of the additional sound sources. This process would ensure that the data used to investigate the characteristics of the pulses of interest are not contaminated by acoustic energy from elsewhere in the environment.

Given the consistent pattern associated with decreasing impulsiveness in all four modelled metrics, a single metric that is related to impacts on hearing may be a sufficient proxy to inform how signals change their impulsive characteristics with range. Such a metric would need to be assessed for cross-correlation, ease of implementation, and ideally be weighted depending on their use in hearing loss studies. For instance, peak sound pressure level is already included in noise exposure criteria (Southall et al. 2019), and could act as such a proxy, although it does not explicitly characterise the shape of the signal. Therefore, readily established metrics used for noise impact assessments should continue to be investigated alongside metrics like kurtosis to allow TTS and PTS thresholds to be further refined. Alternatively, a multi-level criterion of impulsiveness could be developed, in which several metrics could be used to establish when signals transition from being impulsive to non-impulsive.

It is also helpful to highlight that some upcoming noise abatement technologies aim to increase the impact time between hammer and anvil (Koschinski and Lüdemann 2013). This has the potential to reduce source levels but also change other signal characteristics. Both will be expected to influence the distance when a signal changes from impulsive to non-impulsive.

A key knowledge gap persists, being the values for these metrics which can reliably be used to define impulsiveness. Moreover, the definitions or thresholds for impulsiveness we seek are those sounds that result in threshold shifts in the marine mammalian ear. Specifically, it is necessary to understand if sounds with, for example, a kurtosis of 40 or 30 impact the ear in the same manner. Similarly, it is currently unknown if a crest factor of 15 dB is an appropriate cutoff to define impulsiveness. Conducting hearing experiments with marine mammals using playbacks of sounds with known impulsiveness characteristics could provide improved knowledge in this area (i.e., estimating threshold shift under different impulsiveness conditions). Such an approach could help guide which impulsive characteristics are most impactful and help identify the impulsiveness thresholds (and so ranges from

the source) where a transition from impulsive to non-impulsive reliably occurs. Nonetheless, the challenges associated with designing such studies in a realistic and robust manner are acknowledged. Southall (2021) highlighted the issues related to using small reverberant pools and artificial near-field conditions during exposure experiments and recommended instead the design of studies in open ocean conditions that would allow a more realistic presentation of the stimuli. Additionally, Southall (2021) recommended the deployment of acoustic recorders at various distances from the exposed animals rather than the use of speakers closely placed to them to better capture the far-field propagation of the signals.

6.2 PTS framework

The presented model is a useful and valuable framework for estimating PTS impact ranges. The framework allows the user to test a list of scenarios which may vary by how the soundscape is modelled (by changing the source level and transmission loss as well as the frequency of piling), by how animals react to piling (by changing the fleeing speed), and by the assumed distance threshold at which sound becomes non-impulsive. The framework also allows for an easy simultaneous testing of multiple scenarios.

Overall, the results of this study highlight that the assumptions assessed in EIAs may result in substantial overestimation of PTS ranges. Often in EIAs this is highlighted as a caveat to the predicted impact ranges. However, consent must be considered on the basis of the maximum design envelope (which considers a realistic worst case to maximise flexibility in construction if consent is awarded). As wind farm foundations (e.g., pile diameter) and installation techniques (e.g. greater hammer energy) develop further, there is the potential for impact ranges to increase. As such, it is critical that researchers, engineers, regulators, and advisors proactively engage on this topic to find a path forward.

In the absence of progression in this topic, then the likely endpoint is for noise abatement approaches to be mandatory to help reduce levels close to the source. Noise abatement potentially represents a substantial investment decision for developers (and potential slowing of offshore wind expansion due to supply chain limitations associated with noise abatement). As such, it is important that design envelopes and the presentation and review of noise impact assessments appropriately consider the conservatisms highlighted in this study (and the potential to demonstrate further overestimation of impact described below), as this is critical to the industry and to help progression towards Net Zero objectives. The findings and recommendations of this report could be considered further to improve impact assessments. Engagement among relevant stakeholders can help establish a sustainable path forward.

Currently, impacts are assessed based on a worst case scenario without any assessment of how likely the worst case is to be realised. Increasingly, the use of noise abatement is being discussed to mitigate the risk of cumulative SEL_{cum} PTS impacts on marine mammals. Understanding the potential conservatisms in these SEL_{cum} PTS assessments is a critical and pressing need to help proportionality in assessments and discussions.

The modelled scenarios presented focused on one of the variables that has the potential to be controlled during the installation of piles – the temporal pattern of hammer blows. Varying this parameter had a marked effect on the resulting PTS impact ranges and areas (with three quarters of scenarios showing a reduction of impact >57%, compared to a simulated EIA baseline).

Given the number of offshore foundations that have been installed to date around Europe – it would be pertinent to broaden the assessment of piling schedules across the industry to ensure that the true range of piling hammer logs is captured. This can help improve our understanding of how precautionary the design envelope is, and how this could be refined. Specifically, this means for each piling log, the impact range of the 'as built' foundations could be compared to the realistic worst case design envelope approach used in the impact assessment in the consent application.

The PTS framework currently assumes the animal is experiencing the loudest exposure at a given range (approximately equivalent to being in the loudest part of the water column), which is a further conservatism. It could be possible to further refine this by considering animal dive behaviour if known from studies using animal-borne dive-depth recording tags. However, it is important to balance the tradeoffs of computation time and these conservatisms, especially given the large reductions from ranges using the design envelope approach demonstrated here. Similarly, the PTS framework currently involves animals fleeing continuously in one direction away from the piling location, after the first strike. This could be amended in future iterations of the framework by implementing more complex movement patterns or changes in swim speed within a given simulation. Lastly, the framework uses a constant source level as an input parameter, which comes with a high level of conservatism. This parameter would therefore not capture the variations in source level during phases such as the soft start, when hammer energies are expected to be lower than during the rest of the installation. The inclusion of hammer energy as an input parameter into the framework would allow the source level to be corrected, for instance, by using energy-transfer methods (Wood et al. 2023).

Further discussion on PTS assessments and their implications is needed between developers and their engineers, and with the engagement of regulators and their advisors. It is important that developers consider the consequences of decision in formulating the design envelope for the project (e.g., the potential for noise abatement to be a condition, coupled with the associated costs of implementing such solutions) and that developers have the information available to help assess the likelihood of impacts (and not only the worst case to consider). It is also important for the scientific community to understand the decision-making process related to the temporal patterns of pile strikes and whether they can be adapted to reduce PTS impact ranges. This likely requires a facilitated discussion to help better understand perspectives and to allow for improved processes to help conservation, management, and investment decisions.

The framework developed here could be used to help design installation blow patterns to help mitigate impacts at the design or pre-consent stage. Additionally, the tool can be further developed to address some of its inherent conservatisms. The ways in which this could be done are described further below.

6.2.1 Framework expansion

Although this tool was not designed to match the noise modelling software currently used to estimate PTS impact ranges, it could be adapted to better capture the complexity of sound propagation and make it more comparable to such software. A valuable assessment would involve modelling the same scenario with this framework and a noise modelling tool (e.g., the Inspire Light model), so that impact ranges could be compared.

Currently, the framework assumes a constant 'source level' during a simulation (a value of 220 dB re 1 µPa at 1m was used here, aligned with current EIA assumptions). Using a constant source level is

unrealistic as piles are typically installed with some form of soft start or ramp-up in which hammer energies start well below the maximum energy and gradually increase (up to the required maximum hammer energy to allow the pile to be safely installed). This ramp-up of energy is likely to correlate strongly with the source level increasing though this needs to be carefully considered (see Verfuss et al. 2023).

Previous studies have investigated the energy transfer from the hammer and into the pile during impact pile driving and proposed means of calculating the sound pressure level at the location of the pile (Wood et al. 2023). Moreover, the hammer logs generated during impact pile driving installations record the hammer energy of each hammer strike. Utilising the outputs of the ReCON project (Verfuss et al. 2023) could be helpful to validate and improve estimates of sound pressure level close to the piling site, and therefore improve the predictions of this framework. Additionally, more complex sound propagation models could be integrated into the framework to better predict the intensity of the sound waves at various points in the water column.

The speed at which animals are assumed to flee away from the source had a marked effect on estimated PTS ranges. For instance, in EIA applications for English waters, all HF and VHF cetaceans were assumed to start moving away at a swim speed of 1.5 m/s once the piling had started (based on reported sustained swimming speeds for harbour porpoises, Otani et al. (2000)). Low frequency cetaceans like minke whales are assumed to swim at a speed of 3.25 m/s (Blix and Folkow 1995). In this study, we tested swim speed values of between 0.2 and 5 m/s to allow for different speed over ground for cases in which animals do not move away from the source in a straight line. For many species of marine mammal there is limited information to inform fleeing speeds over ground in response to pile driving and for how long they can sustain fleeing speeds. Determining this requires controlled exposure experiments to be carried out, likely involving fitting animals with movement tags close in time and space to pile driving to better understand this sensitive parameter. This is a gap that requires further information if there is concern about assumed fleeing speeds. The best approach to plug these gaps is via controlled or observational behavioural response studies (Harris and Thomas 2015).

The potential for the auditory system to recover in between pile strikes must also be considered. During the most intensive periods of pile driving, pile strikes are typically separated by 1-2 seconds. This can result in a lower overall threshold shift, compared to a continuous exposure at the same SEL. Kastelein et al. (2013, 2014, 2015) have highlighted in various species (including harbour seals, California sea lions and harbour porpoises) that the equal energy hypothesis assumption behind the SEL_{cum} threshold is violated. This means models will likely overestimate the level of threshold shift experienced from intermittent noise exposures, like those from pile driving. Pile strikes are relatively short signals; the signal duration of monopile pile strikes may range between 0.1 seconds (De Jong and Ainslie 2008) and approximately 0.3 seconds (Dähne et al. 2017) measured at a distance of 3.3 km to 3.6 km. Duration will however increase with increasing distance from the pile site. Together, this means that there is significant potential for animals to experience a lower threshold shift than predicted under the worst case assumptions in an EIA. For example, harbour porpoise exposed to sonar with a 25% duty cycle (i.e., 25% of the exposure duration contained sound) experienced a reduction in threshold shift of 5.5 - 8.3 dB compared to a continuous sound (Kastelein et al. 2014). The inclusion of a 1-second silent period in between pulses resulted in a 3 to 5 dB lower threshold shift compared to those generated following exposure to an equivalent continuous sound source.

Given pile strike durations of 0.1-0.3 seconds and maximum blow rates of 32 – 36 blows per minute (i.e., blows separated by 1.7-1.8 seconds) this equates to a duty cycle of approximately 5-15% - which would likely lead to animals experiencing smaller threshold shifts than those present above (where duty cycle = 25%). This could be explored formally within the framework with further development.

6.3 Caveats and assumptions

It is important to highlight the assumptions and potential caveats to the results of this study. Whilst we have used the best available information and well-established thresholds and approaches, it is important to highlight there are no empirical data on the threshold for auditory injury in the form of PTS onset for marine mammals. PTS onset thresholds have been estimated based on extrapolating from measured TTS onset thresholds on the assumption that PTS occurs from exposures that generated a TTS of 40 dB (measured approximately four minutes after exposure (NMFS 2018)).

It is important to highlight that not all animals would be predicted to experience a temporary threshold shift at the onset level. That is, fixed thresholds are highly unlikely to exist in biology or ecology (i.e. that all animals respond above a threshold and all animals do not respond below the same threshold). This means that a probabilistic relationship is more appropriate (though as yet challenging to derive for PTS). However, some studies have explored this. For example, using the SAFESIMM (Statistical Algorithms For Estimating the Sonar Influence on Marine Megafauna) model and data from Finneran et al. (2005), Donovan et al. (2017) estimated a probability of 0.18-0.19 of TTS occurring at the onset level (i.e., if 100 animals were exposed to sounds loud enough to exceed the onset level, 18-19 would be likely to experience a temporary threshold shift). Therefore, when using PTS onset ranges it is reasonable to assume that not all individuals within that range will experience PTS. This means estimates of animals predicted to be within PTS onset ranges are likely to be precautionary because they assume all animals are impacted. Of course, this potential conservatism must be balanced against the state of knowledge regarding the level of threshold shift that generated permanent damage and the different regulatory contexts in which this is applied.

7 Summary and recommendations

This study used empirical data from foundation installations at 11 offshore wind farms to assess the changes in impulsive characteristics of sounds produced during impact pile driving. Four metrics of impulsiveness were assessed in terms of changes with increasing distance from the piling location and all four metrics showed a decrease in impulsiveness as sounds travel further away from the sound source. Although there is still insufficient evidence to establish a range of distances from which these sounds are no longer impulsive, a marked decline in each metric was noted within the first five kilometres from the sound source. Underwater noise modelling approaches for EIAs should continue to assume that sounds produced during impact pile driving keep their impulsive characteristics irrespective of distance, but further studies should be carried out to investigate the effects of partially impulsive sounds on hearing in order to improve the assessment of the hazardous nature of these signals.

This study also highlighted that other factors may play a role in determining the size of PTS impact areas for marine mammals. Assuming that animals flee the pile driving site, the speed at which these

animals move may lead to lower estimated impact ranges. However, it is essential to understand the variations in speed and direction of the exposed animals during activities such as impact pile driving. Other factors like the time between subsequent pile strikes could be addressed by developers and engineers to achieve smaller PTS impact ranges and allow the hearing of animals to recover in between pile strikes.

Recommendations - Summary

- Threshold shift playback experiments to known sounds with known impulsiveness characteristics to better understand the impulsiveness points at which sounds become less damaging to the auditory system.
- Further development of the framework to address potential conservatisms within the current formation (e.g., ramp-up, recovery between blows) to better understand PTS risks.
- Census of real world hammer logs (as constructed) and comparison to EIA assumptions (design envelope) to understand how often worst case assumptions are realised.
- Swim speed is important to better understand. A complete review or dedicated behavioural response studies would be needed to support this.
- Use framework to explicitly design hammer logs that can minimize impact ranges and coordinate with engineers to ensure feasibility.
- Facilitated engagement between engineers, regulatory advisors, acousticians, and marine mammal specialists to develop solutions to streamline EIA processes.
- Carry out studies of swim speeds of animals relative to pile driving activities.

8 References

Ahroon, W. A., R. P. Hamernik, and R. I. Davis. 1993. Complex noise exposures: An energy analysis. The Journal of the Acoustical Society of America **93**:997-1006.

Amaral, J. L., J. H. Miller, G. R. Potty, K. J. Vigness-Raposa, A. S. Frankel, Y.-T. Lin, A. E. Newhall, D. R. Wilkes, and A. N. Gavrilov. 2020. Characterization of impact pile driving signals during installation of offshore wind turbine foundations. The Journal of the Acoustical Society of America **147**:2323-2333.

Bellmann, M. A., J. Brinkmann, A. May, T. Wendt, S. Gerlach, and P. Remmers. 2020. Underwater noise during the impulse pile-driving procedure: Influencing factors on pile-driving noise and technical possibilities to comply with noise mitigation values. 10036866, Federal Ministry for the Environment, Nature Conservation and Nuclear Safety (Bundesministerium für Umwelt, Naturschutz und nukleare Sicherheit (BMU)).

Blix, A., and L. Folkow. 1995. Daily energy expenditure in free living minke whales. Acta Physiologica Scandinavica **153**:61-66.

BSH. 2011. Offshore wind farms: Measuring instruction for underwater sound monitoring. Federal Maritime and Hydrographic Agency (BSH).

Canlon, B. 1988. The effect of acoustic trauma on the tectorial membrane, stereocilia, and hearing sensitivity: possible mechanisms underlying damage, recovery, and protection. Scand Audiol Suppl **27**:1-45.

Dähne, M., J. Tougaard, J. Carstensen, A. Rose, and J. Nabe-Nielsen. 2017. Bubble curtains attenuate noise from offshore wind farm construction and reduce temporary habitat loss for harbour porpoises. Marine Ecology Progress Series **580**:221-237.

De Jong, C. A. f., and M. A. Ainslie. 2008. Underwater radiated noise due to the piling for the Q7 Offshore Wind Park. Journal of the Acoustical Society of America **123**:2987.

De Jong, C. A. F., M. A. Ainslie, and G. Blacquiere. 2011. Standard for measurement and monitoring of underwater noise, Part II: procedures for measuring underwater noise in connection with offshore wind farm licensing. Den Haag, The Netherlands.

DIN 45641. 1990. Akustik, NA: Lärmminderung und Schwingungstechnik (NALS) im DIN und VDI: DIN 45641, Mittelung von Schallpegeln. Norm, DIN Deutsches Institut Für Normung e. V., Berlin.

Donovan, C. R., C. M. Harris, L. Milazzo, J. Harwood, L. Marshall, and R. Williams. 2017. A simulation approach to assessing environmental risk of sound exposure to marine mammals. Ecology and Evolution.

Dunn, D. E., R. R. Davis, C. J. Merry, and J. R. Franks. 1991. Hearing loss in the chinchilla from impact and continuous noise exposure. The Journal of the Acoustical Society of America **90**:1979-1985.

Dunn, P. K. 2022. Tweedie: Evaluation of Tweedie exponential family models. R package version 2.3.

Erdreich, J. 1986. A distribution based definition of impulse noise. The Journal of the Acoustical Society of America **79**:990-998.

Finneran, J. J. 2015. Noise-induced hearing loss in marine mammals: A review of temporary threshold shift studies from 1996 to 2015. The Journal of the Acoustical Society of America **138**:1702-1726.

Finneran, J. J., D. A. Carder, C. E. Schlundt, and R. L. Dear. 2010. Temporary threshold shift in a bottlenose dolphin (*Tursiops truncatus*) exposed to intermittent tones. Journal of the Acoustical Society of America **127**:3267-3272.

Finneran, J. J., D. A. Carder, C. E. Schlundt, and S. H. Ridgway. 2005. Temporary threshold shift in bottlenose dolphins (Tursiops truncatus) exposed to mid-frequency tones. The Journal of the Acoustical Society of America **118**:2696-2705.

Finneran, J. J., R. Dear, D. A. Carder, and S. H. Ridgway. 2003. Auditory and behavioral responses of California sea lions (Zalophus californianus) to single underwater impulses from an arc-gap transducer. The Journal of the Acoustical Society of America **114**:1667-1677.

Finneran, J. J., K. Lally, M. G. Strahan, K. Donohoe, J. Mulsow, and D. S. Houser. 2023. Dolphin conditioned hearing attenuation in response to repetitive tones with increasing level. The Journal of the Acoustical Society of America **153**:496-504.

Finneran, J. J., C. E. Schlundt, B. K. Branstetter, J. S. Trickey, V. Bowman, and K. Jenkins. 2015. Effects of multiple impulses from a seismic air gun on bottlenose dolphin hearing and behavior. The Journal of the Acoustical Society of America **137**:1634-1646.

Finneran, J. J., C. E. Schlundt, D. A. Carder, J. A. Clark, J. A. Young, J. B. Gaspin, and S. H. Ridgway. 2000. Auditory and behavioral responses of bottlenose dolphins (Tursiops truncatus) and a beluga whale (Delphinapterus leucas) to impulsive sounds resembling distant signatures of underwater explosions. The Journal of the Acoustical Society of America **108**:417-431.

Finneran, J. J., C. E. Schlundt, R. Dear, D. A. Carder, and S. H. Ridgway. 2002. Temporary shift in masked hearing thresholds in odontocetes after exposure to single underwater impulses from a seismic watergun. The Journal of the Acoustical Society of America **111**:2929-2940.

Forrest, T., G. Miller, and J. Zagar. 1993. Sound propagation in shallow water: Implications for acoustic communication by aquatic animals. Bioacoustics **4**:259-270.

Fox, J., and S. Weisberg. 2019. An R companion to applied regression. Third Edition. Thousand Oaks CA: Sage. URL: https://socialsciences.mcmaster.ca/jfox/Books/Companion/.

Gao, W.-y., D.-l. Ding, X.-y. Zheng, F.-m. Ruan, and Y.-j. Liu. 1992. A comparison of changes in the stereocilia between temporary and permanent hearing losses in acoustic trauma. Hearing Research **62**:27-41.

Goley, G. S., W. J. Song, and J. H. Kim. 2011. Kurtosis corrected sound pressure level as a noise metric for risk assessment of occupational noises. The Journal of the Acoustical Society of America **129**:1475-1481.

Grimm, V., U. Berger, F. Bastiansen, S. Eliassen, V. Ginot, J. Giske, J. Goss-Custard, T. Grand, S. K. Heinz, G. Huse, A. Huth, J. U. Jepsen, C. Jorgensen, W. M. Mooij, B. Muller, G. Pe'er, C. Piou, S. F. Railsback, A. M. Robbins, M. M. Robbins, E. Rossmanith, N. Ruger, E. Strand, S. Souissi, R. A. Stilmann, R. Vabo, U. Visser, and D. L. DeAngelis. 2006. A standard protocol for describing individual-based and agent- based models. Pages 115-126 Ecological Modelling.

Grimm, V., U. Berger, D. L. DeAngelis, G. Polhill, J. Giske, and S. F. Railsback. 2010. The ODD protocol: A review and first update. Pages 2760-2768 Ecological Modelling.

Guan, S., T. Brookens, and R. Miner. 2022. Kurtosis analysis of sounds from down-the-hole pile installation and the implications for marine mammal auditory impairment. JASA Express Letters **2**:071201.

Hamernik, R. P., W. A. Ahroon, K. D. Hsueh, S. F. Lei, and R. I. Davis. 1993. Audiometric and histological differences between the effects of continuous and impulsive noise exposures. The Journal of the Acoustical Society of America **93**:2088-2095.

Hamernik, R. P., and D. Henderson. 1976. The potentiation of noise by other ototraumatic agents. Effects of Noise on Hearing, D. Henderson, R. Hamernik, D. Dosanj, and JH Mills, Eds., Raven Press, New York:291-307.

Hamernik, R. P., and W. Qiu. 2001. Energy-independent factors influencing noise-induced hearing loss in the chinchilla model. The Journal of the Acoustical Society of America **110**:3163-3168.

Hamernik, R. P., W. Qiu, and B. Davis. 2003. The effects of the amplitude distribution of equal energy exposures on noise-induced hearing loss: The kurtosis metric. The Journal of the Acoustical Society of America **114**:386-395.

Hamernik, R. P., W. Qiu, and B. Davis. 2007. Hearing loss from interrupted, intermittent, and time varying non-Gaussian noise exposure: The applicability of the equal energy hypothesis. The Journal of the Acoustical Society of America **122**:2245-2254.

Hamernik, R. P., G. Turrentine, M. Roberto, R. Salvi, and D. Henderson. 1984. Anatomical correlates of impulse noise-induced mechanical damage in the cochlea. Hear Res **13**:229-247.

Harris, C. M. 1998. Handbook of Acoustical Measurements and Noise Control. Acoustical Society of America, Huntington, NY.

Harris, C. M., and L. Thomas. 2015. Status and future of research on the behavioural responses of marine mammals to US Navy sonar.

Hastie, G., N. D. Merchant, T. Götz, D. J. Russell, P. Thompson, and V. M. Janik. 2019. Effects of impulsive noise on marine mammals: investigating range-dependent risk. Ecological Applications **29**:e01906.

Heinrich, U.-R., and R. Feltens. 2006. Mechanisms underlying noise-induced hearing loss. Drug Discovery Today: Disease Mechanisms **3**:131-135.

Henderson, D., and R. P. Hamernik. 1986. Impulse noise: Critical review. The Journal of the Acoustical Society of America **80**:569-584.

Henderson, D., and R. P. Hamernik. 2012. The Use of Kurtosis Measurement in the Assessment of Potential Noise Trauma. Pages 41-55 *in* C. G. Le Prell, D. Henderson, R. R. Fay, and A. N. Popper, editors. Noise-Induced Hearing Loss: Scientific Advances. Springer New York, New York, NY.

Hu, B. H., D. Henderson, and T. M. Nicotera. 2006. Extremely rapid induction of outer hair cell apoptosis in the chinchilla cochlea following exposure to impulse noise. Hearing Research **211**:16-25.

ISO. 2017a. ISO 18405 Underwater Acoustics—Terminology. International Organization for Standardization Geneva.

ISO. 2017b. ISO 18406:2017 Underwater Acoustics—Measurement of radiated underwater sound from percussive pile driving. International Organization for Standardization Geneva.

Kastak, D., M. Holt, C. Kastak, B. Southall, J. Mulsow, and R. Schusterman. 2005. A voluntary mechanism of protection from airborne noise in a harbor seal. Page 148 *in* 16th Biennial Conference on the Biology of Marine Mammals. San Diego CA.

Kastelein, R. A., R. Gransier, J. Schop, and L. Hoek. 2015. Effects of exposure to intermittent and continuous 6–7 kHz sonar sweeps on harbor porpoise (Phocoena phocoena) hearing. The Journal of the Acoustical Society of America **137**:1623-1633.

Kastelein, R. A., L. Helder-Hoek, J. Covi, and R. Gransier. 2016. Pile driving playback sounds and temporary threshold shift in harbor porpoises (Phocoena phocoena): Effect of exposure duration. The Journal of the Acoustical Society of America **139**:2842-2851.

Kastelein, R. A., L. Helder-Hoek, S. Van de Voorde, A. M. von Benda-Beckmann, F.-P. A. Lam, E. Jansen, C. A. de Jong, and M. A. Ainslie. 2017. Temporary hearing threshold shift in a harbor porpoise (*Phocoena phocoena*) after exposure to multiple airgun sounds. The Journal of the Acoustical Society of America **142**:2430-2442.

Kastelein, R. A., L. Hoek, R. Gransier, and N. Jennings. 2013. Hearing thresholds of two harbor seals (Phoca vitulina) for playbacks of multiple pile driving strike sounds. Journal of the Acoustical Society of America **134**:2307-2312.

Kastelein, R. A., L. Hoek, R. Gransier, M. Rambags, and N. Claeys. 2014. Effect of level, duration, and inter-pulse interval of 1-2 kHz sonar signal exposures on harbor porpoise hearing. The Journal of the Acoustical Society of America **136**:412-422.

Ketten, D. 2004a. Marine mammal auditory systems: A summary of audiometric and anatomical data and implications for underwater acoustic impacts. Polarforschung **72**:79-92.

Ketten, D. R. 1995. Estimates of blast injury and acoustic trauma zones for marine mammals from underwater explosions. Sensory systems of aquatic mammals:391-407.

Ketten, D. R. 2004b. Experimental measures of blast and acoustic trauma in marine mammals. WOODS HOLE OCEANOGRAPHIC INST MA BIOLOGY DEPT.

Ketten, D. R., J. A. Simmons, H. Riquimaroux, and A. M. Simmons. 2021. Functional Analyses of Peripheral Auditory System Adaptations for Echolocation in Air vs. Water. Frontiers in Ecology and Evolution **9**.

Koschinski, S., and K. Lüdemann. 2013. Development of Noise Mitigation Measures in Offshore Wind Farm Construction 2013.

Lei, S. F., W. A. Ahroon, and R. P. Hamernik. 1994. The application of frequency and time domain kurtosis to the assessment of hazardous noise exposures. The Journal of the Acoustical Society of America **95**:3005-3005.

Liberman, M. C. 1987. Chronic ultrastructural changes in acoustic trauma: Serial-section reconstruction of stereocilia and cuticular plates. Hearing Research **26**:65-88.

Liberman, M. C., and S. G. Kujawa. 2017. Cochlear synaptopathy in acquired sensorineural hearing loss: Manifestations and mechanisms. Hearing Research **349**:138-147.

Lucke, K., U. Siebert, P. A. Lepper, and M.-A. Blanchet. 2009. Temporary shift in masked hearing thresholds in a harbor porpoise (Phocoena phocoena) after exposure to seismic airgun stimuli. The Journal of the Acoustical Society of America **125**:4060-4070.

Martin, B., K. Lucke, and D. Barclay. 2020. Techniques for distinguishing between impulsive and non-impulsive sound in the context of regulating sound exposure for marine mammals. The Journal of the Acoustical Society of America **147**:2159-2176.

Mooney, T. A., P. E. Nachtigall, M. Breese, S. Vlachos, and W. W. L. Au. 2009. Predicting temporary threshold shifts in a bottlenose dolphin (Tursiops truncatus): The effects of noise level and duration. The Journal of the Acoustical Society of America **125**:1816-1826.

Müller, R. A. J., A. M. v. Benda-Beckmann, M. B. Halvorsen, and M. A. Ainslie. 2020. Application of kurtosis to underwater sound. The Journal of the Acoustical Society of America **148**:780-792.

Nachtigall, P. E., A. Y. Supin, A. F. Pacini, and R. A. Kastelein. 2018. Four odontocete species change hearing levels when warned of impending loud sound. Integrative Zoology **13**:160-165.

National Marine Fisheries Service. 2018. Revisions to: Technical Guidance for Assessing the Effects of Anthropogenic Sound on Marine Mammal Hearing (Version 2.0): Underwater Thresholds for Onset of Permanent and Temporary Threshold Shifts. Page 167. U.S. Department of Commerce, NOAA, Silver Spring.

NMFS. 2018. Revisions to: Technical Guidance for Assessing the Effects of Anthropogenic Sound on Marine Mammal Hearing (Version 2.0): Underwater Thresholds for Onset of Permanent and Temporary Threshold Shifts. Page 167. U.S. Department of Commerce, NOAA, Silver Spring.

Nordmann, A. S., B. A. Bohne, and G. W. Harding. 2000. Histopathological differences between temporary and permanent threshold shift11A portion of this study formed the basis of a pre-doctoral M.A. thesis in Biological Sciences, Washington University School of Medicine (A.S.N.). This study was presented in part at the 22nd Midwinter Research Meeting of the Association for Research in Otolaryngology, February 1999. Hearing Research **139**:13-30.

Otani, S., Y. Naito, A. Kato, and A. Kawamura. 2000. Diving behavior and swimming speed of a free-ranging harbor porpoise, *Phocoena phocoena*. Marine Mammal Science **16**:811-814.

Patterson, J. H., and R. P. Hamernik. 1997. Blast overpressure induced structural and functional changes in the auditory system. Toxicology **121**:29-40.

Pekkarinen, J., and J. Starck. 1983. Impulse noise in a shipyard. Pages 15-16 *in* Proceedings of the 11th International Congress on Acoustics.

Popper, A., A. Hawkins, R. Fay, D. Mann, S. Bartol, T. Carlson, S. Coombs, W. Ellison, R. Gentry, and M. Halvorsen. 2014. Sound exposure guidelines for fishes and sea turtles. Springer Briefs in Oceanography. DOI **10**:978-973.

Price, G. R. 1983. Relative hazard of weapons impulses. The Journal of the Acoustical Society of America **73**:556-566.

Reichmuth, C., A. Ghoul, J. M. Sills, A. Rouse, and B. L. Southall. 2016. Low-frequency temporary threshold shift not observed in spotted or ringed seals exposed to single air gun impulses. The Journal of the Acoustical Society of America **140**:2646-2658.

Roberto, M., R. P. Hamernik, and G. A. Turrentine. 1989. Damage of the Auditory System Associated with Acute Blast Trauma. Annals of Otology, Rhinology & Laryngology **98**:23-34.

Robinson, S. P., P. A. Lepper, and R. A. Hazelwood. 2014. Good Practice Guide for Underwater Noise Measurement.

Robinson, S. P., L. Wang, S.-H. Cheong, P. A. Lepper, J. P. Hartley, P. M. Thompson, E. Edwards, and M. Bellmann. 2022. Acoustic characterisation of unexploded ordnance disposal in the North Sea using high order detonations. Marine Pollution Bulletin **184**:114178.

Rosowski, J. J., P. J. Davis, K. M. Donahue, S. N. Merchant, and M. D. Coltrera. 1990. Cadaver Middle Ears as Models for Living Ears: Comparisons of Middle Ear Input Immittance. Annals of Otology, Rhinology & Laryngology **99**:403-412.

Ryan, A. F., S. G. Kujawa, T. Hammill, C. Le Prell, and J. Kil. 2016. Temporary and Permanent Noise-induced Threshold Shifts: A Review of Basic and Clinical Observations. Otology & Neurotology **37**:e271-e275.

Scott-Hayward, L., C. S. Oedekoven, M. L. Mackenzie, C. Walker, and E. Rexstad. 2017. MRSea package (version 1.0-beta): Statistical Modelling of bird and cetacean distributions in offshore renewables development areas. Retrieved from http://creem2.st-and.ac.uk/software.aspx.

Scott-Hayward, L., C. Walker, and M. Mackenzie. 2021. Vignette for the MRSea Package v1.3: Statistical Modelling bird and cetacean distributions in offshore renewables development areas." University of St. Andrews. Centre for Research into ecological and Environmental Modelling, <https://github.com/lindesaysh/MRSea/tree/master/vignettes>.

Sills, J. M., B. Ruscher, R. Nichols, B. L. Southall, and C. Reichmuth. 2020. Evaluating temporary threshold shift onset levels for impulsive noise in seals. The Journal of the Acoustical Society of America **148**:2973-2986.

Southall, B., J. J. Finneran, C. Reichmuth, P. E. Nachtigall, D. R. Ketten, A. E. Bowles, W. T. Ellison, D. Nowacek, and P. Tyack. 2019. Marine Mammal Noise Exposure Criteria: Updated Scientific Recommendations for Residual Hearing Effects. Aquatic Mammals **45**:125-232.

Southall, B. L. 2021. Evolutions in Marine Mammal Noise Exposure Criteria. Acoust. Today **17**:52-60.

Southall, B. L., A. E. Bowles, W. T. Ellison, J. J. Finneran, R. L. Gentry, C. R. Greene, D. Kastak, D. R. Ketten, J. H. Miller, P. E. Nachtigall, W. J. Richardson, J. A. Thomas, and P. L. Tyack. 2007. MARINE MAMMAL NOISE-EXPOSURE CRITERIA: INITIAL SCIENTIFIC RECOMMENDATIONS. Bioacoustics **17**:273-275.

Starck, J., and J. Pekkarinen. 1987. Industrial impulse noise: Crest factor as an additional parameter in exposure measurements. Applied Acoustics **20**:263-274.

Urick, R. J. 1983. Principles of underwater sound, 3rd ed. Peninsula Publishing, Los Altos.

Verfuss, U., P. Remmers, M. Ryder, K. Palmer, J. Wood, and M. Bellmann. 2023. Reducing uncertainty in underwater noise assessments (ReCon). Offshore Renewables Joint Industry Programme.

von Benda-Beckmann, A. M., G. Aarts, H. Ö. Sertlek, K. Lucke, W. C. Verboom, R. A. Kastelein, D. R. Ketten, R. van Bemmelen, F.-P. A. Lam, and R. J. Kirkwood. 2015. Assessing the impact of underwater clearance of unexploded ordnance on harbour porpoises (*Phocoena phocoena*) in the southern North Sea. Aquatic Mammals **41**:503.

von Benda-Beckmann, A. M., D. R. Ketten, F. P. A. Lam, C. A. F. de Jong, R. A. J. Müller, and R. A. Kastelein. 2022. Evaluation of kurtosis-corrected sound exposure level as a metric for predicting onset of hearing threshold shifts in harbor porpoises (Phocoena phocoena). The Journal of the Acoustical Society of America **152**:295-301.

Walker, C., M. Mackenzie, C. Donovan, and M. O'Sullivan. 2011. SALSA–a spatially adaptive local smoothing algorithm. Journal of Statistical Computation and Simulation **81**:179-191.

Ward, W. D., E. M. Cushing, and E. M. Burns. 1976. Effective quiet and moderate TTS: Implications for noise exposure standards. The Journal of the Acoustical Society of America **59**:160-165.

Wilson, R. J., D. C. Speirs, A. Sabatino, and M. R. Heath. 2018. A synthetic map of the north-west European Shelf sedimentary environment for applications in marine science. Earth System Science Data **10**:109-130.

Wood, M., M. Ainslie, and R. Burns. 2023. Energy Conversion Factors in Underwater Radiated Sound from Marine Piling. Review of the method and recommendations. JASCO Applied Sciences (UK) Ltd.

Xie, H.-w., W. Qiu, N. J. Heyer, M.-b. Zhang, P. Zhang, Y.-m. Zhao, and R. P. Hamernik. 2016. The Use of the Kurtosis-Adjusted Cumulative Noise Exposure Metric in Evaluating the Hearing Loss Risk for Complex Noise. Ear and Hearing **37**:312-323.

Yamamura, K., K. Aoshima, S. Hiramatsu, T. Hikichi, and S. Hiramatsu. 1980. An investigation of the effects of impulse noise exposure on man: impulse noise with a relatively low peak level. European Journal of Applied Physiology and Occupational Physiology **43**:135-142.

Zhao, Y.-m., W. Qiu, L. Zeng, S.-s. Chen, X.-r. Cheng, R. I. Davis, and R. P. Hamernik. 2010. Application of the Kurtosis Statistic to the Evaluation of the Risk of Hearing Loss in Workers Exposed to High-Level Complex Noise. Ear and Hearing **31**:527-532.

9 Appendix 1 – Outcomes of literature review

9.1 Objective

This literature review aimed to evaluate the current understanding of the mechanism of noise induced hearing loss at the mammalian ear, with focus on the impulsiveness of noise, and the potential to transfer the knowledge obtained from studies on terrestrial mammals, to marine mammals. Furthermore, this review aims to assess the available metrics of impulsiveness, and how the characteristics of impulsive sounds change with increasing distance from the source.

9.2 Methods

The research papers presented in the proposal were reviewed alongside additional studies from scientific journals such as *The Journal of the Acoustical Society of America, Ear and Hearing, Hearing research*, and *Noise and Health*. Additional literature sources were provided by Dr. Dorian Houser (Director of Conservation and Biological Research at the National Marine Mammal Foundation), Dr. Colleen Reichmuth (Physical & Biological research scientist at the Institute of Marine Sciences, Santa Cruz), and Dr. Darlene Ketten (Senior research scientist at the Biomedical Engineering, Hearing Research Center, Boston University).

9.3 Results

A total of 77 scientific papers and reports were included in the repository, with each literature source categorised based on their main topic and presented in Table 10. Overall, there were more studies

which investigated the effects of impulsive sounds on hearing that used terrestrial mammals as subjects (n = 26) compared to marine mammals (n = 15).

Table 10. Number of scientific papers reviewed for the RaDIN project work package 1 split by category. Two papers were included in two different sections, thus resulting in a total of 77 papers.

Topic	Number of papers	Marine/terrestrial
Definition of impulsiveness	8	
Changes in acoustic properties of impulses with range	5	Marine (5)
Effects on impulses on the mammalian ear	41	Marine (15), terrestrial (26)
Effects on blast waves on the mammalian ear	5	Marine (3), terrestrial (2)
Mechanism of hearing loss	12	Marine (1), terrestrial (11)
Transferability of observations from terrestrial mammals to marine mammals	8	

9.3.1 Definitions of impulsiveness

Impulsive sounds can be broadly characterised as brief, transient signals with a rapid rise time from onset to peak sound pressure level (Southall et al. 2007). These signals often cover a broad frequency range (i.e., up to several hundreds of kilohertz in the case with explosions (Robinson et al. 2022)) as a result of the rapid rise time, which leads to greater energy content into the high frequency portion of the spectrum due to the presence of short wavelength components (Henderson and Hamernik 1986). The degree of impulsiveness has been described by metrics such as **kurtosis** (Erdreich 1986), **crest factor** (Pekkarinen and Starck 1983), and the **Harris impulse factor** (Harris 1998), which are defined in Table 1. For instance, a kurtosis value of 40 has been used to describe “fully-impulsive” signals (Hamernik et al. 2007) whereas (Pekkarinen and Starck 1983) suggested that a signal should be considered impulsive if it has an A-weighted crest factor greater than 15 decibels. The Harris impulse factor has been proposed as a metric to indicate the presence of an impulse when there is a difference greater than 3 decibels between the received level using impulse versus the equivalent continuous time constant (Southall et al. 2007).

9.3.2 Characterisation of impulses at various distances from the source

As sound travels further away from the source, its energy is dissipated and gets absorbed by the surrounding particles. This absorption effect impacts higher frequencies to a greater extent than lower frequencies (Urick 1983), thus altering the characteristics of a broadband signal as it propagates away from the sound source (Hastie et al. 2019). Moreover, when transient sounds like impulses are received at long distances from the source, their temporal characteristics can be influenced by multi-path reflections, due to the added arrivals following reflections against the sea surface and sea floor (Martin

et al. 2020). Five studies were reviewed which investigated how the properties of impulsive signals change with range, and a summary of the results has been provided in Table 11.

Two of these five studies measured the acoustic properties of individual impact pile driving strikes and seismic airguns, and reported marked changes for several metrics, such as rise time, at various ranges from the source (Hastie et al. 2019, Amaral et al. 2020). For example, (Hastie et al. 2019) reported a marked decrease in the peak sound pressure level of a pulse approximately five kilometres away from the sound source and an increase in signal duration especially at distances greater than around 20 kilometres. The authors also observed a relatively poor relationship between crest factor and the distance from the sound source due to the high level of variation of this metric (Hastie et al. 2019). The crest factor represents the difference between the peak and average levels of a signal (Pekkarinen and Starck 1983), therefore one possible reason for the observed level of variation could be the complex multipath propagation of impulse reflections, which may have elevated the background noise levels around some of the analysed signals. Similarly, (Amaral et al. 2020) reported a decrease in peak sound pressure level at greater distances from impact piling activities, and an increase in pulse duration and rise time, indicating that the signals became less impulsive.

Two other studies used kurtosis as metric of impulsiveness to investigate the changes in acoustic properties of signals with range but computed this metric using a longer time window of analysis. Rather than taking measurements strictly from the periods containing single strikes (shorter than two seconds, as shown by (Hastie et al. 2019) and (Amaral et al. 2020)), (Guan et al. 2022) and Martin et al. (2020) used a 60-second analysis window to capture more of the variability present in the acoustic data. These studies also reported a decrease in the impulsiveness of sounds with increasing distance from the sound sources (Martin et al. 2020, Guan et al. 2022). For instance, (Guan et al. 2022) reported a decrease in kurtosis further away from down-the-hole pile driving and drilling, however there was a high degree of variation throughout the data, presumably due to complexity of the sounds produced during this activity. The pile installation technology discussed in this study is relatively new, and uses a combination of impact piling and rotating drilling to advance a pile into the sediment, thus generating complex sounds which include both impulsive and non-impulsive components (Guan et al. 2022).

Lastly, (Robinson et al. 2022) reported a decrease in peak sound pressure level and sound exposure level compared to those measured at close distances from unexploded ordnance disposals. This study also reported a decrease in the frequency bandwidth at distances greater than 10 kilometres from the source.

The above studies indicate a gradual change in the degree of impulsiveness of the analysed signals but (Hastie et al. 2019) showed that some of the metrics reach the non-impulsive threshold at variable distances from the source. This variability would be further complicated by external factors such as the seabed sediment type, sea state, and other variables that may influence how sounds propagate during construction activities. For these reasons, a single threshold may not be suitable for establishing when signals are no longer impulsive, whereas a transition or intermediary zone could be established instead to account for some of these uncertainties.

Table 11. Summary of metrics and analysis methodology from several studies which investigated the changes of acoustic properties of impulses with range.

Reference	Sound source	Acoustic metric analysis	Metrics of impulsiveness	Effects of range
Hastie et al. (2019)	Seismic air guns and impact pile driving	The characteristics of each signal were measured	Rise time Pulse duration Peak pressure Crest factor	Increase Increase Decrease No clear effect
Amaral et al. (2020)	Impact pile driving	The characteristics of each individual hammer strike were measured[5]	Rise time Decay time Pulse duration Kurtosis Sound received levels	Increase Increase Increase No clear effect Decrease
Martin et al. (2020)	Drilling, vessel noise, vibratory & impact piling, seismic airguns, naval sonar	The characteristics of each individual hammer strike were measured[6]	Kurtosis Crest factor Harris impulse factor	Decrease Decrease Decrease
Guan et al. (2022)	Down-the-hole pile driving and drilling	Metric computed using a 60-second time window	Kurtosis	Decrease
Robinson et al. (2022)	Unexploded ordnance disposal	Protocol from BEIS 2020, time window not mentioned	Peak sound pressure level Sound exposure level	Decrease Decrease

9.4 Knowledge available from studies involving terrestrial mammals

Hearing loss has been studied more closely in terrestrial mammals, compared to marine mammals, due to the possibility to expose larger numbers of terrestrial animals in controlled environments, and

[5] The kurtosis was calculated for each hammer strike using a one-second window that encompassed the peak in the signal. The window was defined as 0.1 s before to 0.9 s after the time of the peak.

[6] The kurtosis was calculated for each hammer strike using a one-second window that encompassed the peak in the signal. The window was defined as 0.1 s before to 0.9 s after the time of the peak.

assess the degree of acoustic trauma both physiologically and histologically. The main terrestrial mammal used in the reviewed studies was the chinchilla (Hamernik and Qiu 2001), although other terrestrial mammals such as cats (Price 1983), pigs and sheep (Roberto et al. 1989), and humans (Yamamura et al. 1980) have also been studied in noise exposure experiments and/or hearing loss assessments. Furthermore, the degree of impulsiveness of stimuli could also be artificially modified to investigate the effects of various types of impulses on hearing as outlined in (Hamernik et al. 2003, Hamernik et al. 2007). The studies of (Goley et al. 2011) and (Xie et al. 2016) also integrated corrections related to the degree of impulsiveness into energetic measurements, to predict the likelihood of hearing loss following exposures to complex or intermittent sounds.

Multiple studies concluded that in general, at comparable sound levels, impulsive or complex noise (consisting of a combination of continuous and impulsive noise) is more hazardous than continuous noise with respect to hearing damage (Hamernik and Henderson 1976, Henderson and Hamernik 1986, Dunn et al. 1991, Ahroon et al. 1993, Henderson and Hamernik 2012). Kurtosis is the primary metric of impulsiveness which has been implemented in hearing loss studies. This metric was used in 13 of the reviewed studies involving terrestrial mammals, which are summarised in Table 12. The use of signals with variable degrees of kurtosis, but the same energy and spectral content, provided valuable information about how this metric of impulsiveness relates to noise induced hearing loss. In chinchillas, exposure to impulsive signals with a higher degree of kurtosis has been shown to induce more hair cell loss than exposure to signals with a lower degree of kurtosis for a similar sound exposure. For human workers, chronic exposure to sound with a higher value of kurtosis was correlated with a higher prevalence of measured hearing loss.

Table 12. Overview of hearing loss studies involving terrestrial mammals which used kurtosis to measure impulsiveness.

Reference	Species	Metric	Outcome
Davis et al. (2012)	Humans	Kurtosis	Noise induced PTS increased with kurtosis
Goley et al. (2011)	Chinchillas	Kurtosis correction	Kurtosis correction improved correlation of noise measurements with PTS
Hamernik and Qiu (2001)	Chinchillas	Kurtosis	Greater outer hair cell loss following exposures with higher kurtosis values
Hamernik et al. (1993)	Chinchillas	Kurtosis	Exposures with higher kurtosis produced more PTS at the high frequencies
Hamernik et al. (2003)	Chinchillas	Kurtosis	PTS increased with kurtosis and reached an asymptote at a kurtosis value of ~40
Hamernik et al. (2007)	Chinchillas	Kurtosis	Increase in kurtosis at a fixed energy was accompanied by an increase in noise induced trauma
Lei et al. (1994)	Chinchillas	Kurtosis	Consistent positive relation between kurtosis and outer hair cell loss
Qiu et al. (2013)	Chinchillas	Kurtosis	Hearing trauma increased with increasing kurtosis
Xie et al. (2016)	Humans	Kurtosis correction	Kurtosis correction improved the correlation of cumulative noise exposure index with noise induced hearing loss
Xin et al. (2022)	Humans	Kurtosis correction	Likelihood of noise induced PTS increased with kurtosis
Zhang et al. (2021a)	Humans	Kurtosis	Increased likelihood of high frequency noise induced hearing loss for kurtosis ≥ 10
Zhang et al. (2021b)	Humans	Kurtosis	Noise induced PTS increased with kurtosis
Zhao et al. (2010)	Humans	Kurtosis correction	Higher prevalence of noise induced hearing loss following exposures to noise with higher kurtosis compared to continuous noise

The benefits of using kurtosis include the fact that this metric is sensitive to temporal characteristics of complex noise, and extensive data are available from exposures to stimuli with variable levels of kurtosis and associated degrees of hearing loss. Additionally, the combination of kurtosis and energy metrics like sound pressure level (SPL) or sound exposure level (SEL) is considered to be a good predictor of the relative magnitude of acoustic trauma between signals that differ in impulsiveness. As

this metric of impulsiveness is energy independent, it always needs to be accompanied by energy metrics in order to provide a suitable amount of information about hearing hazards.

Additional metrics such as crest factor have been associated with possible impulse hazards for human workers (Pekkarinen and Starck 1983) but no studies could be found that explicitly varied this metric to assess the degree of observed hearing loss. (Henderson and Hamernik 1986) provided a comprehensive overview of additional metrics used to measure impulses during experimental noise exposures. These metrics included rise time, pulse amplitude and duration, and pulse repetition rate. Rise time, for example, may be considered more suitable for identifying the onset of damage temporally, whereas signal duration at peak pressure could provide information about the extent of mechanical stress experienced by the inner ear (Ketten 2004a).

Lastly, (Martin et al. 2020) investigated the degree of correlation between three metrics of impulsiveness and reported that the kurtosis, crest factor, and Harris impulse factor were well correlated and responded similarly to changes in the data. (Martin et al. 2020) also recommended kurtosis as a metric for quantifying impulsiveness. Kurtosis is therefore highly recommended in the literature reviewed, as one of the metrics to be included in the analysis conducted in WP 3 alongside several others. The degree of correlation between the selected metrics will also be assessed as part of the modelling component of this project.

9.5 Knowledge available from studies involving marine mammals

The degree of impulsiveness of acoustic stimuli used for marine mammal studies has, to our knowledge, not been neither systematically nor artificially modified to assess the relationship between impulsiveness and degree of hearing loss following distinct exposures. Instead, playbacks of real impulsive sounds from activities such as pile driving (Kastelein et al. 2016), seismic surveys (Finneran et al. 2015) and explosions (Finneran et al. 2000), have been used to induce temporary threshold shifts (TTS) in captive marine mammals. The properties of exposures, which have been varied, include peak sound pressure level (Finneran et al. 2003), frequency weighted cumulative sound exposure level (Kastelein et al. 2017), exposure duration (Mooney et al. 2009), and number of impulses (Sills et al. 2020).

The exposures to single impulses known to date did not induce TTS in seals (Reichmuth et al. 2016) nor delphinids (Finneran et al. 2000). However, in the (Finneran et al. 2000) study involving delphinids, only sounds which resembled distant underwater explosions were used during the experiments, with ranges from 1.5 to 55.6 kilometres. Additional studies involving single pulses would be valuable, particularly if variable degrees of impulsiveness and energy levels could be used to assess whether TTS is more likely to occur following exposures to stimuli with a higher degree of impulsiveness.

Previous studies have found that exposures to multiple impulsive sounds caused TTS in several marine mammal species, including the bottlenose dolphin (*Tursiops truncatus*; (Finneran et al. 2015), beluga whale (*Delphinapterus leucas*; (Finneran et al. 2002), bearded seal (*Erignathus barbatus*; Sills et al. (2020)) and harbour porpoise (*Phocoena phocoena*; Kastelein et al. (2017)). Some of these studies varied the duration of playbacks or number of impulses that individuals were exposed to in order to identify the TTS onset or assess the amount of sound energy required to reach higher TTS levels (e.g., Lucke et al. (2009); Mooney et al. (2009); Kastelein et al. (2017); Sills et al. (2020).

In hearing loss studies involving terrestrial mammals such as (Goley et al. 2011) and (Xie et al. 2016), the temporal complexity of stimuli was assessed by using the kurtosis metric. This metric of impulsiveness was integrated into corrections applied to energetic measurements, in order to better predict the likelihood of hearing loss following exposures containing impulsive sounds. The first application of such kurtosis corrections in the case of marine mammals was recently performed by (von Benda-Beckmann et al. 2022). (von Benda-Beckmann et al. 2022) applied the kurtosis corrections from the (Goley et al. 2011) and (Xie et al. 2016) studies to frequency weighted sound exposure levels measured during previous harbour porpoise studies, where the subjects were exposed to acoustic stimuli of varying degrees of impulsiveness (pile driving, airguns, and intermittent and continuous sonar). One of these corrections, proposed by (Goley et al. 2011), was developed to predict the likelihood of permanent threshold shifts (PTS) in chinchillas and humans, and provided consistent predictions of porpoise TTS onset following exposures to signals with different degrees of impulsiveness (von Benda-Beckmann et al. 2022). This study by (von Benda-Beckmann et al. 2022) is the first one, to our knowledge, to apply this correction to sounds from marine mammal exposures. It is important to note that the authors expressed caution regarding the transferability of this measurement to other marine mammal species, unless more studies are performed to assess its suitability.

9.6 Mechanism of noise induced hearing loss

The analysis of histological samples from terrestrial mammals exposed to noise has provided key information regarding the mechanism of hearing loss and the cellular structures impacted by stimuli of varying intensity and temporal characteristics. The components of the inner ear which have been observed to suffer from noise induced damage include the stereocilia of hair cells (Liberman 1987, Gao et al. 1992), the synapses between hair cells and the primary afferent neurons (Canlon 1988, Ryan et al. 2016, Liberman and Kujawa 2017), and the hair cells themselves via metabolic and physiological alterations (Canlon 1988, Heinrich and Feltens 2006).

9.6.1 Differences between temporary and permanent noise induced trauma

Exposure to intense sounds can either produce TTS, characterised by acute changes in hearing sensitivity which recover over time, or PTS, which involves a loss of inner ear hair cells or neural synapses which cannot recover to preexposure levels (Ryan et al. 2016). (Nordmann et al. 2000), for example, investigated the differences in TTS and PTS in chinchillas, and for the former case reported a buckling of the inner ear supporting cells which led to the uncoupling of the outer hair cell stereocilia from the tectorial membrane. Inner ears with PTS also exhibited focal losses of inner ear hair cells and afferent nerve fibres (Nordmann et al. 2000).

9.6.2 Effects of impulsive sounds on the inner ear

Exposures to impulsive sounds have also provided insight into the effects of brief, intense transient signals on the inner ear cellular integrity. For instance, (Hu et al. 2006) reported a rapid induction of outer hair cell body shrinkage and apoptosis in chinchillas after 5 and 30 minutes of being exposed to intense, impulsive noise. (Hamernik et al. 1984) described a complete separation of the inner ear sensory epithelia (consisting of outer hair cells and support cells) from the basilar membrane, and changes in the stereocilia arrays following exposures of chinchillas to blast waves. These forms of

mechanical damage induced by impulsive stimuli with a rapid rise time are distinct from the metabolic stress experienced by the inner ear cells during exposures to continuous noise (Henderson and Hamernik 2012).

9.6.3 Interactions between continuous and impulsive sounds

(Hamernik and Henderson 1976), as cited in (Henderson and Hamernik 2012)) highlighted a possible synergistic interaction between continuous and impulsive noise, which may lead to enhanced hearing trauma. During this study, the group of chinchillas exposed to a combination of continuous and impulsive noise (where the total energy was less than one decibel greater compared to either condition individually) suffered hearing losses greater by 20-30 decibels compared to the groups exposed only to continuous or impulsive noise ((Hamernik and Henderson 1976)). This interaction has been described by (Henderson and Hamernik 2012) in light of the new observations at a cellular level – inner ear cells exposed to continuous noise produce toxic free radicals over time, which make the sensory cells more vulnerable to the mechanical damage that is observed during exposures to impulsive sounds. Although this interaction cannot be accounted during this project, further consideration should be given to the underwater continuous noise that marine mammals may be exposed to during construction activities that generate impulsive sounds.

9.7 Auditory effects from blast waves

Unlike the reverberant impulses produced during activities like impact pile driving, the blast waves generated during the denotation of unexploded ordnances are in fact shock waves. These waves are characterised by a very sudden increase in amplitude and animals exposed to these intense impulsive stimuli often show signs of compressive-rarefactive blast trauma (e.g., middle ear ossicular fractures, haemorrhages, and brain trauma) (Ketten 2004b).

Terrestrial mammals which have been involved in studies investigating blast wave induced trauma include pigs, sheep, and chinchillas (e.g., (Roberto et al. 1989). In the study of (Roberto et al. 1989), live animals were exposed to acoustic stimuli in controlled conditions prior to histological assessments of their ear components. In the case of marine mammals, the only study performed in a controlled environment, used fresh post-mortem specimens equipped with pressure sensors, rather than live animals (Ketten 2004b), given the similar mechanical properties of live and post-mortem ears (Rosowski et al. 1990), as cited in (Ketten 2004b). The effects of the blast waves on the inner ears of the tested subjects were similar for terrestrial and marine mammals and involved damage to the sensory epithelium (Patterson and Hamernik 1997), mechanical fracture and separation of the Organ of Corti from the basilar membrane (Roberto et al. 1989), and inner ear haemorrhage (Ketten 2004b). Additionally, a relationship between body mass and the severity of damage was observed for both terrestrial and marine mammals, where smaller animals were found to be at risk of suffering more trauma compared to larger animals exposed to stimuli with the same peak pressure (Ketten 2004b). Theoretical models have also been designed to assess the potential of blast waves to induce acoustic trauma in marine mammals (Ketten 1995, von Benda-Beckmann et al. 2015), and it has been suggested that in spite of the adaptations of marine mammals to underwater hearing (e.g., use of soft tissue channels to conduct sound to the ear, believed to reduce the received acoustic power), these animals are still at risk of suffering permanent hearing loss as well as compressive-rarefactive blast trauma due to the air-filled middle ear (Ketten 1995).

9.8 Transferability of observations from terrestrial mammals to marine mammals

Anatomically, marine mammal inner ears generally resemble those of terrestrial mammals, given their fluid-filled cochlear canal and resonating basilar membrane with a similar cellular structure, which supports mechano-sensory receptors (Ketten et al. 2021). However, differences in the degree of stiffness, width, and thickness of the basilar membrane have been observed across these two mammalian groups, which are believed to be primarily a result of marine mammals adapting their auditory system to the reception and transduction of underwater sounds (Ketten 2004a) (Ketten 2004b).

Although the sound transduction and mechanisms of auditory damage may share some similarities across these two groups of mammals, direct extrapolations of auditory system responses to impulsive sounds from terrestrial mammal to marine species may be inappropriate. It is therefore recommended by the authors of this report that future studies should involve marine mammal species from various hearing groups, (e.g., as proposed by Southall et al. (2019)), which should include various intermediary levels of impulsiveness and exposure patterns (i.e., duty cycle, exposure duration, number of impulses) at a constant sound exposure level when assessing hearing loss.

The transferability of auditory responses from terrestrial mammals to marine species is further complicated by differences in study design and methodology. These differences are related to the characteristics of the study location (i.e., anechoic chambers for terrestrial mammals compared to reverberant pools or pens exposed to background noise for marine mammals), the duration of noise exposures (which can last for multiple hours for terrestrial mammals compared to usually no more than a couple of hours for marine mammals), and the number of individuals used for experiments (usually greater in terrestrial mammal studies). Additionally, due to ethical considerations, marine mammals cannot be exposed to high levels of noise which could induce PTS, nor can they be killed and have their ear structures investigated after exposures, thus limiting this auditory response to modelled estimates and the use of observations at a cellular level from terrestrial mammal studies.

Lastly, the age of the subjects and their familiarity with an experimental routine may impact the outcome of hearing loss studies. The former variable is supported by evidence of age-related hearing loss (process termed presbycusis), which causes natural hearing cell and tissue deterioration as animals age (Ketten 2004a). If the same captive marine mammals are used for multiple noise exposures over the years, their age and likely degree of ear tissue wear and tear should be considered before extrapolating values related to TTS onset and growth to wild animals. Additionally, regarding the familiarity of the subjects with the study settings, it has been observed that multiple marine mammals attenuated their hearing sensitivity during intense noise exposures when they could predict the onset of repetitive acoustic stimuli (Nachtigall et al. 2018, Finneran et al. 2023).

10 Appendix 2 – Metrics extracted from field data

10.1 Definitions of acoustic metrics

All mathematical operations were performed via a software package called IONIS.evaluation (v0.5.1), developed by *itap*, based on the Python Scientific Stack. The generation of the energy-equivalent continuous sound pressure level (SPL) was done according to the DIN 45641 (1990).

10.1.1 Energy-equivalent continuous Sound Pressure Level (SPL)

The SPL is the most common measure in acoustics, and it is defined in ISO (2017b) as follows:

$$SPL = 10 \log\left(\frac{1}{T}\int_0^T \frac{p(t)^2}{p_0^2} dt\right) \text{ [dB]} \qquad \text{Equation (1)}$$

with

$p(t)$ - time-variant sound pressure,

p_0 - reference sound pressure (in water 1 µPa),

T - averaging time.

10.1.2 Sound Exposure Level (SEL)

For characterization of impact pile driving impulses, SPL solely is an insufficient measure, since it depends on both the strength of the pile driving blows, and on the averaging time and the breaks between the blows of pile driving. The Sound Exposure Level (SEL) is more appropriate, and it is defined in ISO (2017b) as follows:

$$SEL = 10 \log\left(\frac{1}{T_0}\int_{T_1}^{T_2} \frac{p(t)^2}{p_0^2} dt\right) \text{ [dB re 1 µPa}^2\text{]} \qquad \text{Equation (2)}$$

with

T_1 and T_2 - starting and ending time of the averaging window (should be determined so that the signal of interest is between T_1 and T_2),

T_0 - reference 1 second.

Therefore, the Sound Exposure Level of an impulse (e.g., a pile driving strike) is the level of a continuous sound of a duration of one second and the same acoustic energy as the impulse.

10.1.3 Cumulative Sound Exposure Level (SEL_{cum})

The amount of acoustic energy from transient sounds like impulses that a subject is exposed to (e.g., a fleeing marine mammal) can be quantified via the cumulative Sound Exposure Level (SEL_{cum}), which is defined in ISO (2017b) as follows:

$$SEL_{cum} = 10 \log \frac{E_{cum}}{E_{ref}} \quad [\text{dB re 1 } \mu\text{Pa}^2] \quad \text{Equation (3)}$$

Where the cumulative sound exposure E_{cum} is defined below for n transient events with the unweighted frequency sound exposure E_n.

$$E_{cum} = \sum_{n=1}^{N} E_n \quad \text{Equation (4)}$$

The reference exposure is $E_{ref} = p_{ref}^2 \cdot T_{ref}$, in which p_{ref} is the reference sound pressure of 1 µPa and T_{ref} the reference duration of 1 second.

10.1.4 Zero-to-peak Sound Pressure Level ($L_{p,pk}$)

This parameter is a measure of peaks in the time series as follows:

$$L_{p,pk} = 20 \log \left(\frac{| p_{pk} |}{p_0} \right) \text{[dB]} \quad \text{Equation (5)}$$

with

p_{pk} - maximal determined positive or negative sound pressure level.

An example is depicted in Figure 22. The Peak Sound Pressure Level ($L_{p,pk}$) is always higher than the Sound Exposure Level (SEL). Generally, the difference between $L_{p,pk}$ and SEL during the pile driving strikes is 20 to 25 dB. Some authors prefer the Peak-to-Peak value (L_{p-p}) instead of the $L_{p,pk}$. This study used zero-to-peak sound pressure level which is referred to throughout the report as L_{peak}.

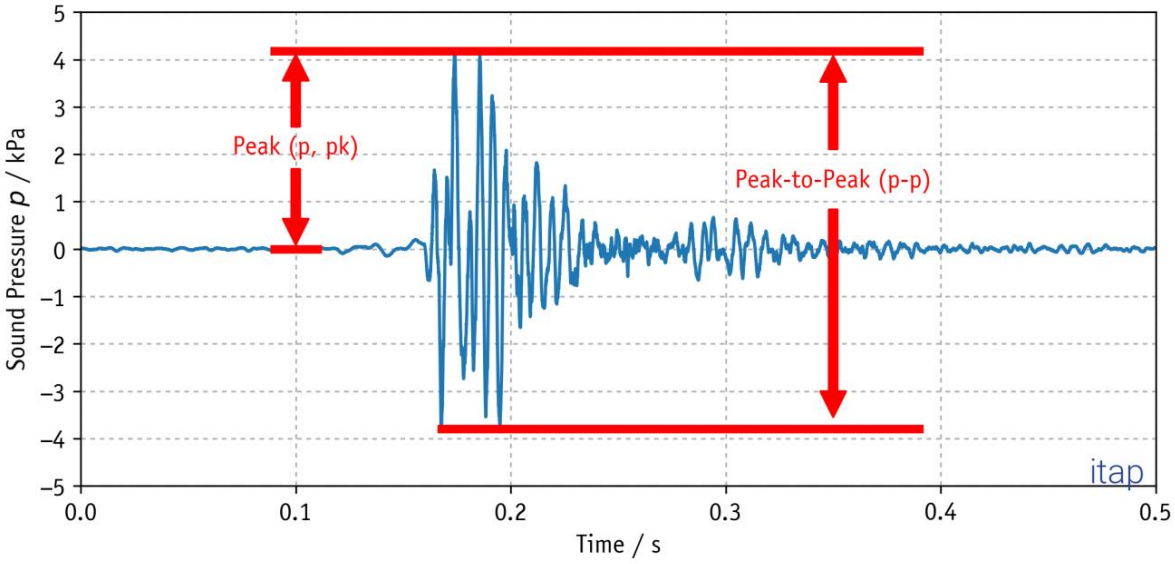

Figure 22. Example of an acoustic signal recorded in the time domain during an impact pile driving strike. The horizontal red lines mark the positive and negative peaks in sound pressure.

10.1.5 Kurtosis

The kurtosis (β) of an acoustic time series is calculated over a specified time interval according to ISO (2017a) t_0 to t_1 as

$$\beta = \frac{\mu_4}{\mu_2^2}$$ Equation (6)

Where

$$\mu_4 = \frac{1}{t_1 - t_0} \int_{T_0}^{T_1} [p\,(t) - \bar{p}]^4\, dt$$ Equation (7)

and

$$\mu_2 = \frac{1}{t_1 - t_0} \int_{T_0}^{T_1} [p\,(t) - \bar{p}]^2 dt$$ Equation (8)

with the variance of the pressure $\bar{p}$ being the mean sound pressure in the time interval.

10.1.5.1 Kurtosis time window selection

In the literature, a variety of time windows have been used to compute kurtosis, ranging from one second (Kastelein et al. 2017, von Benda-Beckmann et al. 2022) to 40 minutes (Zhao et al. 2010). Hamernik et al. (2003) reported that the kurtosis became relatively stable when sample windows longer than 30 seconds were used to compute this metric from noise of variable temporal complexity. Furthermore, Martin et al. (2020) recommended a time window of 60 seconds and reported that the kurtosis stabilised once the window of analysis had a representative number of impulses within the sample. This time window was subsequently used by Guan et al. (2022) for their characterisation of underwater noise.

With the justifications above considered, the time window of analysis for this project was selected by performing tests on a subset of acoustic data using distinct windows of analysis (0.5, 1, 5, 30, and 60 seconds). The effect of the window length on the determined kurtosis values is shown in Figure 23 and Figure 24. The window length of < 1 s produced lower kurtosis values, suggesting there may be a limitation of the metric to identify outliers in the time series if not enough of the background noise is captured around the signal of interest. On the other hand, the window lengths between 1 and 60 s produces similar results.

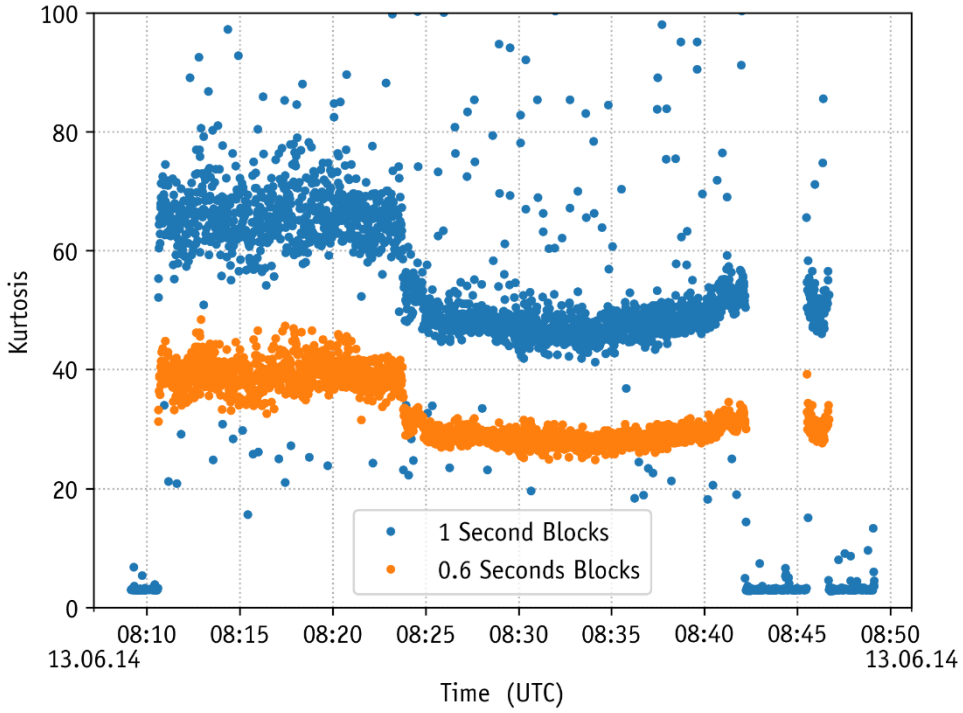

Figure 23 : Example of the determined noise metric kurtosis of a representative impact pile driving measurement in 750 m distance with a time interval length of 1 s and 0.6 s.

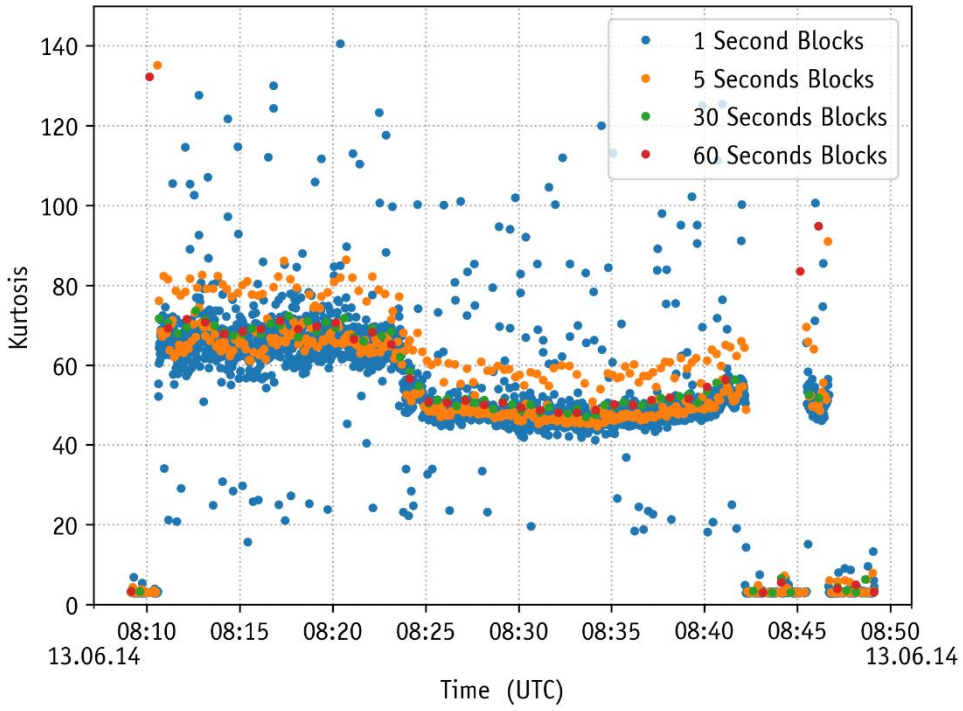

Figure 24 : Example of the determined noise metric kurtosis of the representative impact pile driving measurement of Figure 23 with time interval length varying between 1 and 60 s.

10.1.6 Kurtosis corrected Sound Exposure Level

The kurtosis corrected SEL ($SEL_{W,adj}$) is an adjustment to the SEL that aims to account for the effects of kurtosis. The kurtosis corrected SEL is therefore a modified form of the SEL that attempts to account for the effects of these unusual peak levels or distribution shape (kurtosis) on the average sound level over a period of time. It is important to note that different studies and sources may use different formulas or methods for calculating kurtosis corrected SEL, as there is no universally accepted definition.

The following equation is based on the formula from von Benda-Beckmann et al. (2022), which was initially proposed in Goley et al. (2011) to correct acoustic energy levels from exposures containing impulses in terrestrial mammal studies:

$$SEL_{W,adj} = SEL_W + \lambda \log_{10} \frac{\beta}{\beta_G} \quad \text{Equation (9)}$$

Where β_G is the kurtosis of a Gaussian distribution ($\beta_G = 3$), β is the kurtosis of the exposure, and λ is a positive constant determined by fitting measured threshold shifts to sound exposure levels at different levels of kurtosis. The λ value for humans is 4.02 and that of chinchillas is 3.07, but von Benda-Beckmann et al. (2022) used a constant λ of 13 for harbour porpoises, which was also used in this study.

10.1.7 Rise Time

Rise time represents the time it takes a signal to rise from 10 % to 90 % of its highest peak (National Marine Fisheries Service 2018).

10.1.8 Pulse or signals duration

According to ISO (2017b) the pulse duration ($\boldsymbol{\tau_{90}}$)should be calculated as the length of the time window which captures 90% of the energy of a pulse.

10.1.9 Crest factor

The crest factor (CF) is the peak sound pressure level minus the root-mean-squared (RMS) sound pressure level and it is calculated following the formula from in Martin et al. (2020) as follows:

$$CF = L_{p,pk} - SPL \quad \text{Equation (10)}$$

10.1.10 High frequency content

High frequency content was recommended by Southall (2021) as a proxy of impulsiveness because signals with high frequency content often also have a short rise time. The high frequency content of an impulse was quantified in this study as the energetic sum of three third octave bands centred around 8, 10, and 12.5 kHz. These bands were chosen because of the different sampling rates used to collect the data included in this study, which limited the upper limit of the effective frequency range to 16 kHz.

10.2 Results of acoustic metric extraction

10.2.1 Impact pile driving dataset

The following Figures show each evaluated metric of the dataset (394,002 Pulses) over the distance.

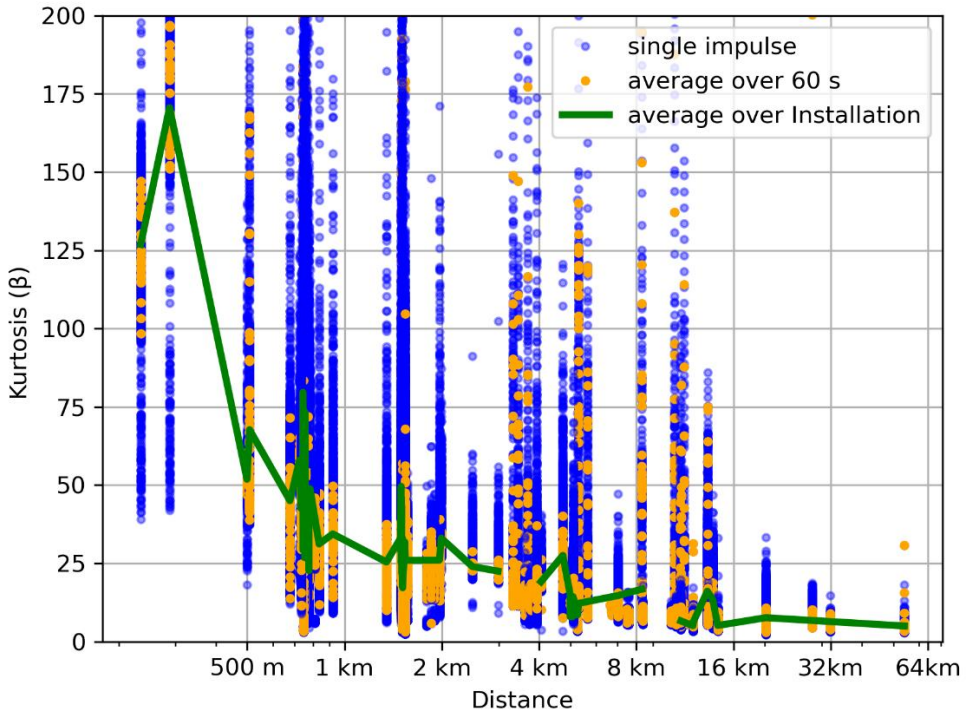

Figure 25. Kurtosis as function of the distance between source and receiver. Blue: for each single impulse, orange: mean over 60 seconds, green: mean over a complete pile installation.

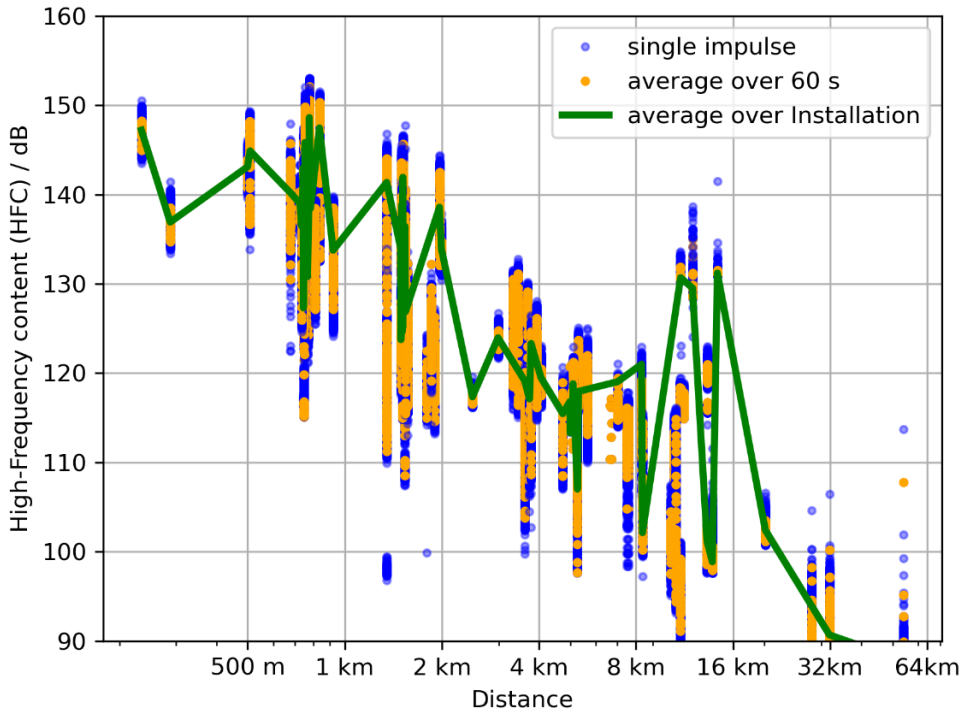

Figure 26. High frequency content as function of the distance between source and receiver. Blue: for each single impulse, orange: mean over 60 seconds, green: mean over a complete pile installation.

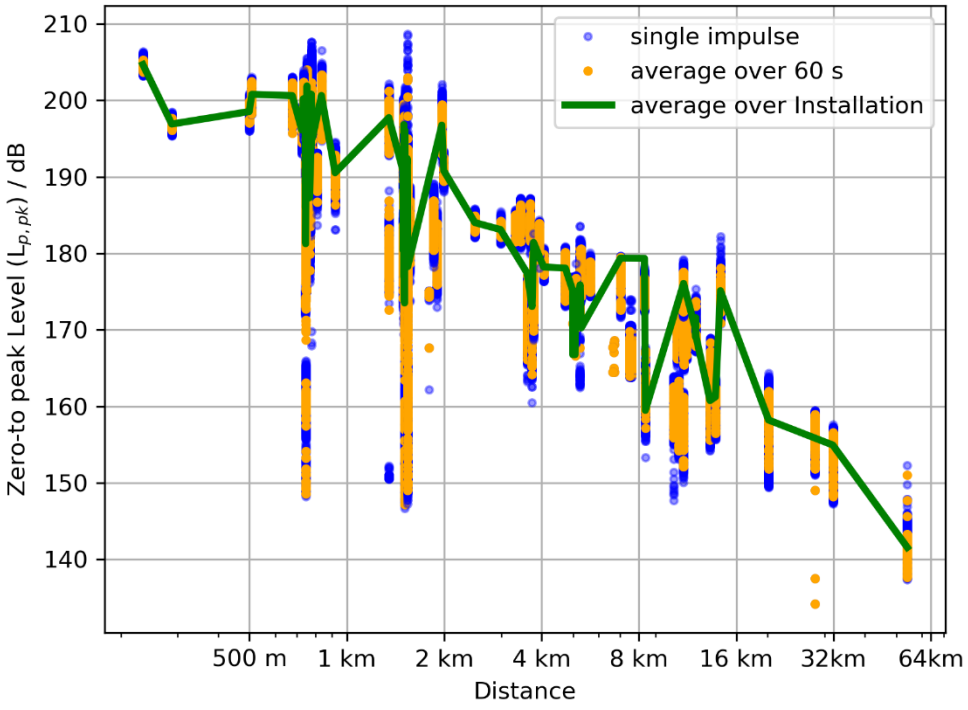

Figure 27. Zero-to-peak Sound Pressure Level as function of the distance between source and receiver. Blue: for each single impulse, orange: mean over 60 seconds, green: mean over a complete pile installation.

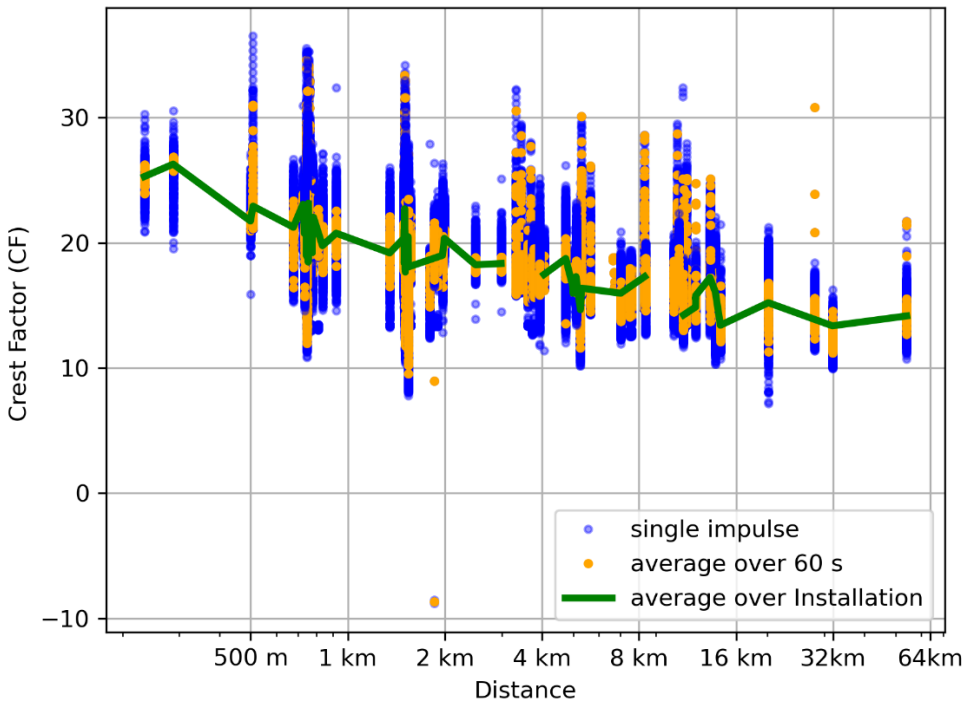

Figure 28. Crest factor as function of the distance between source and receiver. Blue: for each single impulse, orange: mean over 60 seconds, green: mean over a complete pile installation.

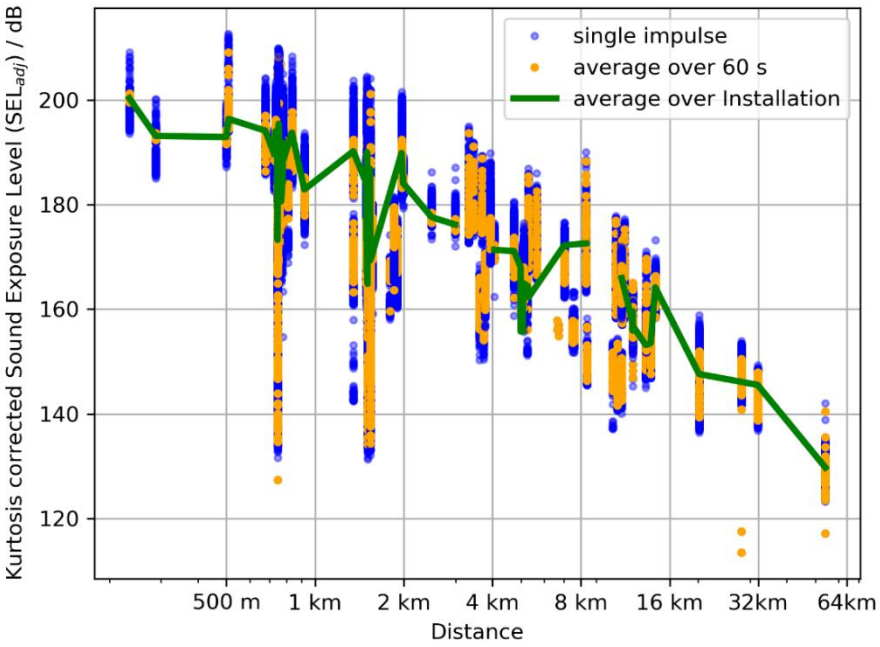

Figure 29. Kurtosis corrected Sound Exposure Level as function of the distance between source and receiver. Blue: for each single impulse, orange: mean over 60 seconds, green: mean over a complete pile installation.

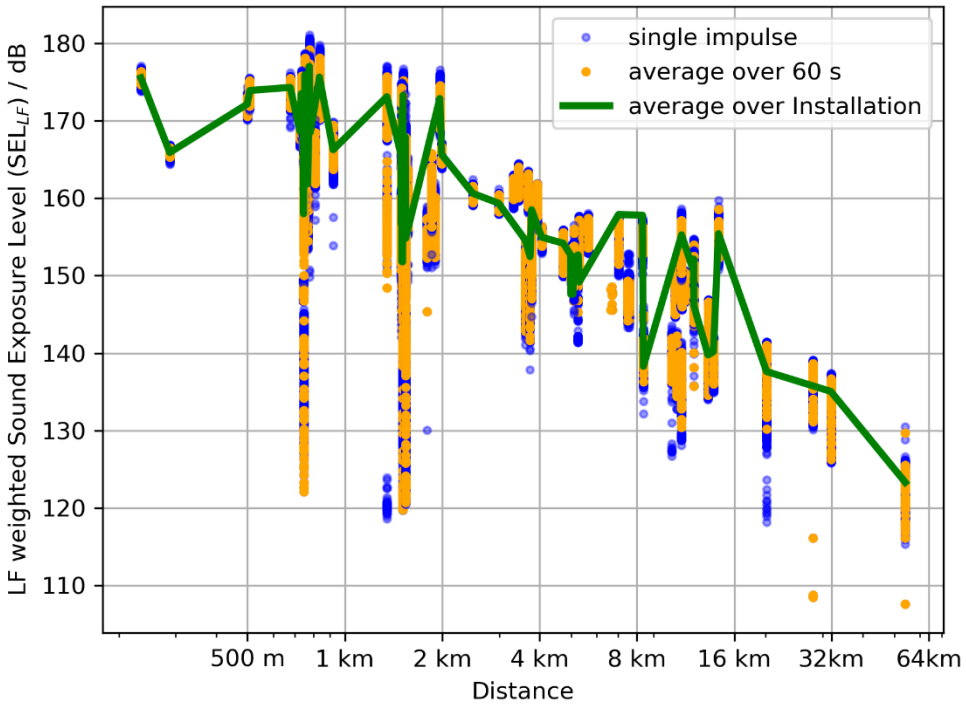

Figure 30. Frequency weighted Sound Exposure Level for low frequency cetaceans (SEL_{lf}) as function of the distance between source and receiver in accordance with Southall et al (2019). Blue: for each single impulse, orange: mean over 60 seconds, green: mean over a complete pile installation.

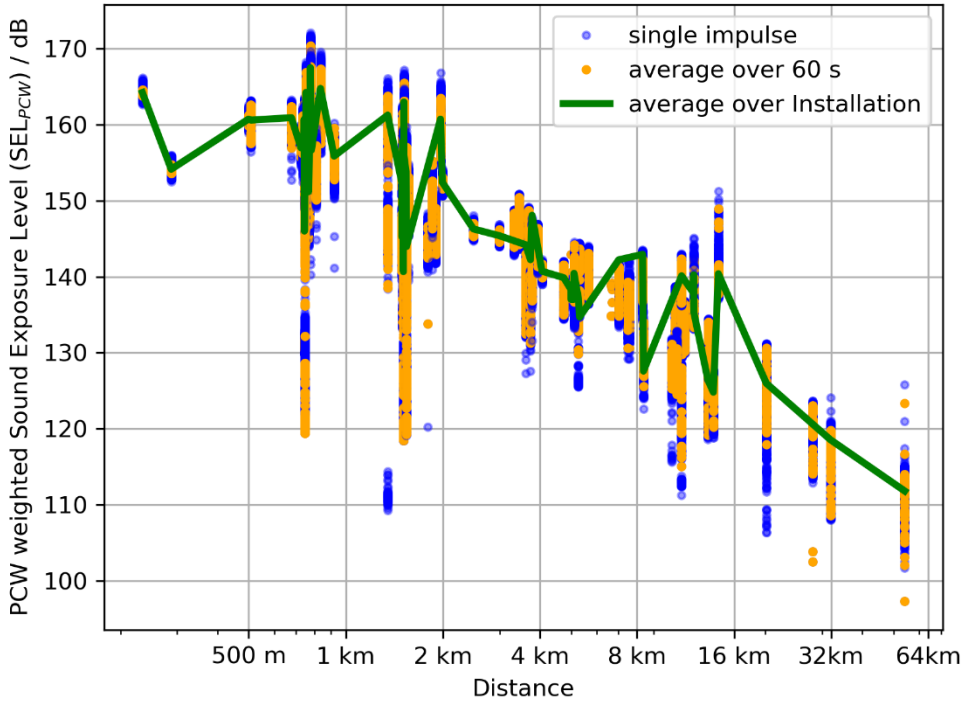

Figure 31. Frequency weighted Sound Exposure Level for pinnipeds (SEL_{pcw}) as function of the distance between source and receiver in accordance with Southall et al (2019). Blue: for each single impulse, orange: mean over 60 seconds, green: mean over a complete pile installation.

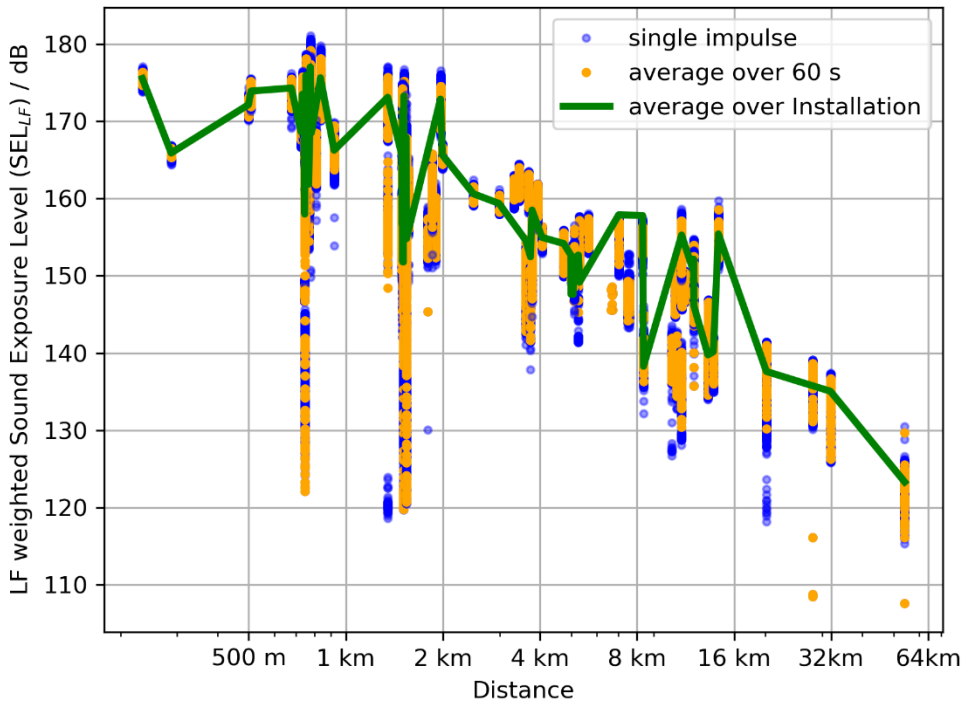

Figure 32. Frequency weighted Sound Exposure Level for high frequency cetaceans (SEL_{hf}) as function of the distance between source and receiver in accordance with Southall et al (2019). Blue: for each single impulse, orange: mean over 60 seconds, green: mean over a complete pile installation.

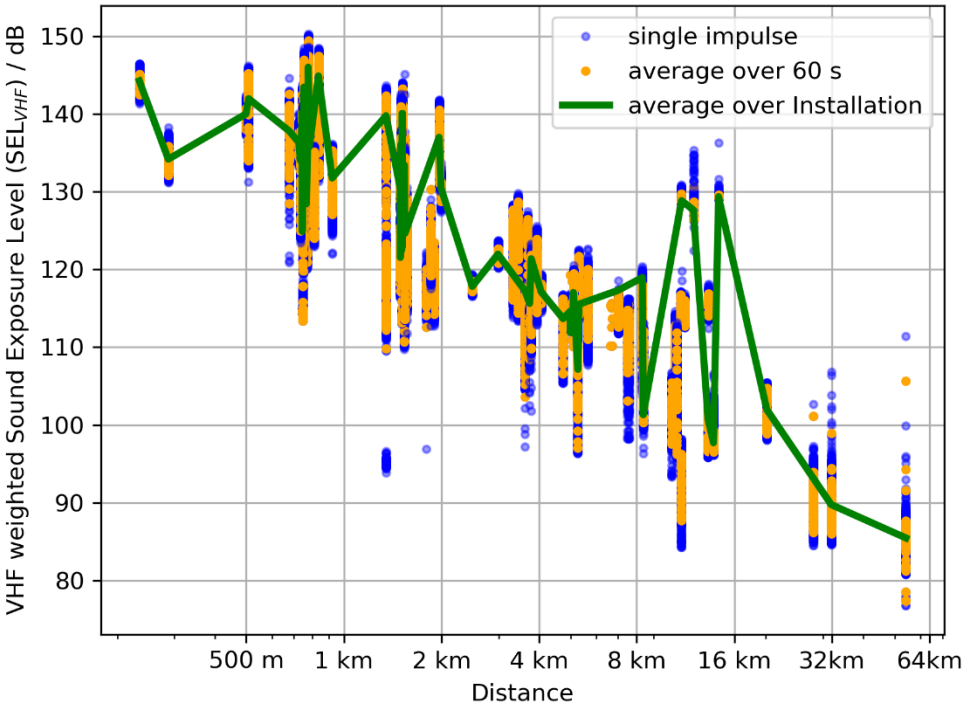

Figure 33. Frequency weighted Sound Exposure Level for very high frequency cetaceans (SEL_{vhf}) as function of the distance between source and receiver in accordance with Southall et al (2019). Blue: for each single impulse, orange: mean over 60 seconds, green: mean over a complete pile installation.

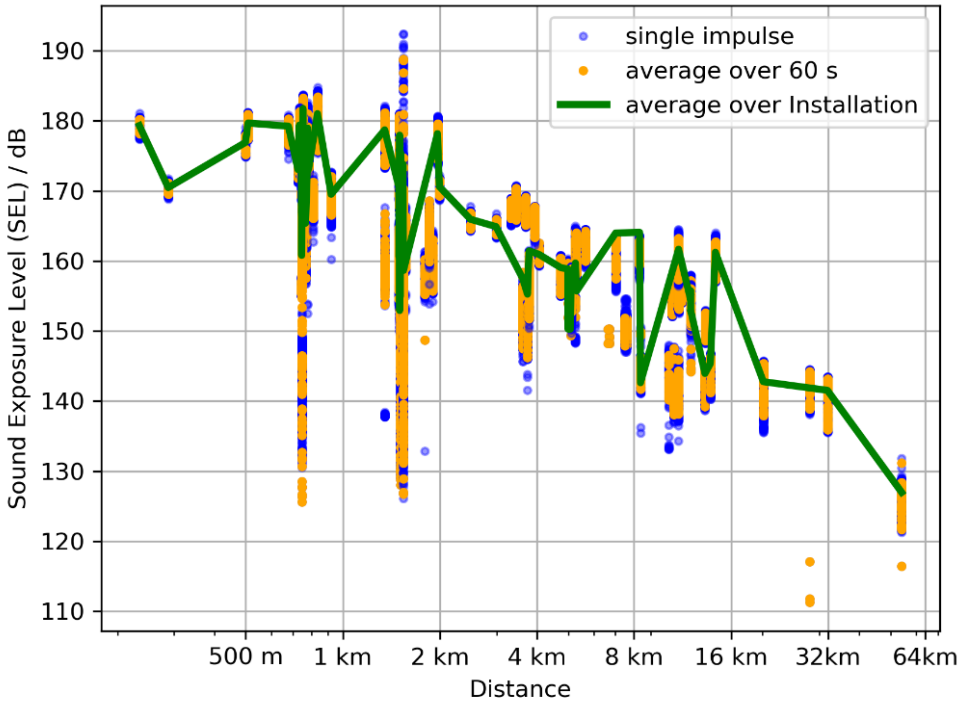

Figure 34. Single strike Sound Exposure Level as function of the distance between source and Receiver. Blue: for each single impulse, orange: mean over 60 seconds, green: mean over a complete pile installation.

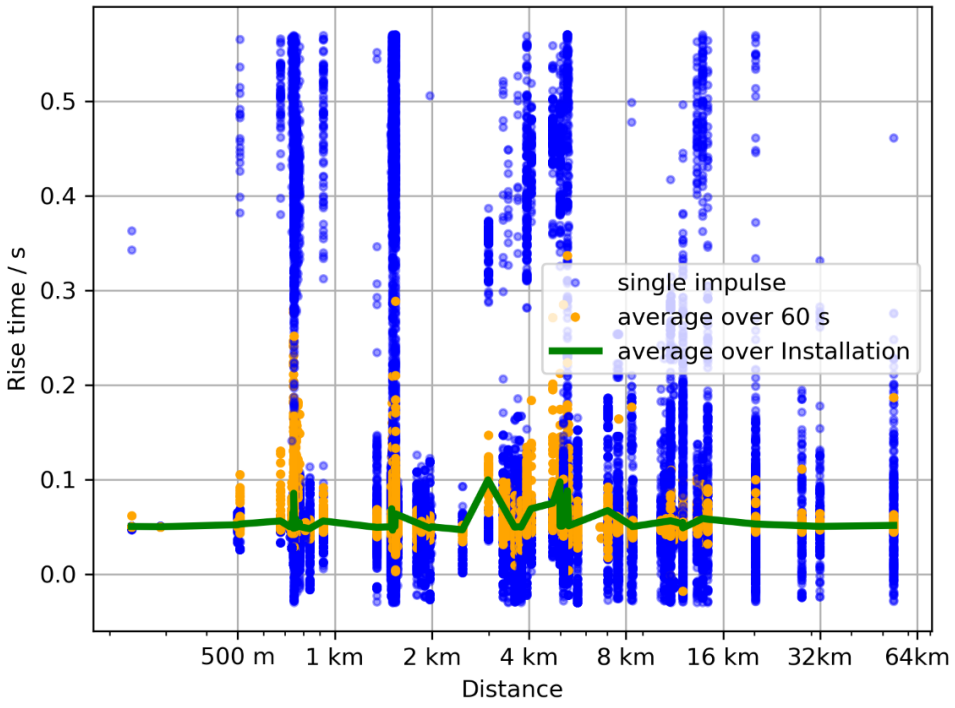

Figure 35. Rising time as function of the distance between source and receiver. Blue: for each single impulse, orange: mean over 60 seconds, green: mean over a complete pile installation.

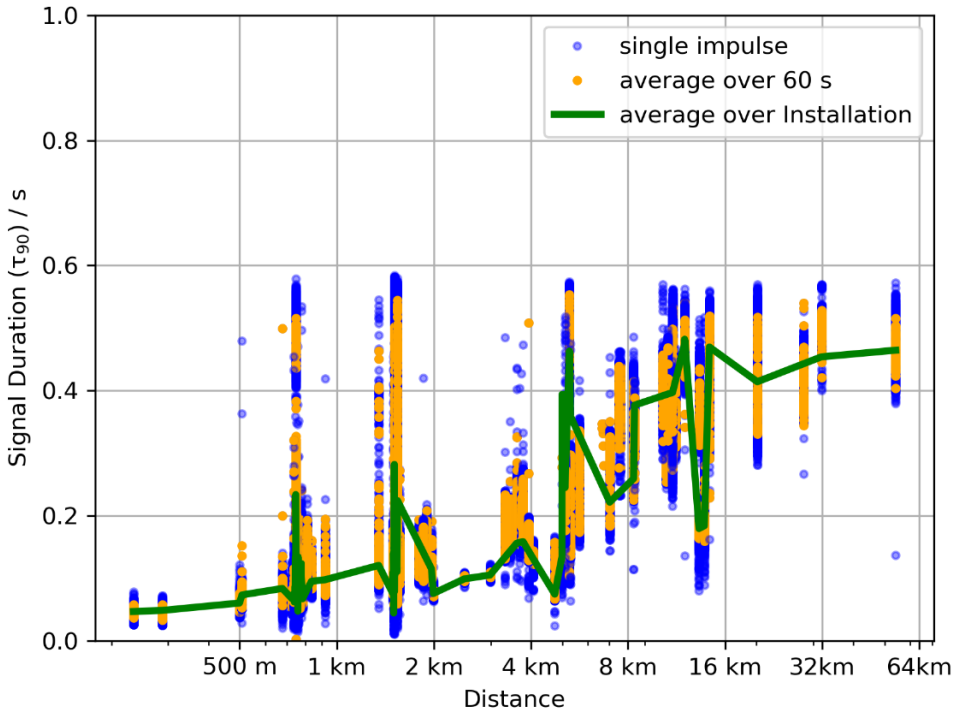

Figure 36. Signal duration of a single strike as function of the distance between source and receiver. Blue: for each single impulse, orange: mean over 60 seconds, green: mean over a complete pile installation.

10.2.2 Unexploded ordnances dataset

The following figures show each evaluated metric of the dataset (38 Pulses) over the distance.

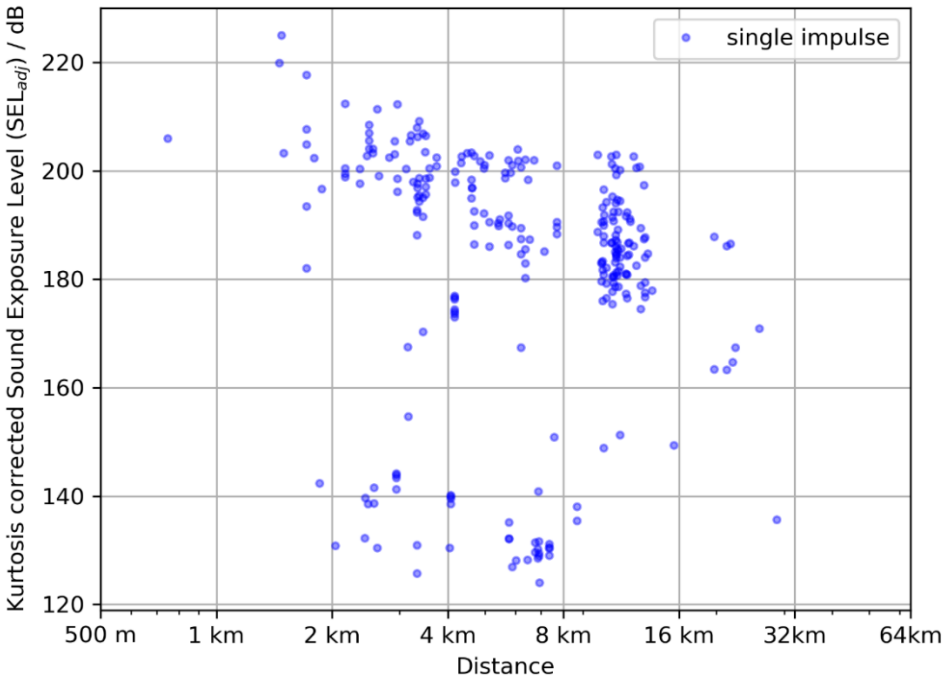

Figure 37. Kurtosis corrected Sound Exposure Level as function of the distance between source and receiver.

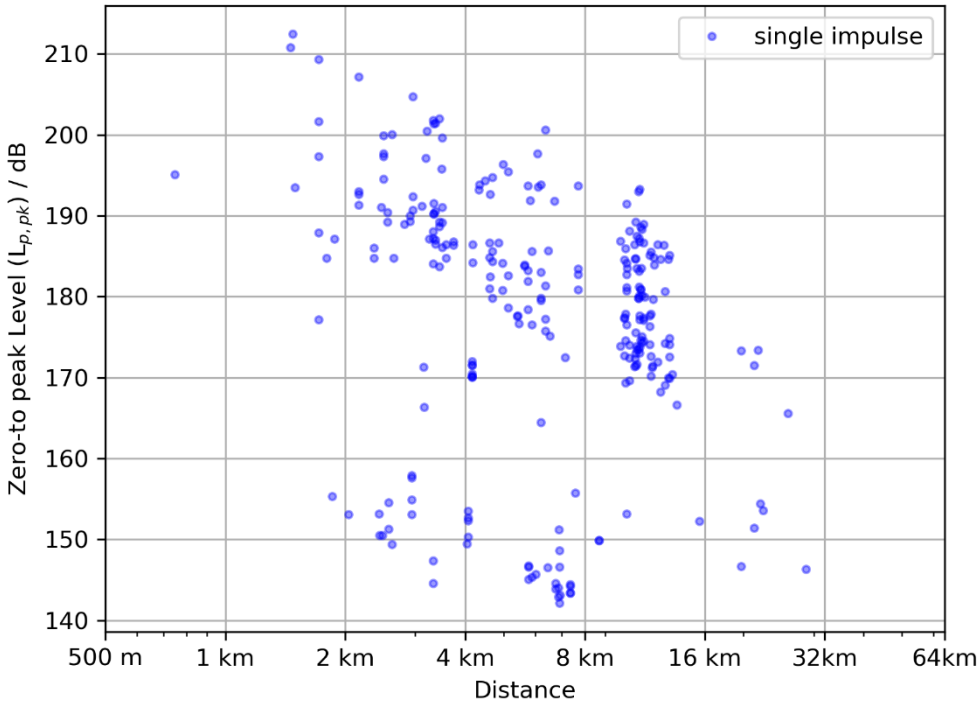

Figure 38. Zero-to-peak Sound Pressure Level as function of the distance between source and receiver.

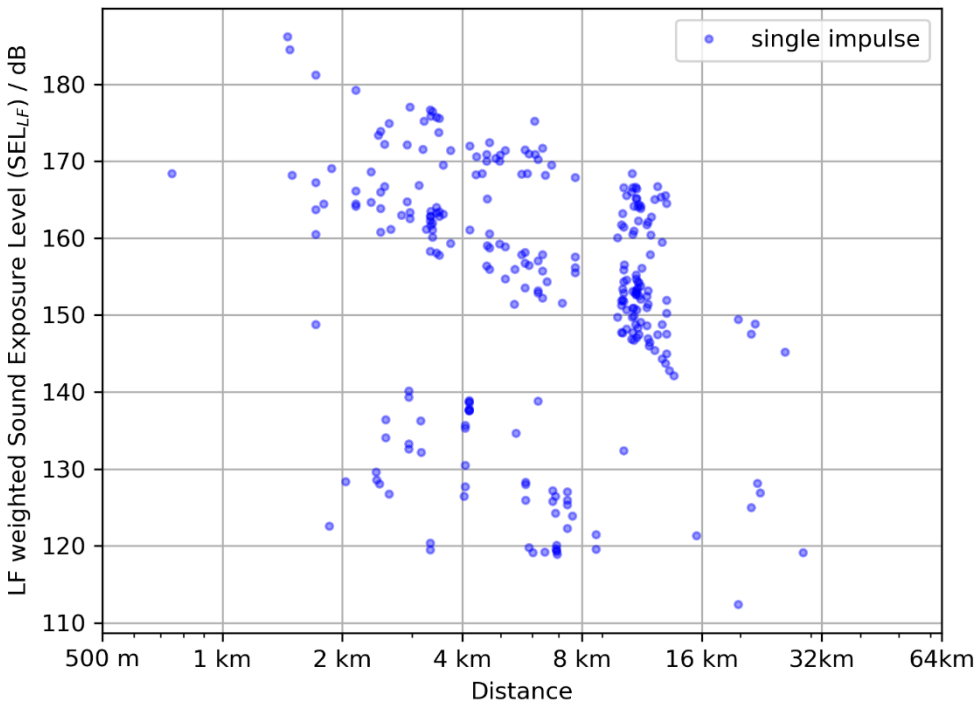

Figure 39. Frequency weighted Sound Exposure Level for low frequency cetaceans (SEL$_{lf}$) as function of the distance between source and receiver in accordance with Southall et al (2019).

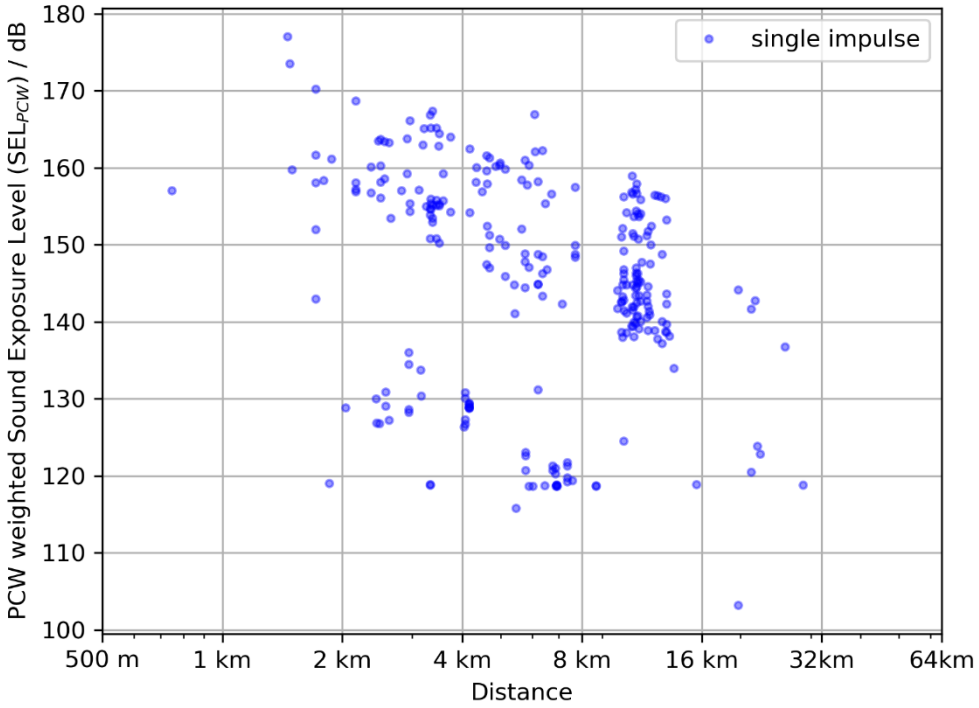

Figure 40. Frequency weighted Sound Exposure Level for pinnipeds (SEL$_{pcw}$) as function of the distance between source and receiver in accordance with Southall et al (2019).

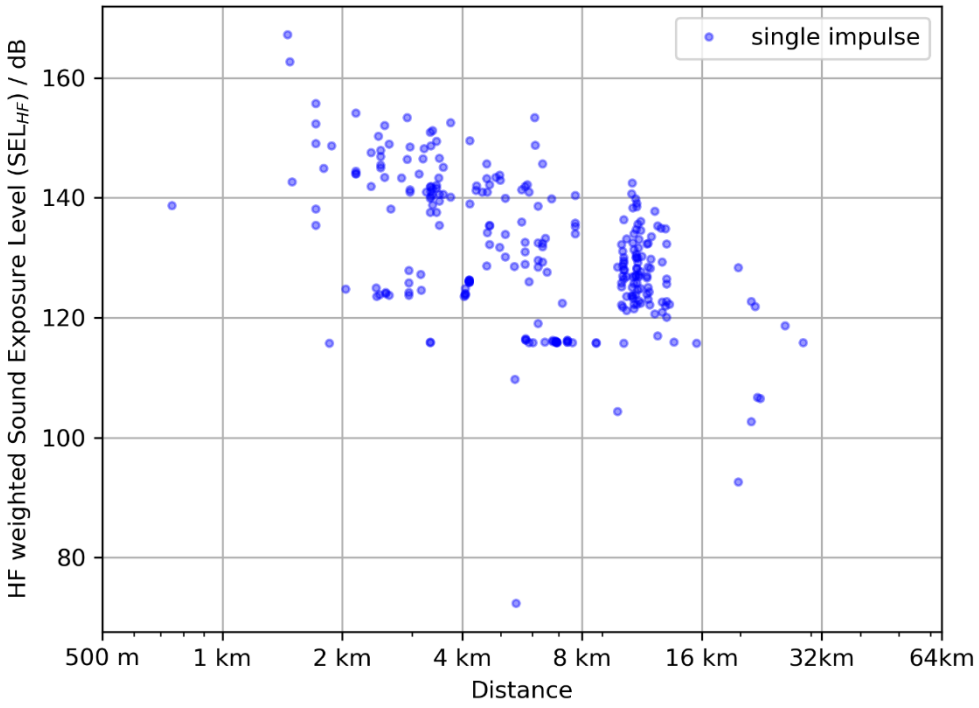

Figure 41. Frequency weighted Sound Exposure Level for high frequency cetaceans (SEL_{hf}) as function of the distance between source and receiver in accordance with Southall et al (2019).

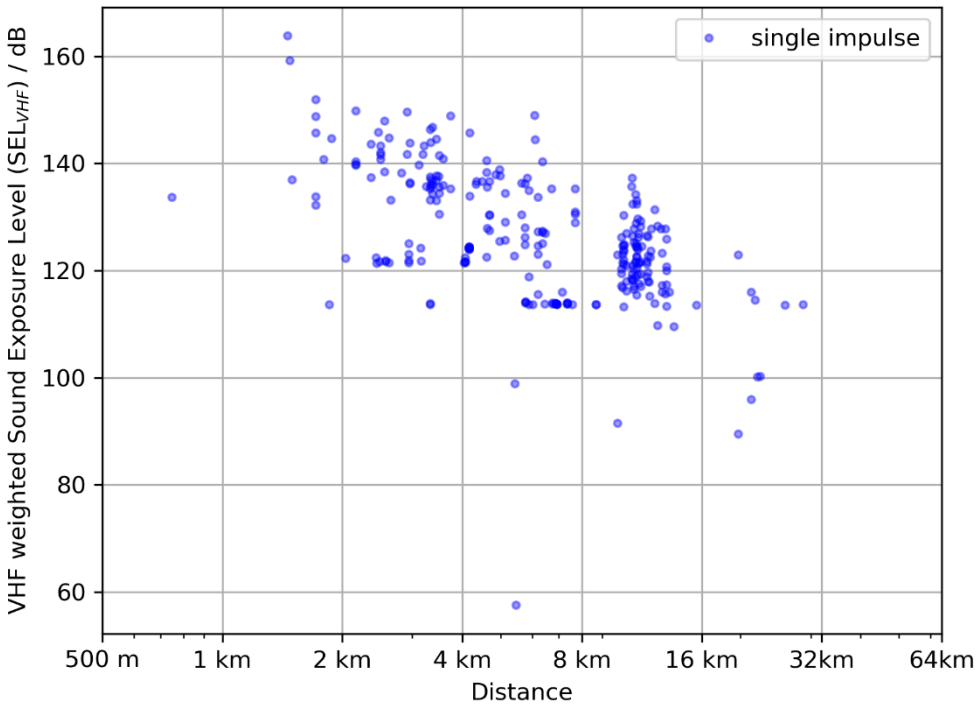

Figure 42. Frequency weighted Sound Exposure Level for very high frequency cetaceans (SEL_{vhf}) as function of the distance between source and receiver in accordance with Southall et al (2019).

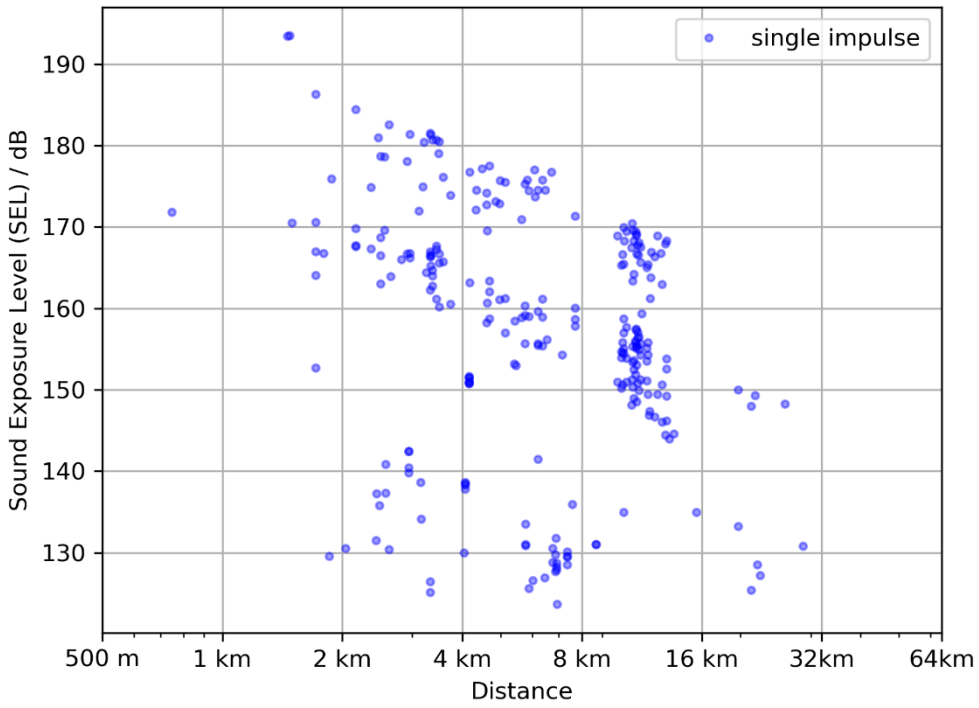

Figure 43. Single strike Sound Exposure Level as function of the distance between source and Receiver.

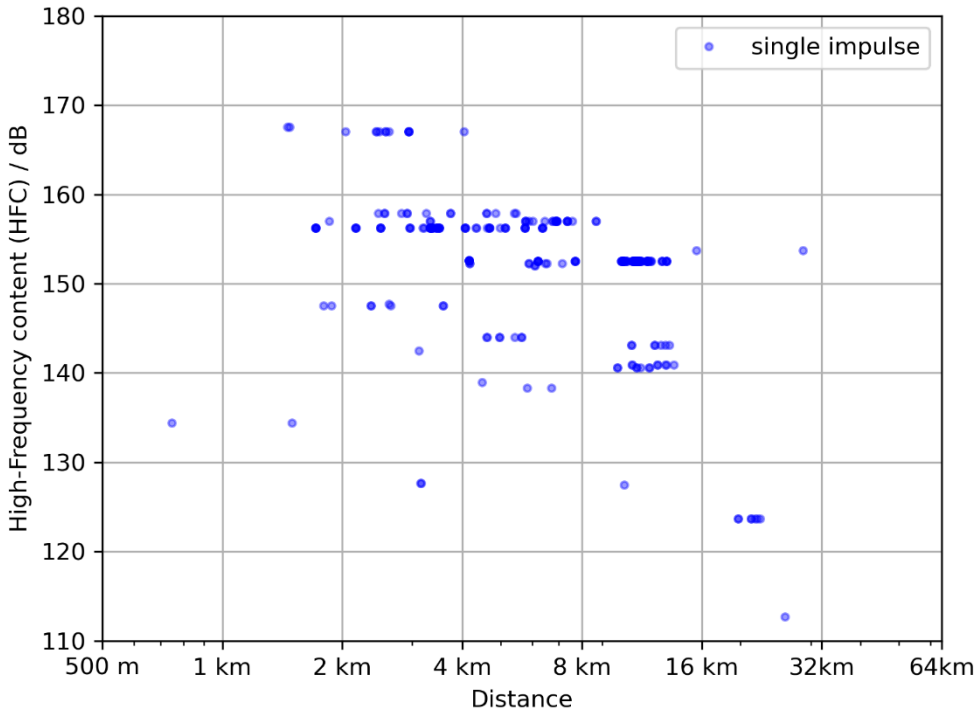

Figure 44. Single strike Sound Exposure Level for the frequency range 8 to 12.5 kHz as function of the distance between source and receiver.

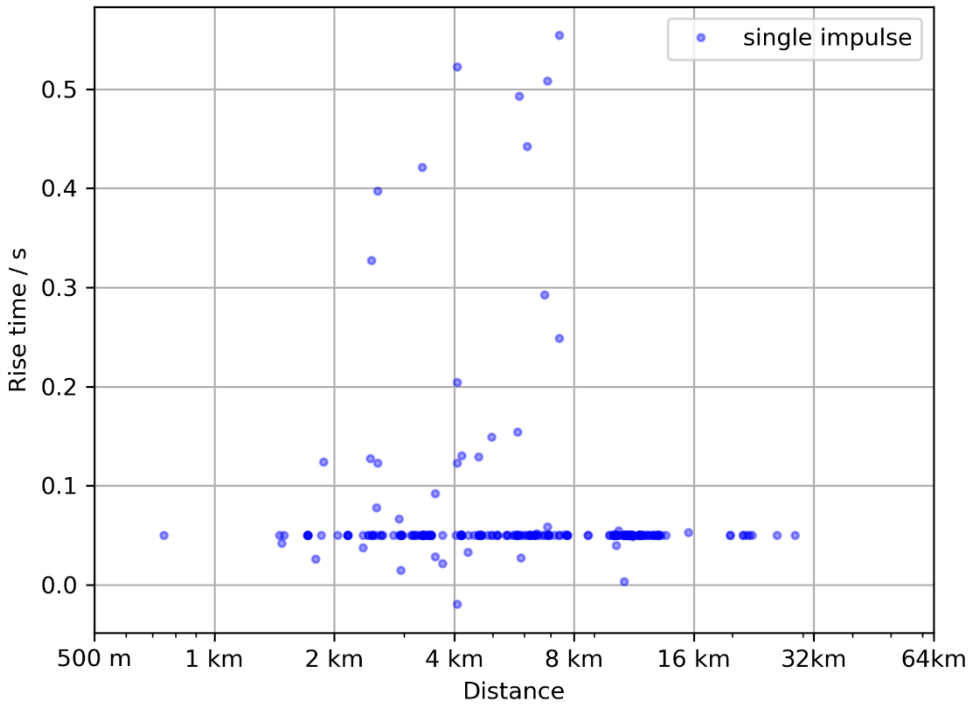

Figure 45. Rising time as function of the distance between source and receiver.

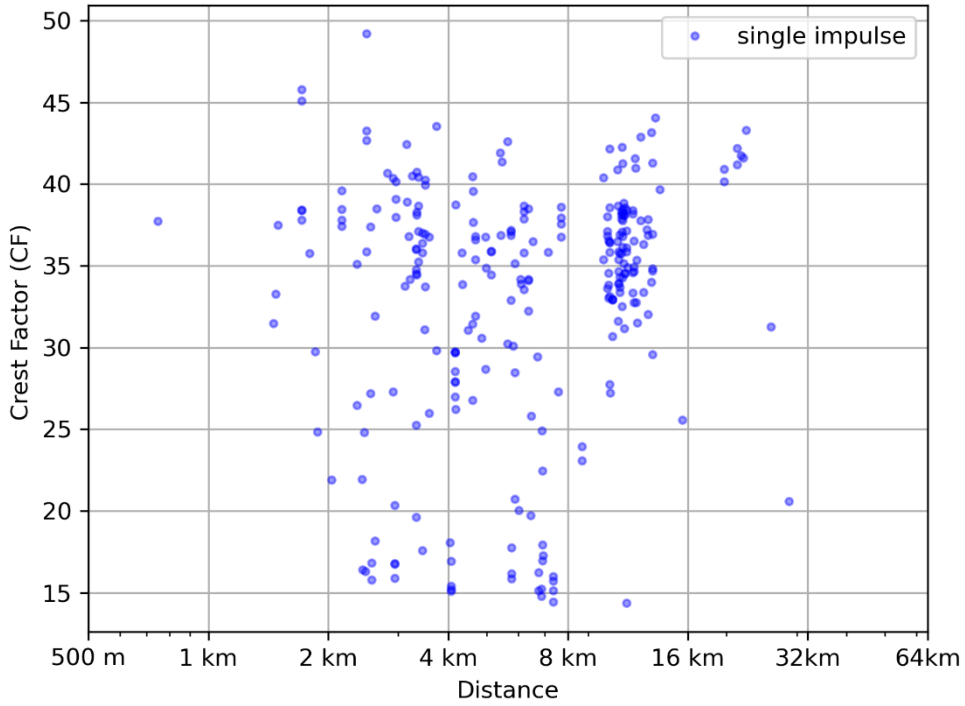

Figure 46. Crest factor as function of the distance between source and receiver

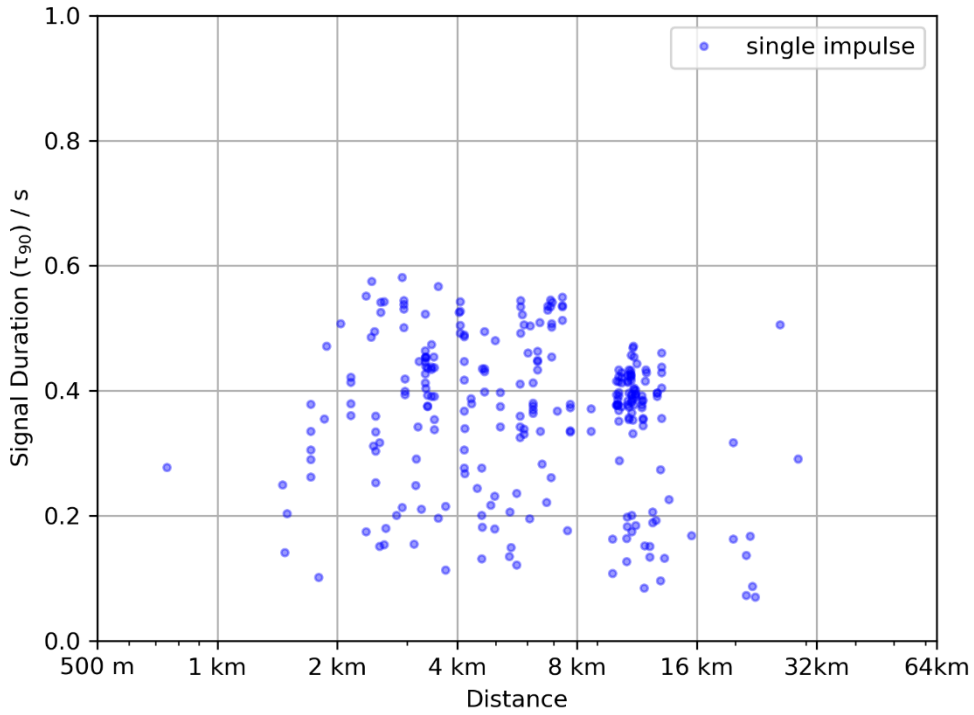

Figure 47. Signal duration of a single strike as function of the distance between source and receiver.

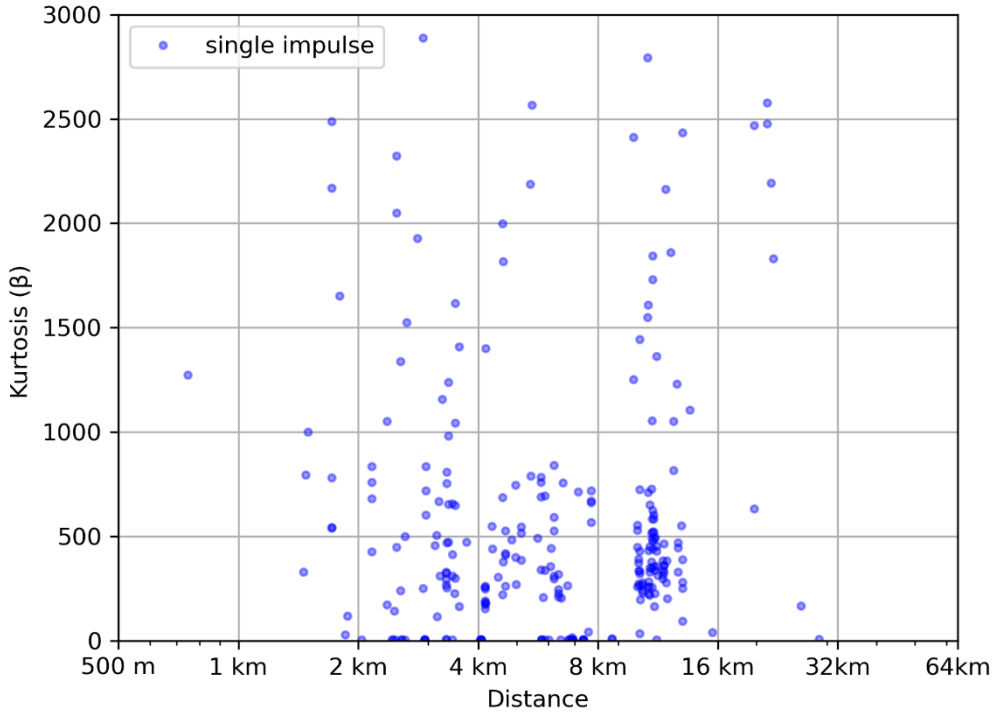

Figure 48. Kurtosis as function of the distance between source and receiver.

11 Appendix 3 – Modelling results and data overview

11.1 Data overview

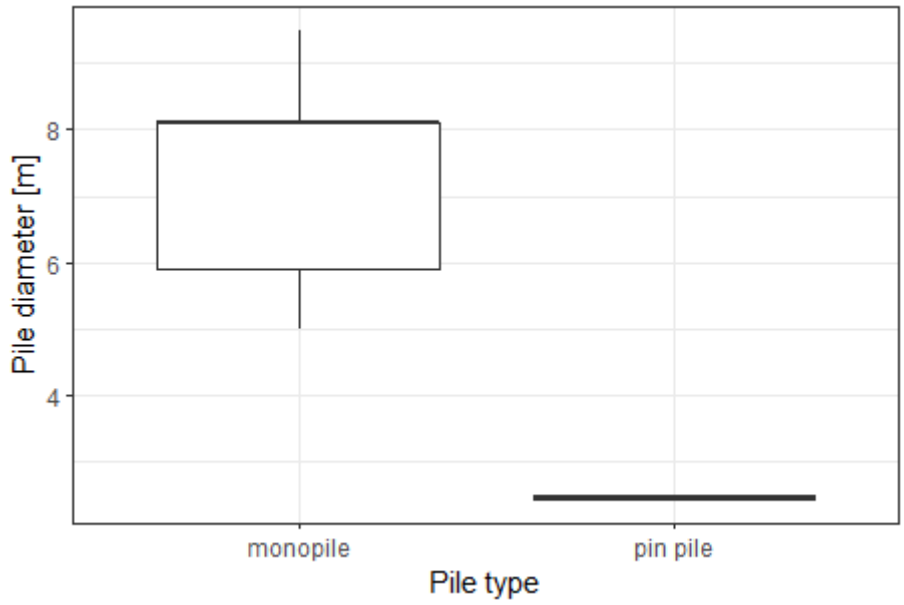

Figure 49. Relationship between pile type and its diameter.

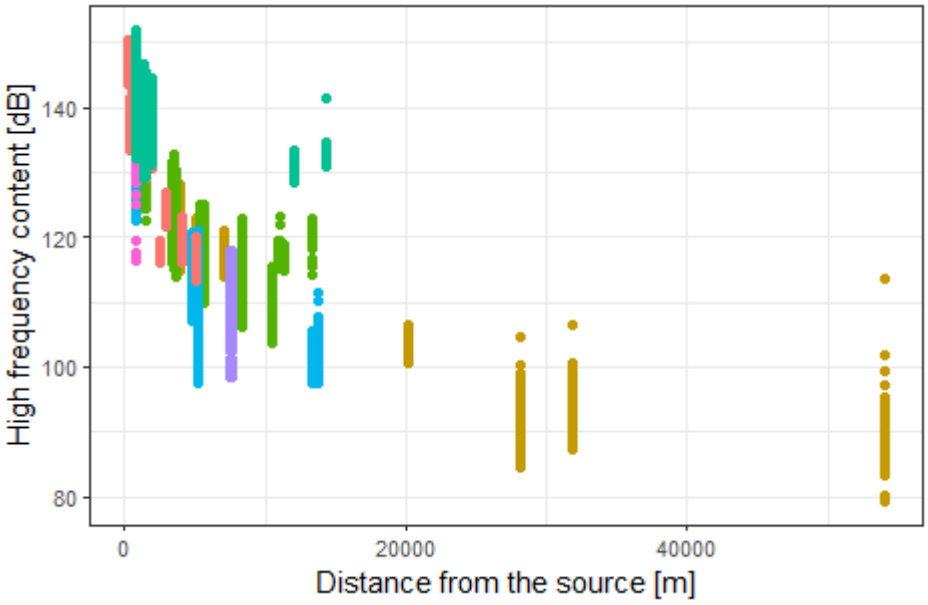

Figure 50. Observed relationship between high frequency content and distance from the piling source colour coded by the seven wind farms.

11.2 Model diagnostics

11.2.1 Kurtosis

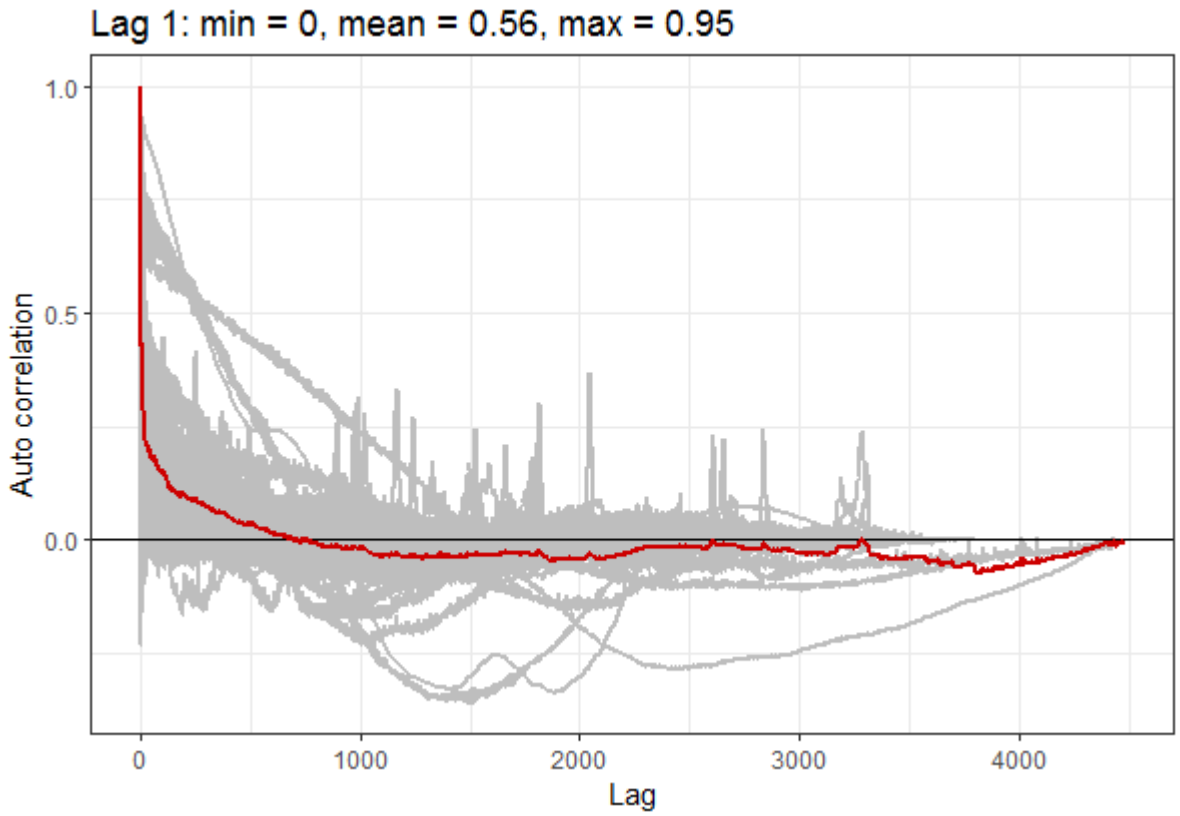

Figure 51. Correlation structure of the model using kurtosis as the response variable. Each grey line is the correlation within a given panel structure: measurements from the same PAM for a given piling operation. The red line is the mean of these correlations.

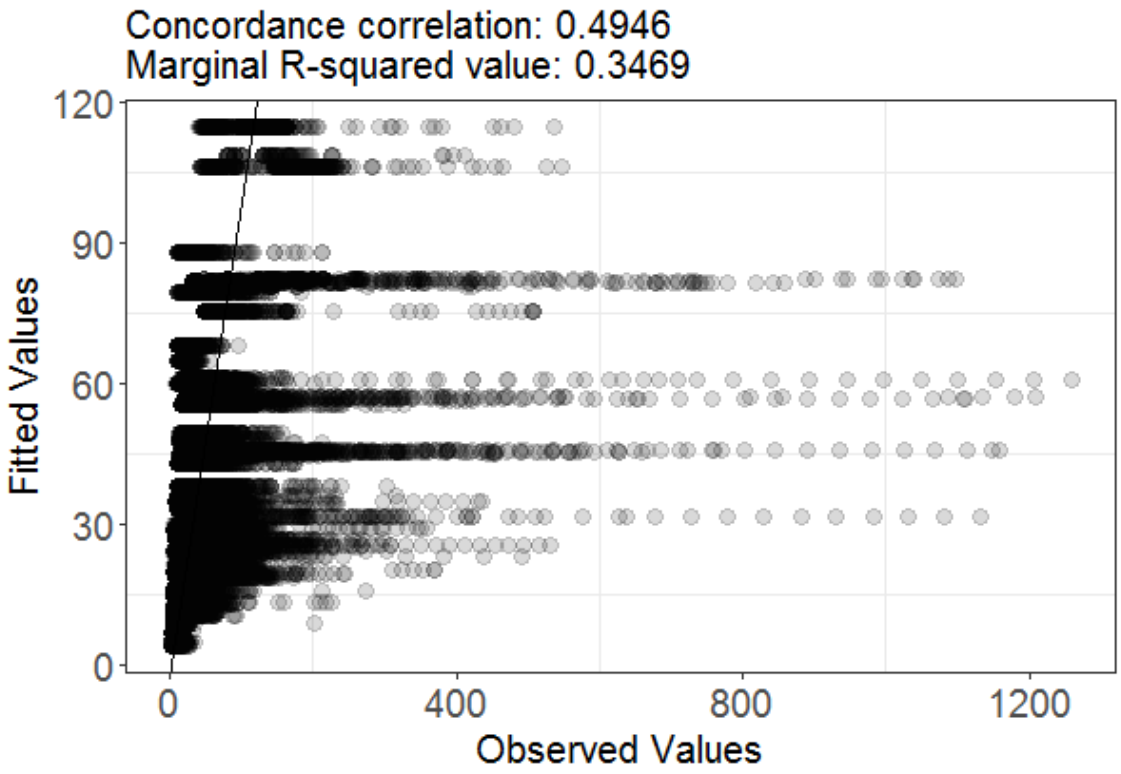

Figure 52. Observed versus fitted values for the model with kurtosis as the response variable. Marginal and concordance correlations are given in the title of the plot. High values of these two corelations indicate a good fit to the data which is medium in the case for this model.

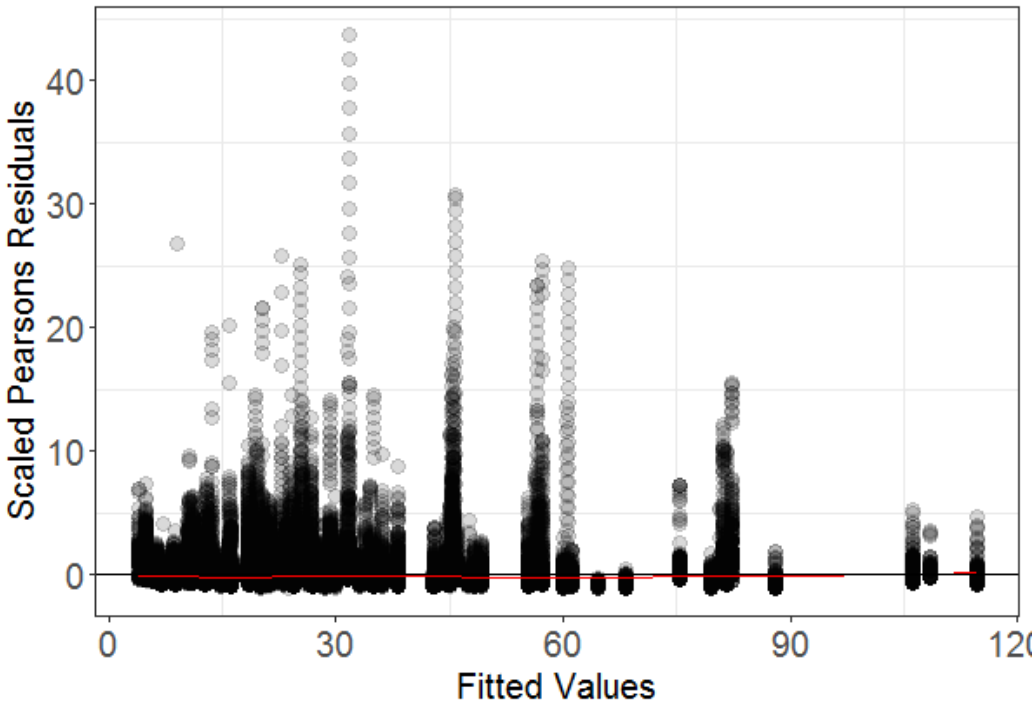

Figure 53. Scaled Pearsons residuals versus fitted values for the model with kurtosis as the response variable. The scaled Pearsons residuals are residuals where the expected relationship given the distribution is taken account of including any extra dispersion estimated via the dispersion parameter.

We would expect to see no pattern and even variance and if this is the case, as for this model, the red line is near horizontal.

11.2.2 Crest factor

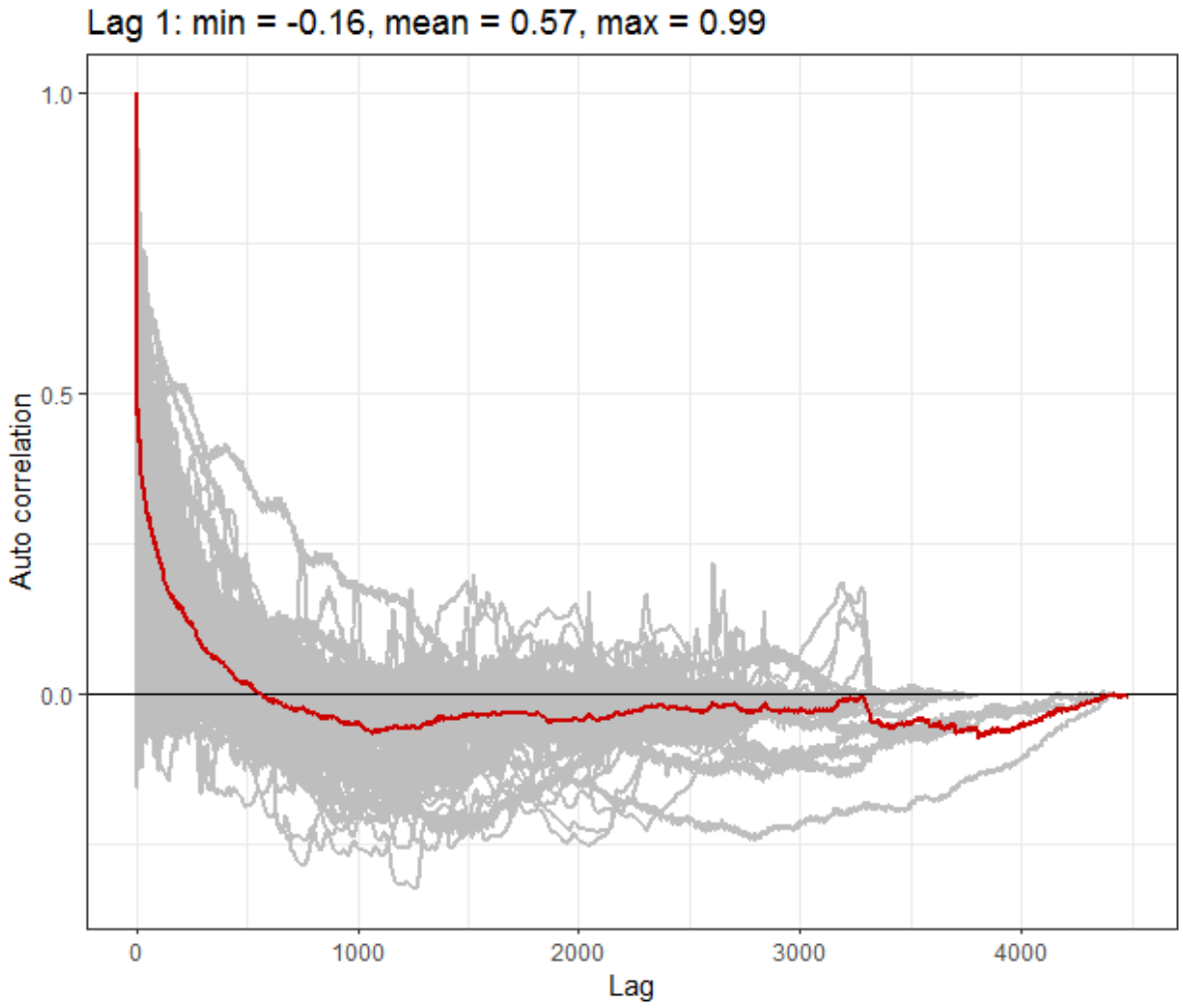

Figure 54. Correlation structure of the model using crest factor as the response variable. Each grey line is the correlation within a given panel structure: measurements from the same PAM for a given piling operation. The red line is the mean of these correlations.

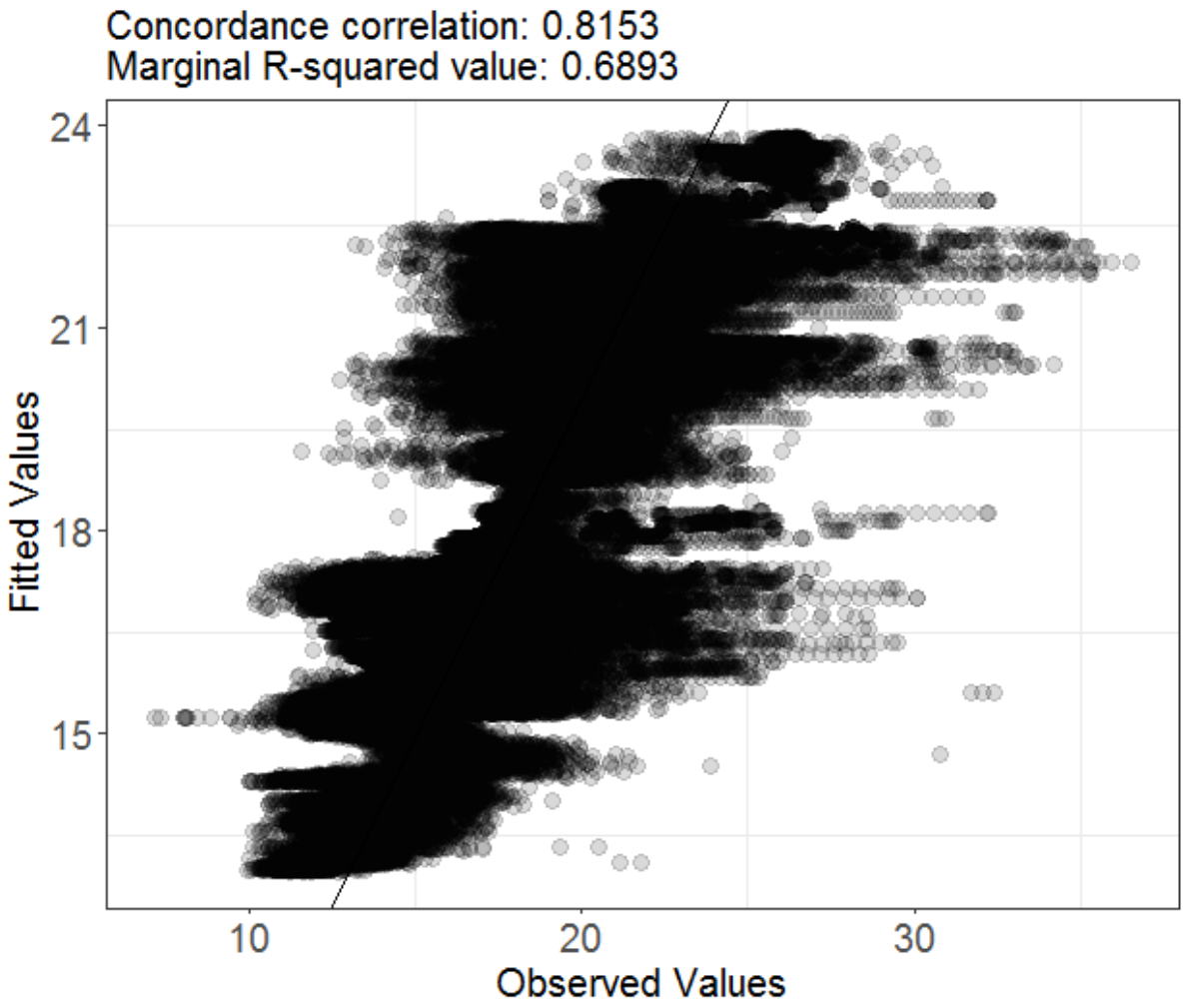

Figure 55. Observed versus fitted values for the model with crest factor as the response variable. Marginal and concordance correlations are given in the title of the plot. High values of these two corelations indicate a good fit to the data which is the case for this model.

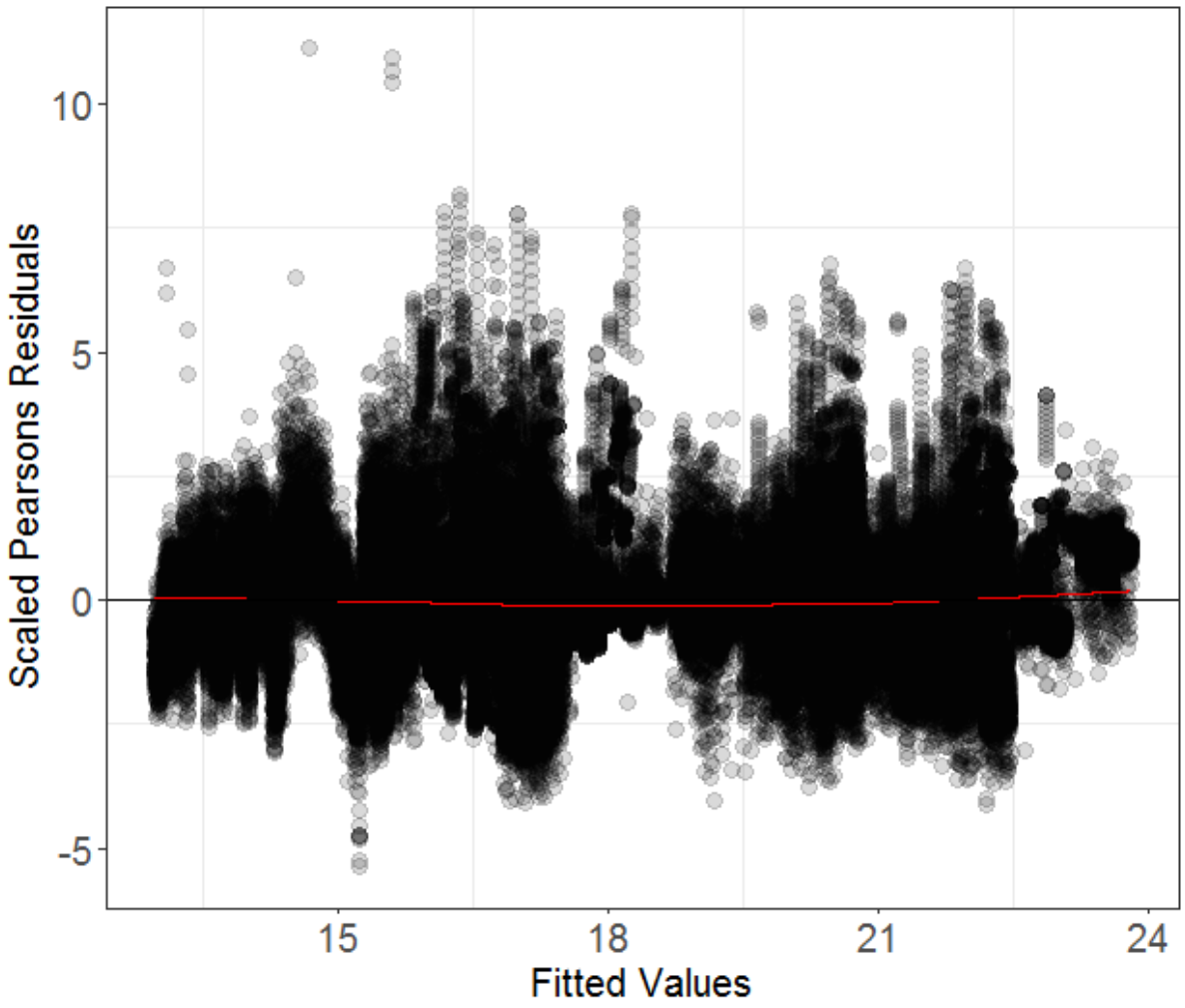

Figure 56. Scaled Pearsons residuals versus fitted values for the model with crest factor as the response variable. The scaled Pearsons residuals are residuals where the expected relationship given the distribution is taken account of including any extra dispersion estimated via the dispersion parameter. We would expect to see no pattern and even variance and if this is the case, as for this model, the red line is near horizontal.

11.2.3 Peak pressure

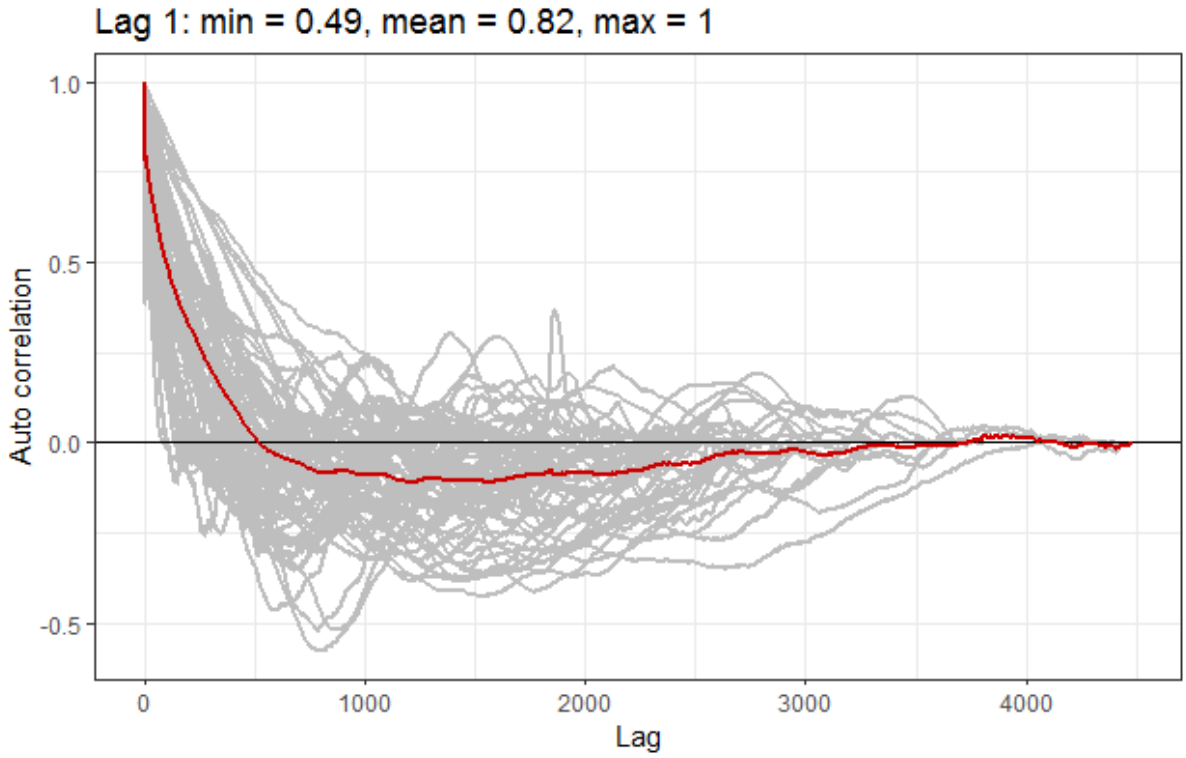

Figure 57. Correlation structure of the model using peak pressure as the response variable. Each grey line is the correlation within a given panel structure: measurements from the same PAM for a given piling operation. The red line is the mean of these correlations.

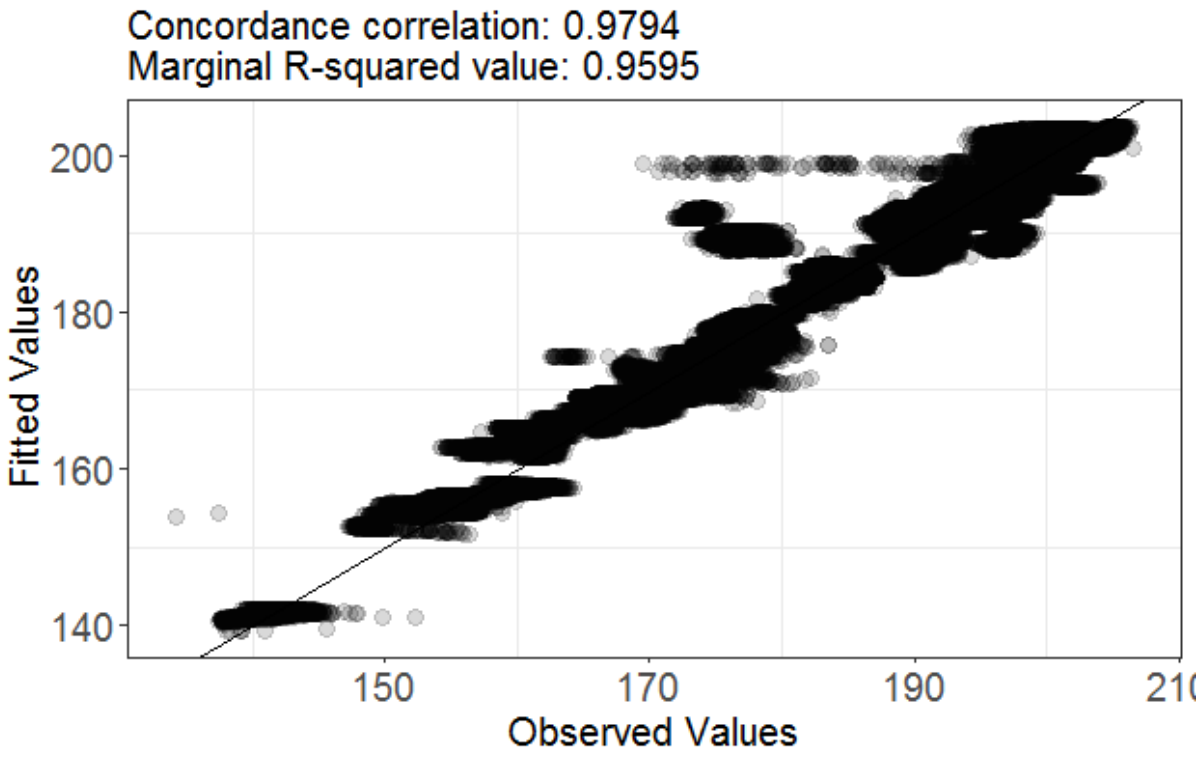

Figure 58. Observed versus fitted values for the model with peal pressure as the response variable. Marginal and concordance correlations are given in the title of the plot. High values of these two corelations indicate a good fit to the data which is the case for this model.

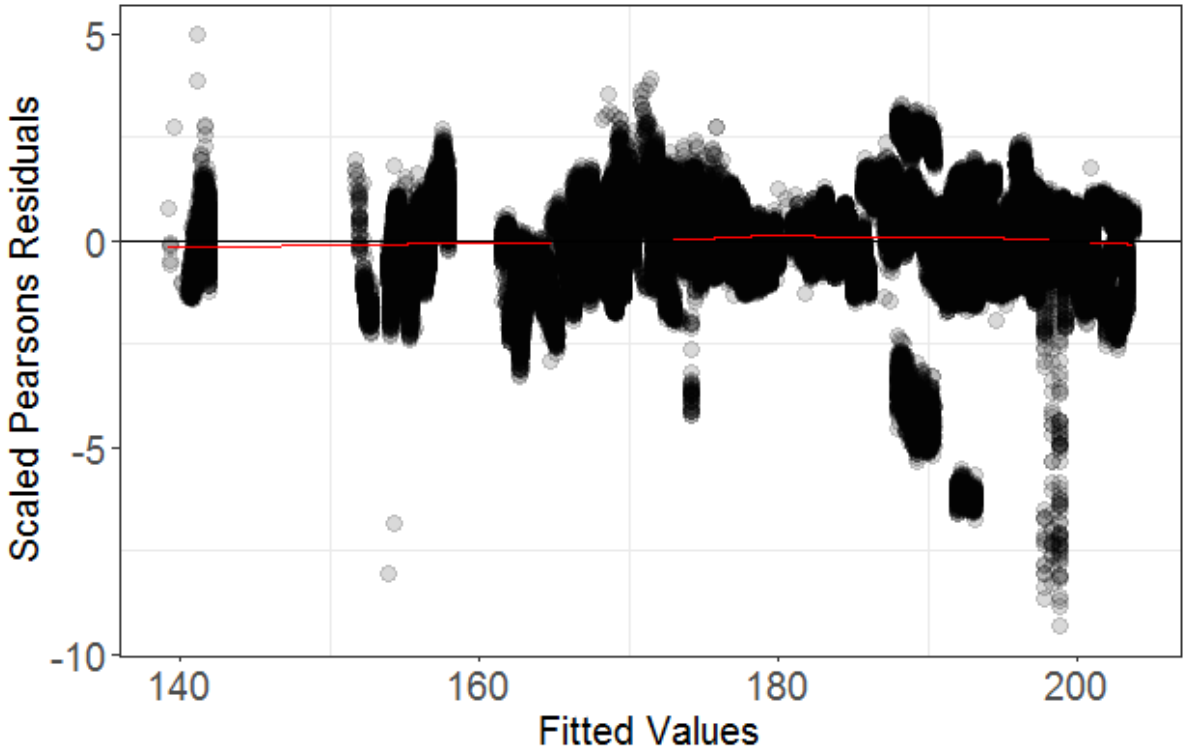

Figure 59. Scaled Pearsons residuals versus fitted values for the model with peak pressure as the response variable. The scaled Pearsons residuals are residuals where the expected relationship given

the distribution is taken account of including any extra dispersion estimated via the dispersion parameter. We would expect to see no pattern and even variance and if this is the case, as for this model, the red line is near horizontal.

11.2.4 High frequency content

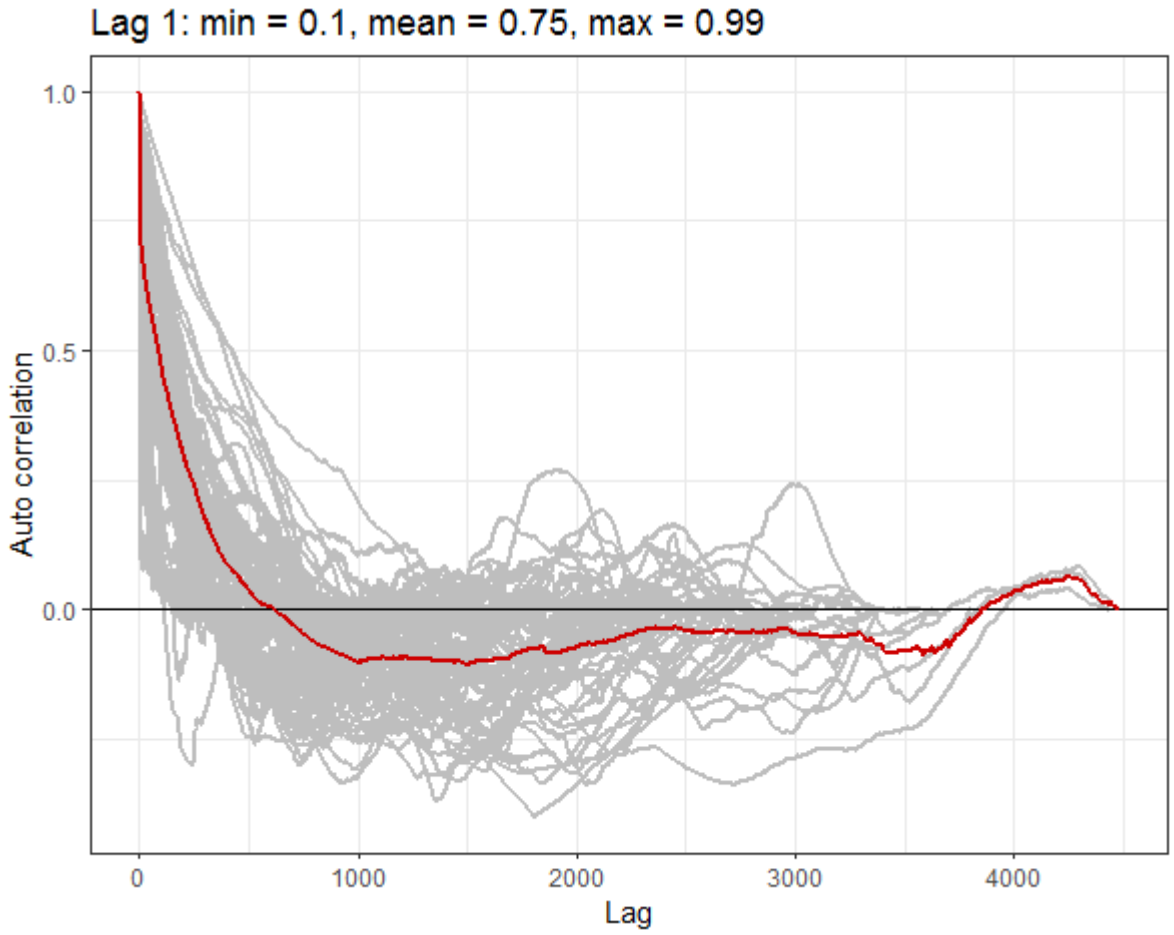

Figure 60. Correlation structure of the model using high frequency content as the response variable. Each grey line is the correlation within a given panel structure: measurements from the same PAM for a given piling operation. The red line is the mean of these correlations.

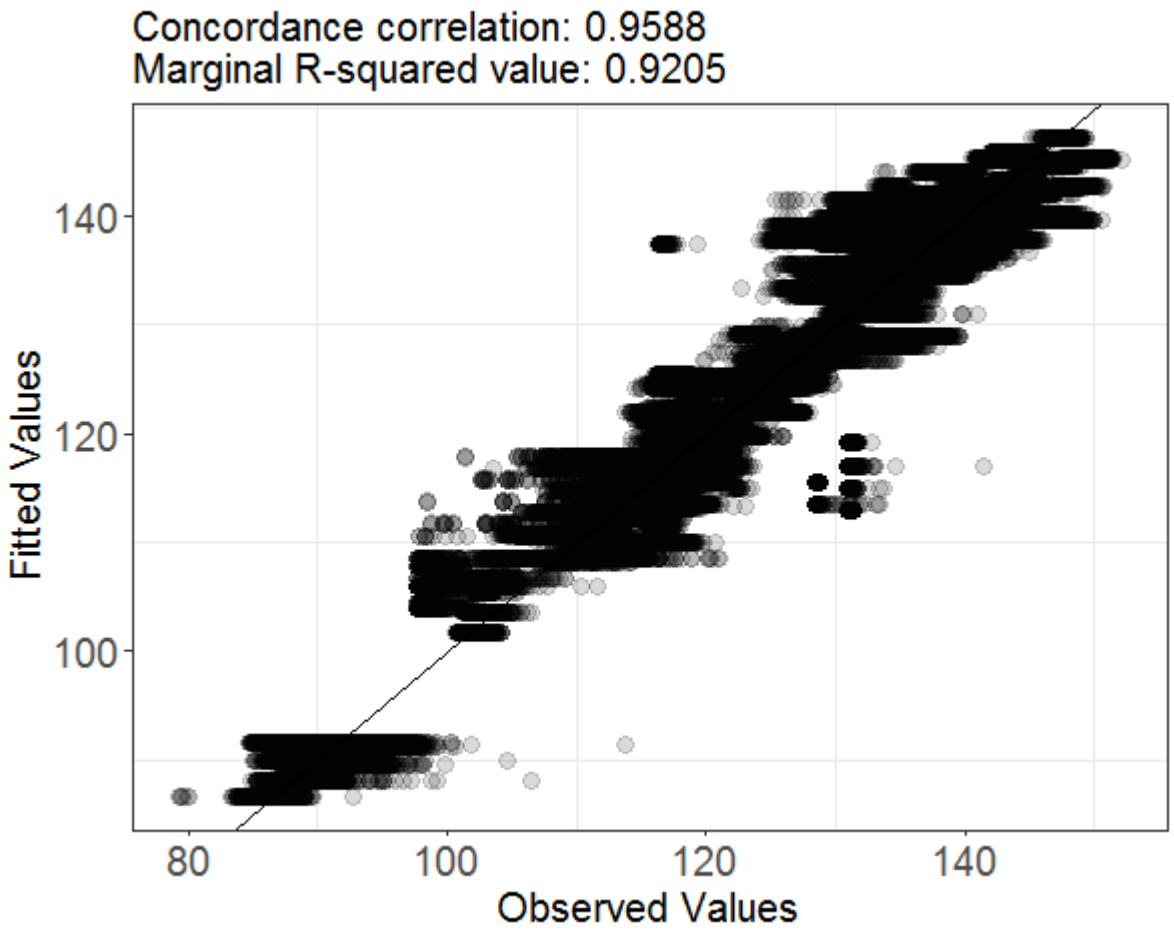

Figure 61. Observed versus fitted values for the model with high frequency content as the response variable. Marginal and concordance correlations are given in the title of the plot. High values of these two corelations indicate a good fit to the data which is the case for this model.

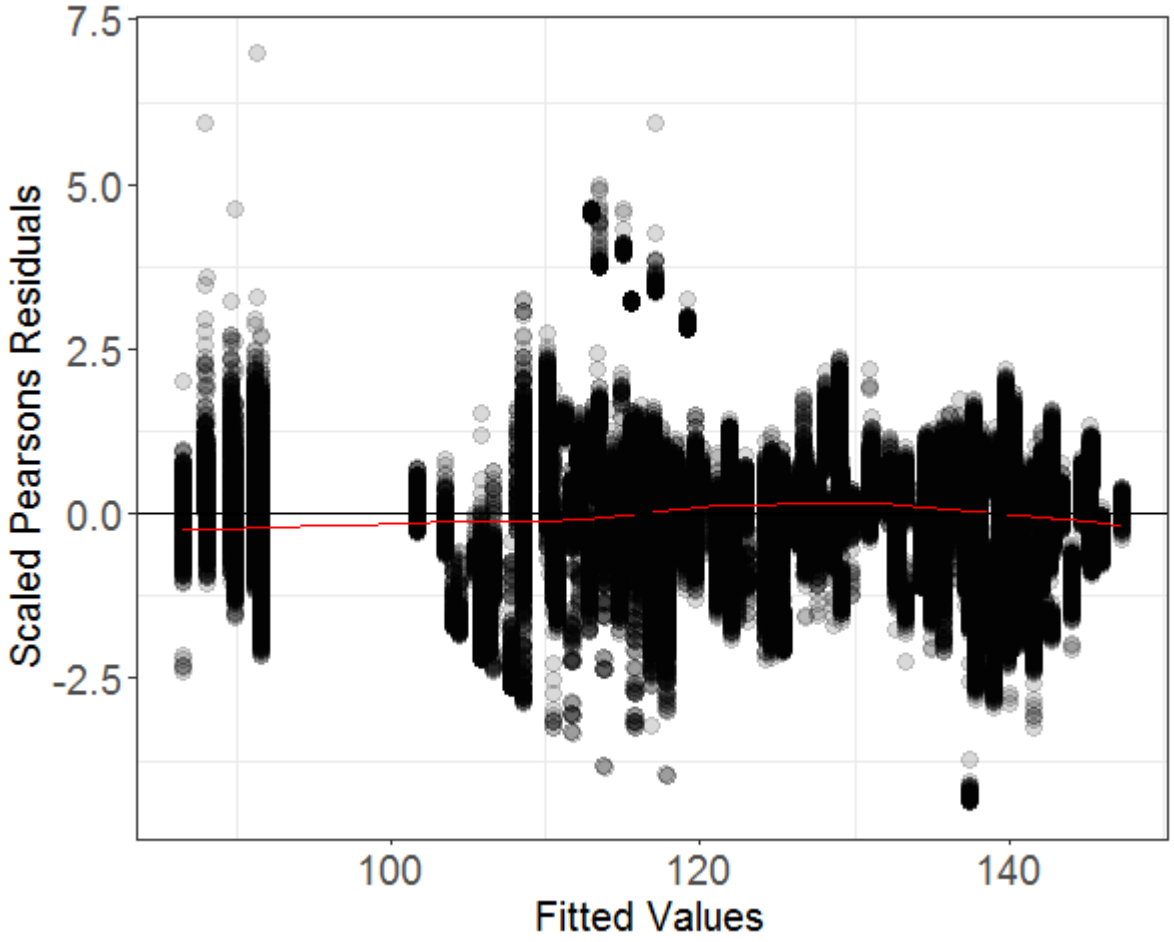

Figure 62. Scaled Pearsons residuals versus fitted values for the model with high frequency content as the response variable. The scaled Pearsons residuals are residuals where the expected relationship given the distribution is taken account of including any extra dispersion estimated via the dispersion parameter. We would expect to see no pattern and even variance and if this is the case, as for this model, the red line is near horizontal.

11.3 Model predictions for the 50 km from the source

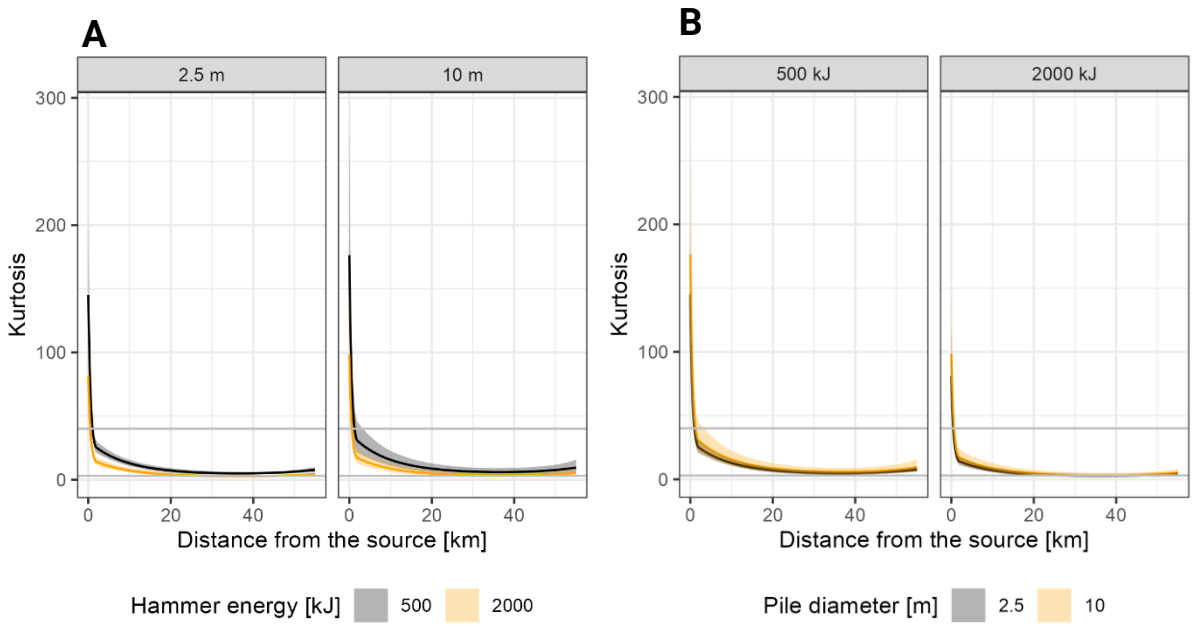

Figure 63. Changes in kurtosis with distance from the piling location plotted for (A) the two pile diameters (2.5 and 10m) and (B) two hammer blow energies (500 and 2000 kJ). The horizontal grey lines indicate kurtosis values thresholds of 40 and 3 respectively. Shaded areas span between upper (95) and lower (5) confidence intervals.

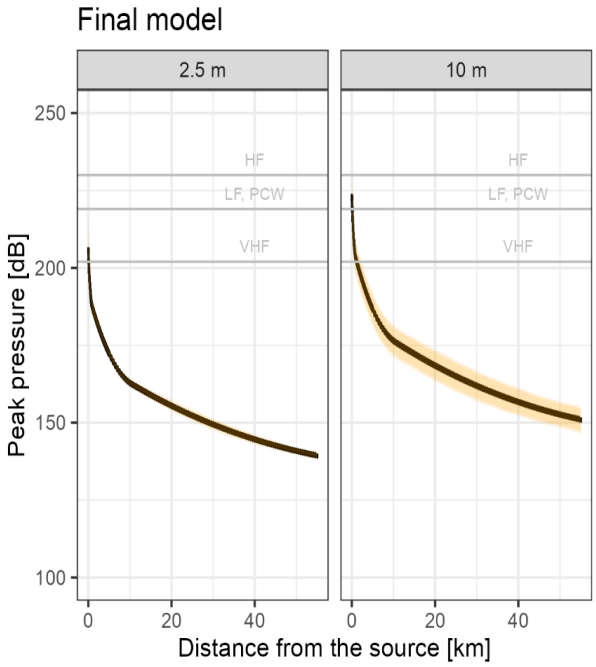

Figure 64. Changes in peak pressure [dB] with distance from the piling location and in the first 30 min of piling for the two pile diameters. The horizontal grey lines indicate thresholds for the four hearing groups of marine mammals: high frequency (HF), low frequency (LF), phocids in water (PCW) and very high

frequency (VHF) as defined in Southall et al. (2019). Shaded areas span between upper (95) and lower (5) confidence intervals.

12 Appendix 4 - Interim workshop report

12.1 Background to workshop

An interim workshop was held to present and discuss the preliminary results of the RaDIN project described in the report. This workshop was hosted by SMRU Consulting and itap GmbH, online on the 19th of June 2023. A total of 34 people attended the interim workshop (Table 13), inclusive of members of regulatory bodies, environmental consultancies, and research institutes. Attendees to the workshop contributed a wide range of knowledge on topics inclusive of environmental impact assessments, acoustic analyses, ecology, and behaviour. The interim workshop began with a series of presentations from SMRU Consulting and itap GmbH on the various streams of work for the RaDIN project, and preliminary results. These presentations were followed by breakout group sessions, in which attendees were split into two breakout groups: "Acoustics", and "Ecological Implications". Each of these groups discussed their titled topic as it relates to the RaDIN project, providing insight and advice as to the best approaches to achieve the goals of the project, as well as discussion of the current progress of the RaDIN project. These breakout group discussions are summarised below.

Table 13. Summary of the attendees to the interim workshop, their affiliations, and breakout group. Note: Some attendees did not participate in breakout group sessions. These are marked with "NA".

Name	Affiliation	Breakout Group
Ross Culloch	APEM	Ecological Implications
Shane Guan	BOEM	Acoustics
Phil New	GoBe	Ecological Implications
Anna Luff	Gobe	Ecological Implications
Caroline Carter	HiDef	Ecological Implications
Michael Bellmann	Itap GmbH	Acoustics
Patrick Remmers	Itap GmbH	Acoustics
Klaus Lucke	JASCO	Acoustics
Sonia Mendes	JNCC	Ecological Implications
Joseph Onoufriou	Marine Scotland Science	Ecological Implications
Tiffini Brookens	Marine Mammal Commission	Acoustics

Name	Affiliation	Breakout Group
Ophelie Humphrey	Natural England	Ecological Implications
Kate Grellier	Natural Power	Ecological Implications
Nicholas Flores Martin	Natural Resources Wales	Acoustics
Rona McCann	NatureScot	Ecological Implications
Amy Scholik-Schlomer	NOAA	Acoustics
Oliver Patrick	ORJIP	Ecological Implications
Matej Simurda	Orsted	Acoustics
Cassie Greenhill	RWE Renewables	Ecological Implications
Ron Kastelein	Seamarco	Ecological Implications
Aimee Kate Darias-O'Hara	SMRU Consulting	Ecological Implications
Cormac Booth	SMRU Consulting	Ecological Implications
Rachael Sinclair	SMRU Consulting	Ecological Implications
Natasha Hardy	SMRU Consulting	NA
Jason Wood	SMRU Consulting	NA
Magda Chudzinska	SMRU Consulting	Ecological Implications
Madalina Matei	SMRU Consulting	Acoustics
Brandon Southall	Southall Environmental Associates	Acoustics
Ashley Leiper	SSE Renewables	Acoustics
Andrew Logie	SSE Renewables	NA
Tim Mason	SubAcoustech	Acoustics
Sander Von Benda-Beckmann	TNO – Expertise group for Acoustics and Sonar	Acoustics
Gordon Hastie	University of St. Andrews	Acoustics
Ewan Edwards	Xodus	Ecological Implications

12.2 Proceedings

12.2.1 Interim workshop presentations

The interim workshop presentation session was led by Dr. Cormac Booth, with Aimee Kate Darias-O'Hara as rapporteur. They provided a brief overview of the aims and objectives of the project, and introductions to the various work packages being undertaken as part of this project. These are inclusive of:

- WP1: Literature review
- WP2: Collation of field data
- WP3: Analysis of field data
- WP4: Interim workshop
- WP5: Animal movement tool to estimate PTS impact ranges

Each of these work packages were subsequently presented on by Cormac Booth, Michael A. Bellmann, and Madalina Matei, providing attendees with an overview of the methods and preliminary results for each work package.

12.2.2 Breakout groups

To facilitate discussions on high priority topics, two breakout groups were formed, focused on the topics of acoustics, and ecological implications. The breakout groups had the objective of discussing the given topic as it relates to the RaDIN project and allow attendees to provide feedback on the current work undertaken by the RaDIN project team, as well as provide recommendations for future research, and next steps in the project. In both breakout groups, online Jamboards were utilised to allow attendees to share feedback and suggestions in note format. Participants were able to add text boxes under different themes in a live and collaborative environment – ensuring the key topics were captured.

12.2.2.1 Acoustics

Dr. Michael A. Bellmann chaired this session, with Madalina Matei as rapporteur. During this breakout group session, various topics were discussed (Figure 65). The breakout group attendees concluded that currently, impact ranges may be overestimated due to a lack of accountability for the transition from impulsive to non-impulsive state of sounds.

Feedback was also provided by participants on the metrics of impulsiveness. A key conclusion was that metrics of impulsiveness computed should consider the characteristics of the target signals. Specifically, their production rate, and additional contextual details such as possible sources of disturbing noise (e.g., the number of vessels present during the monitored activity). Further to this, if construction reports or hammer logs are available, they could be used to contextualise noise levels and extract easy-to-compute metrics such as high frequency content during the periods with impulsive sounds and filter out high frequency noises from other known sound sources. Participants acknowledged that metrics which are complicated to compute (due to the advanced levels of computer power and skillsets required) may be challenging to implement in a variety of cases, especially so where analysts lack the resources to detect and characterise impulses. To combat this, in cases where metrics of impulsiveness are autocorrelated to a high degree, and one of these metrics reliably

translates to impacts on hearing, the easier-to-compute metric could be selected for extraction and estimation of impact. Alternatively, a multi-level criterion was recommended, in which several metrics of impulsiveness could be used to establish when signals transition from being impulsive, to non-impulsive. Effective quiet was also recommended by participants to quantify and assess the risks of hearing loss in cetaceans, depending on the changes in ambient noise levels during activities which produce impulsive sounds.

A key discussion the participants had was on the current knowledge gaps relating to this topic. Participants concluded that there is a lack of empirical data from marine mammals exposed to signals with variable degrees of impulsiveness. There is also a lack of empirical evidence indicating whether signals with kurtosis values between 3 and 40 (considered to not be "fully impulsive") have a lesser impact on the hearing capabilities of marine mammals. It was also noted that metrics of impulsiveness have not yet been used to assess the onset of behavioural responses in marine mammals. Further to this, there is currently a lack of comparable datasets from mitigated construction activities, with participants concluding that the methods developed during the RaDIN project could be applied to acoustic recordings from such activities, but making predictions using only data from unmitigated activities is not recommended. Lastly, participants concluded that there is a need for both methodology and terminology harmonisation (e.g., 'intermittent' versus 'impulsive' sounds). Metrics of impulsiveness such as kurtosis, high frequency content, and crest factor, are not yet part of the ISO standards. The RaDIN project could provide recommendations regarding what should be measured and how results should be reported.

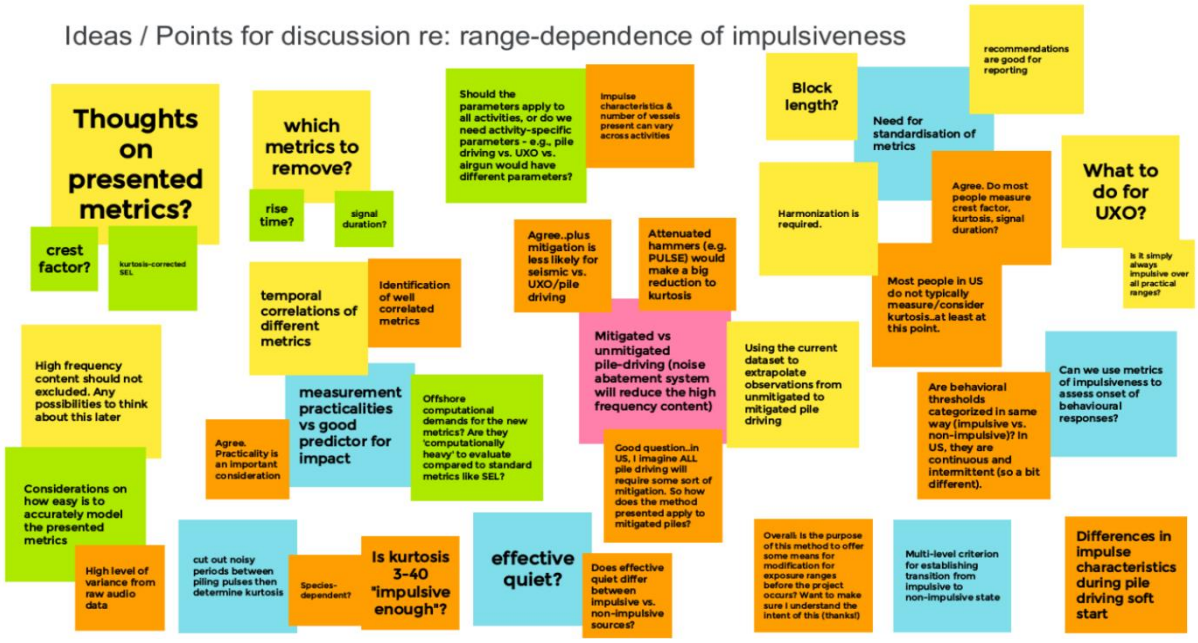

Figure 65 - Jamboard notes from the Acoustics breakout group.

12.2.2.2 Ecological Implications

Cormac Booth chaired this session, with Aimee Kate Darias-O'Hara as rapporteur. This breakout group session covered numerous topics (Figure 66). Amongst the topics discussed, key focus was placed on ensuring that the functionality of the animal movement tool to estimate PTS impact ranges is suitable for use in the impact assessment process. Participants concluded that the following aspects should

be considered by the tool, or future research, such as; recovery during pile driving breaks (inter-pulse intervals), effective quiet (specifically, at what level it is thought that temporary threshold shift (TTS) is still accumulating). Discussions were had on the inclusion of mitigation and abatement (e.g., the use of ADDs) in future work. Considerations should also be made as to individual animals changing their movement speeds over time, it was acknowledged that this would be implementable in theory, but consideration would have to be given as to what parameters are available. This tool was concluded to be useful in future impact assessments, as it was raised during discussions that in some cases, it's not disclosed how precautionary impact assessments have been, in comparison to what the real world data for construction impact reported.

The levels of certainty needed for impact assessments was a key topic discussed amongst participants, with specific thought given to how we consider other species such as minke whales, and what the solutions are when there is very little knowledge on the hearing of many marine mammal species. Consideration was also given to the probability of impulsiveness and dose-response curves. Perhaps most importantly, it was raised that the transparency of results must be considered, in particular, how the results will be reviewed by the regulators and their advisors. The uncertainty will be the most important aspect when determining how this tool will be used in predictive impact assessments.

Participants provided feedback on the RaDIN project as it relates to their individual project needs. This included ensuring that the tool is user-friendly and considering the transferability of the tool to other areas of the globe (or in some cases, within the North Sea itself). To assist with transferability, it was agreed with the project team that depth and salinity will be incorporated at a minimum. It was noted by participants that it will be essential for the RaDIN project to also identify key evidence gaps to guide future research priorities, as well as recommendations on the design of acoustic arrays at wind farms when measuring noise levels, as different array designs may bring additional levels of uncertainty.

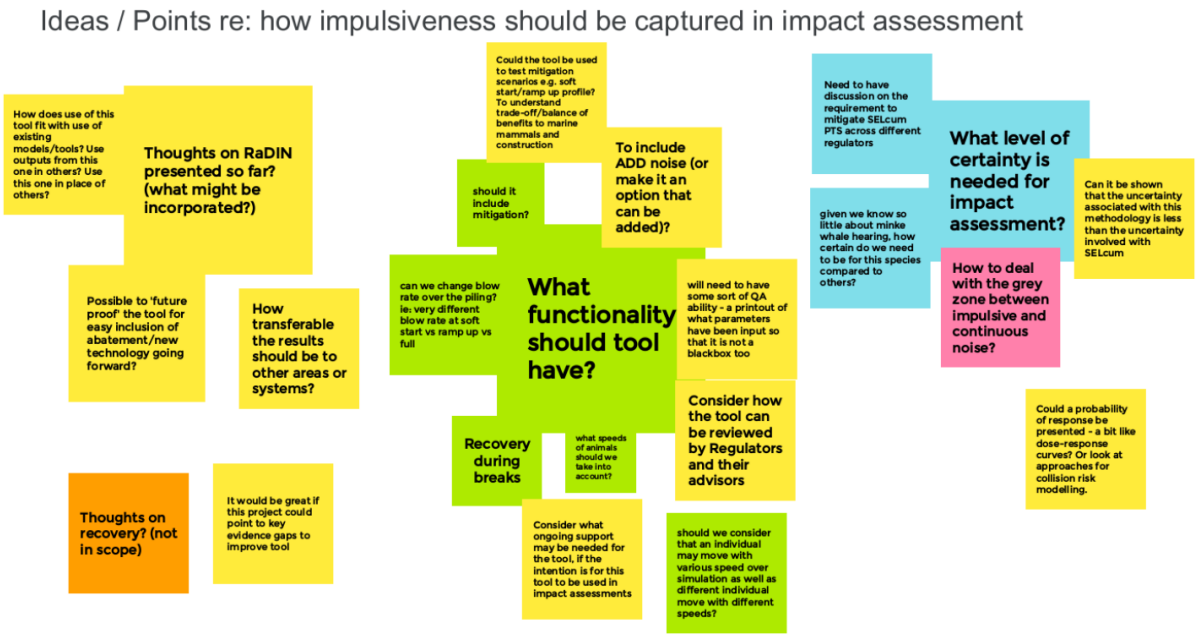

Figure 66 - Jamboard notes from the Ecological Implications breakout group.

12.2.3 Concluding discussions

Following the closure of the breakout groups, the workshop attendees returned to the main session for concluding discussions, chaired by Cormac Booth, with Aimee Kate Darias-O'Hara as rapporteur. This final session included summaries of the breakout group discussions provided by the respective rapporteurs of each breakout group, and a group discussion on the overall RaDIN project. These discussions mainly focused on the challenges for the WP5 tool in that there are currently no threshold shift growth rates available to be incorporated. Further to this, discussions were had on the limitations of the movement tool to estimate PTS impact ranges, to ensure that the results given are robust. It was also discussed amongst participants that the RaDIN project is an initial start to addressing the research questions outlined, and that further work will likely be required in the near future. The interim workshop was closed by Cormac Booth, providing thanks to attendees for their time and input, and reiterating the proposed timeline for the completion of the RaDIN project.

13 Appendix 5 – PTS framework simulation results

13.1 Framework overview

PTS onset impact ranges represent the starting distances from the pile for animals to escape (i.e., move away from the sound source) and prevent them from receiving a dose higher than the PTS onset threshold. We define these as "PTS impact ranges". The aim of this work package is to develop a framework that will allow for the assessment of PTS impact ranges based on a fleeing animal model under different pile driving scenarios.

The purpose of this analysis was to determine the relative differences (i.e., increases or decreases in PTS onset ranges) between different scenarios. The absolute PTS ranges presented are only indicative.

A detailed manual on how to use the model and all the input files necessary to run it are given in a public GitHub repository here https://github.com/SMRU-Consulting-Github/RADIN-framework-development. The model description follows the updated ODD protocol (Overview, Design concepts, Details), suggested by Grimm et al. (2006), (2010). The phrases in *italics* refer to names of a given parameter used in the R code.

13.1.1 Model overview

The model is a one-dimension (1D) agent-based model (ABM) simulating the movement of animals (referred to as *animats*) moving through a soundscape away (set with a source level and transmission loss model) from the source location in a straight line at a user defined speed. In reality, animals may not move in a straight line away from the source. Therefore, we tested a range of speeds between 0.2 and 5 m/s. The lower speed values can account for the fact that animals may not move in a straight line away from the source and, in such cases, their average speed along the straight line could be close to the lowest value chosen. The pattern of blows from pile driving can be fixed to a specified blow rate or by using an input file (which provides the exact pattern of blows, for example, from a real pile installation log).

13.1.1.1 Purpose and patterns

The aim of the model is to simulate movement of animats distributed across the soundscape at different distances from the noise source, and to understand how the movement of animats and soundscape characteristics affect their sound exposure level (SEL) and ultimately PTS onset ranges.

13.1.1.2 Entities, state variables, and scales

The model includes two entities: animats and soundscape patches. Animats are characterised by their position and speed [m/s] and landscape patches are characterised by their ambient noise level, which is quantified using the root-mean-squared sound pressure level metric [dB re 1 µPa].

The spatial extent of the landscape is 50 km and each landscape patch in the model represents 10 m. One time step corresponds to one second.

13.1.1.3 Process overview, scheduling and model initialisation

The model is initialised by creating a user-defined number of animats distributed along the 1D soundscape. At each time step, all animats move away from the first soundscape patch (location of the simulated pile) at a given speed set the same for all individuals for a given simulation.

As the animats move through the soundscape patches, they accumulate noise from impact pile driving strikes (also referred to as 'blows'). This noise is quantified using the single strike sound exposure level metric (SEL_{ss} [dB re 1 µPa^{2}s]). SEL_{ss} at each soundscape patch is calculated as follows (Equation 11):

$$SEL_{ss} = SL_{ss} - x * \log_{10} r + \alpha * \left(\frac{r}{1000}\right) \qquad \text{Equation (11)}$$

where SL_{ss} is single strike source level [dB re 1 µPa] (*source_level*), x is the propagation loss (*log_multiplier)*, r – distance from the source [km], and α absorption coefficient [dB/km] (*attenuation_coefficient*).

The source level is assumed to be located at the first patch of the soundscape. If SEL_{ss} in a given patch is below ambient noise (*ambient_noise*), it is set to ambient noise.

At each time step, the distance of an animat to the source, an indicator whether there was a pile strike or not, and the SEL_{ss} are output.

13.1.2 PTS onset range calculation

PTS onset ranges are calculated using a Movement Analysis R script, which is based on the noise exposure criteria from Southall et al. (2019).

For each animat that accumulates enough SEL_{cum} to experience a TTS onset, this analysis routine continues to accumulate all additional measurements of SEL_{ss} until a 40 dB threshold shift is reached (i.e., the animal accumulates enough threshold shift to reach the PTS threshold). A frequency weighted correction is applied in the process of calculating the cumulative SEL, as shown in Equation 12:

$$SEL_{cum} = 10 * log_{10}\left(\sum_{i=1}^{n} 10^{\frac{SEL_{SS}-SEL_{corr}}{10}}\right)$$ Equation (12)

, where SEL_{ss} is single strike sound exposure level at each time step i [dB re 1µPs^2 s], and SEL_{corr} is the Southall frequency weighted correction specific to each functional hearing group from Southall et al (2007) [dB re 1µPs^2 s] (provided in Table 14). SEL_{ss} is set to zero during time steps *i* without any blow. We, therefore, assume that animals do not accumulate SELs in between the strikes.

Table 14. Functional marine mammal hearing groups, auditory bandwidth (estimated lower to upper frequency hearing cut-off) and levels of cumulative sound exposure level (SELcum) expected to trigger auditory permanent threshold shifts following exposures to impulsive sounds, from Southall et al. (2007; 2019).

Functional hearing group	Estimated auditory bandwidth	SEL_{cum} threshold for triggering PTS (dB re 1 µPa^{2}s) *	SEL_{ss} auditory correction [dB re 1µPa^{2}s]
Low frequency cetaceans	7 Hz to 22 kHz	208 dB	39.9
High frequency cetaceans	150 Hz to 160 kHz	210 dB	35.8
Very high frequency cetaceans	200 Hz to 180 kHz	180 dB	5.6
Pinnipeds in water	75 Hz to 75 kHz	210 dB	18.8

** These thresholds are derived from the TTS onset thresholds for each hearing group plus 40 dB, which indicates the onset of PTS.*

The accumulation process that leads to PTS onset is performed by multiplying the cumulative experienced noise (SEL_{cum}) by a growth rate value which is distinct for continuous and impulsive noise (see Figure 67). For each decibel of continuous noise experienced, the TTS is elevated by 1.6 dB whereas for impulsive sounds, the TTS is elevated by 2.3 dB. These growth rate multipliers are provided in the PTS onset criteria from Southall et al. (2019) and were established following noise exposure studies with chinchillas.

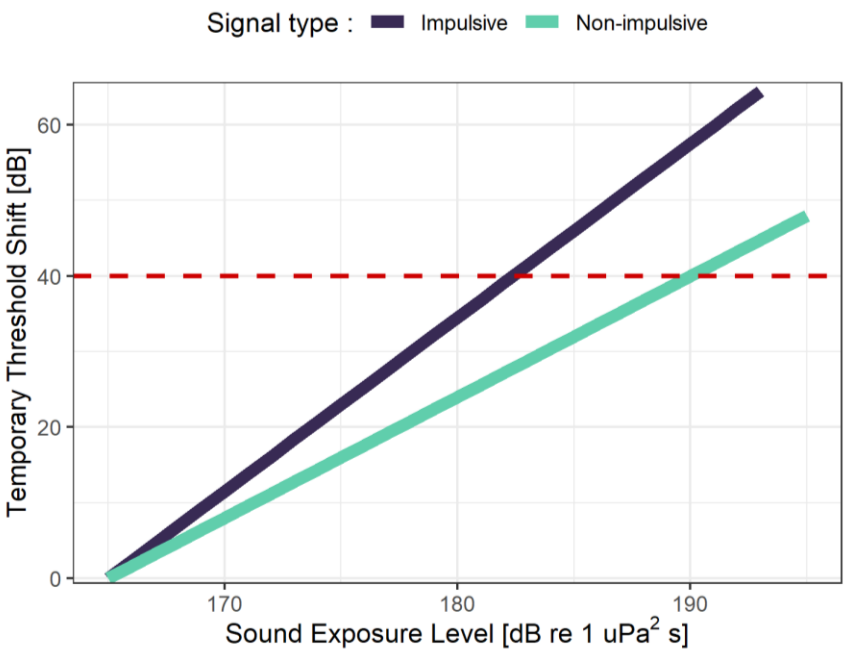

Figure 67. Auditory threshold shift growth rate for impulsive and non-impulsive sounds based on noise exposure criteria from Southall et al. (2019). A threshold shift of 40 dB is used as an indicator of the onset of PTS. Yellow line indicates impulsive growth rate and black line shows the non-impulsive growth rate.

When a TTS value of 40 dB is reached, the given animat is considered to have experienced PTS and their starting distance from the piling location (the first patch in the 1D simulation) is recorded.

The output of the tool is the maximum distance at which animats must be at the start of piling in order to experience PTS. These distances are calculated for four hearing groups: very high frequency (VHF), high frequency (HF), low frequency (LF), and phocids in water (PCW).

13.2 Real world hammer logs

The figures below show changes in PTS ranges (expressed as maximum distance at which animals need to be at the start of piling to receive PTS during piling duration) with animal speed on the x-axis for all 44 real piling schedules. The blow rate pattern is indicated by the line type: the dotted lines show the results of a simulated baseline, and the solid line shows the results for a given hammer log. The distance from the source where sound is assumed to become non-impulsive is indicated by the colour of the lines.

Note that for all simulations grey and orange lines overlap. The title of each graph shows mean and median inter-pile strike interval and the total duration of piling, as well as ID of the piling schedule. The dotted lines show the result of a simulated EIA baseline. The lower panel depicts strike frequency and corresponds to the overview of the strike frequencies shown in Figure 17.

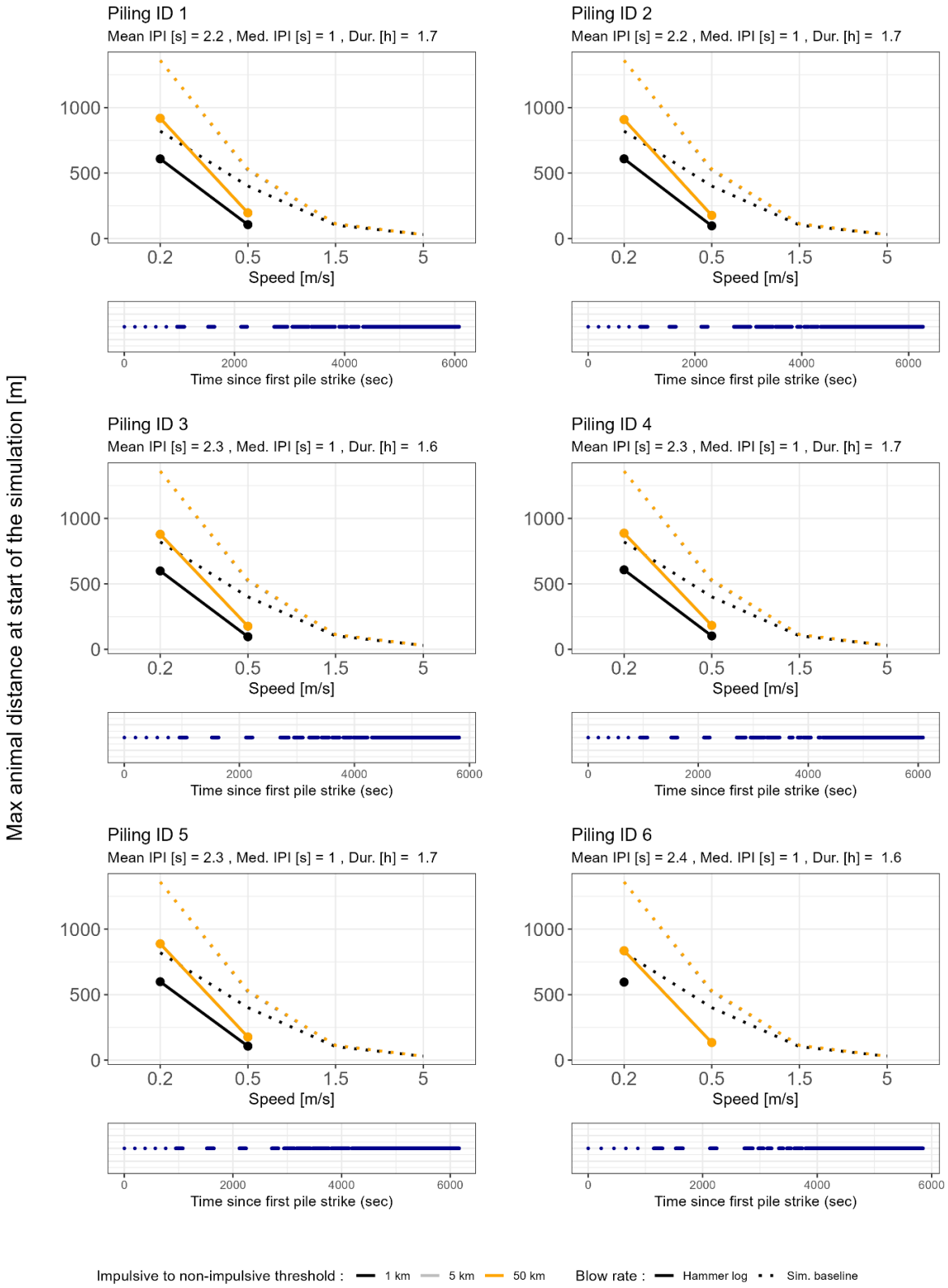

Figure 68. Changes in PTS ranges (expressed as maximum distance at which animals need to be at the start of piling to receive PTS during piling duration) with animal speed on the x-axis for 6 of the 44 real piling schedules (piling IDs 1-6).

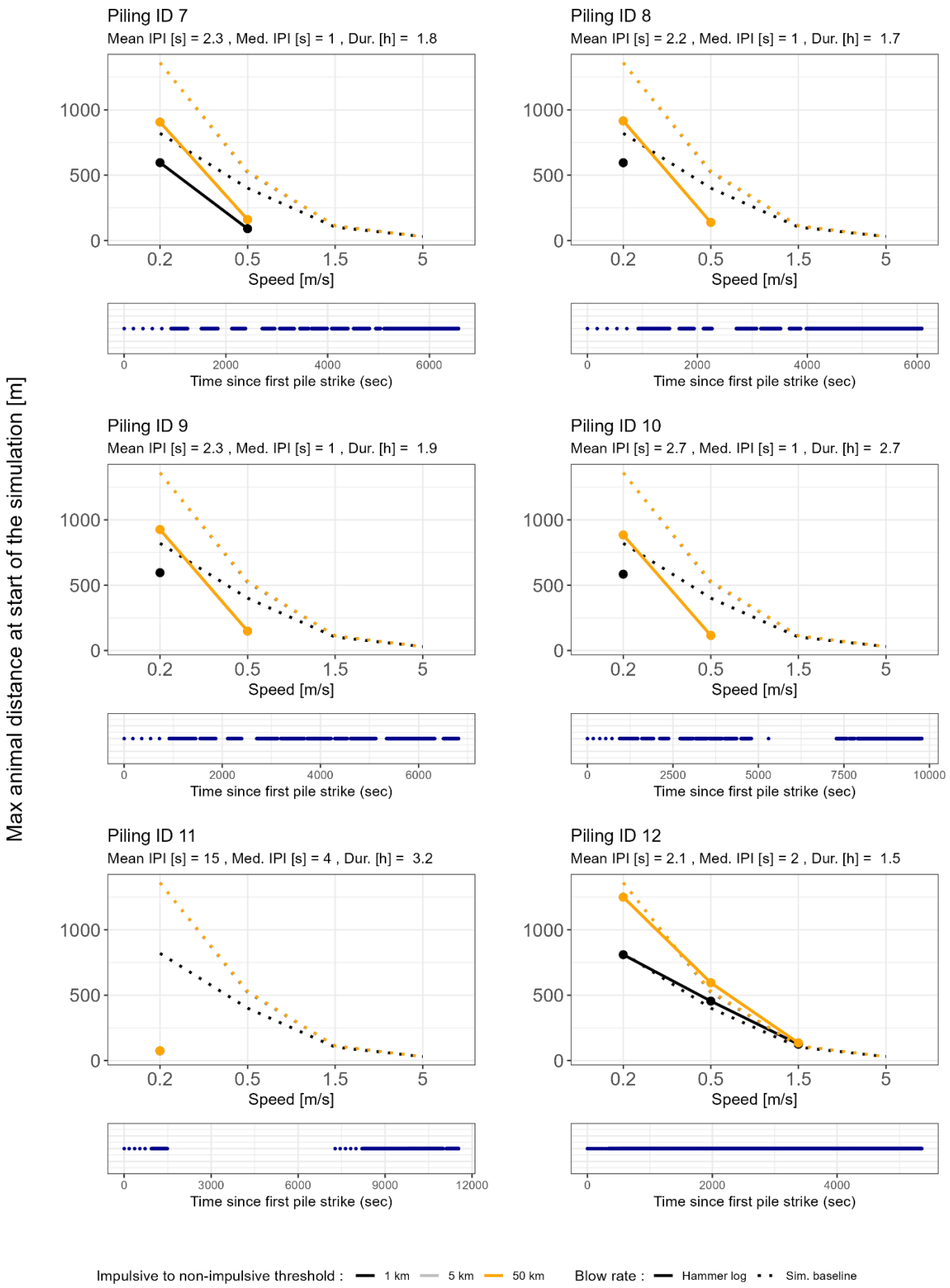

Figure 69. Changes in PTS ranges (expressed as maximum distance at which animals need to be at the start of piling to receive PTS during piling duration) with animal speed on the x-axis for 6 of the 44 real piling schedules (piling IDs 7-12).

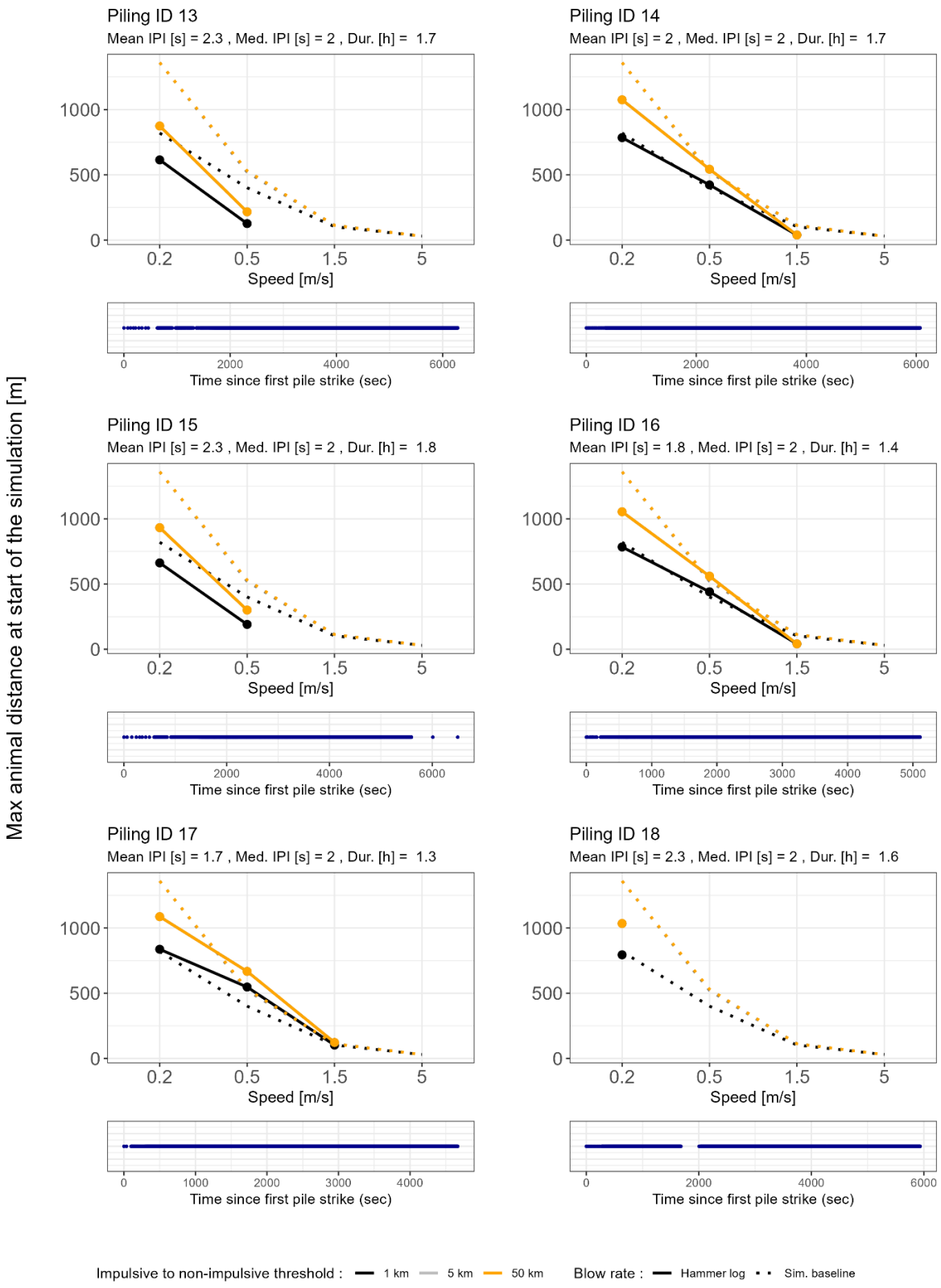

Figure 70. Changes in PTS ranges (expressed as maximum distance at which animals need to be at the start of piling to receive PTS during piling duration) with animal speed on the x-axis for 6 of the 44 real piling schedules (piling IDs 13-18).

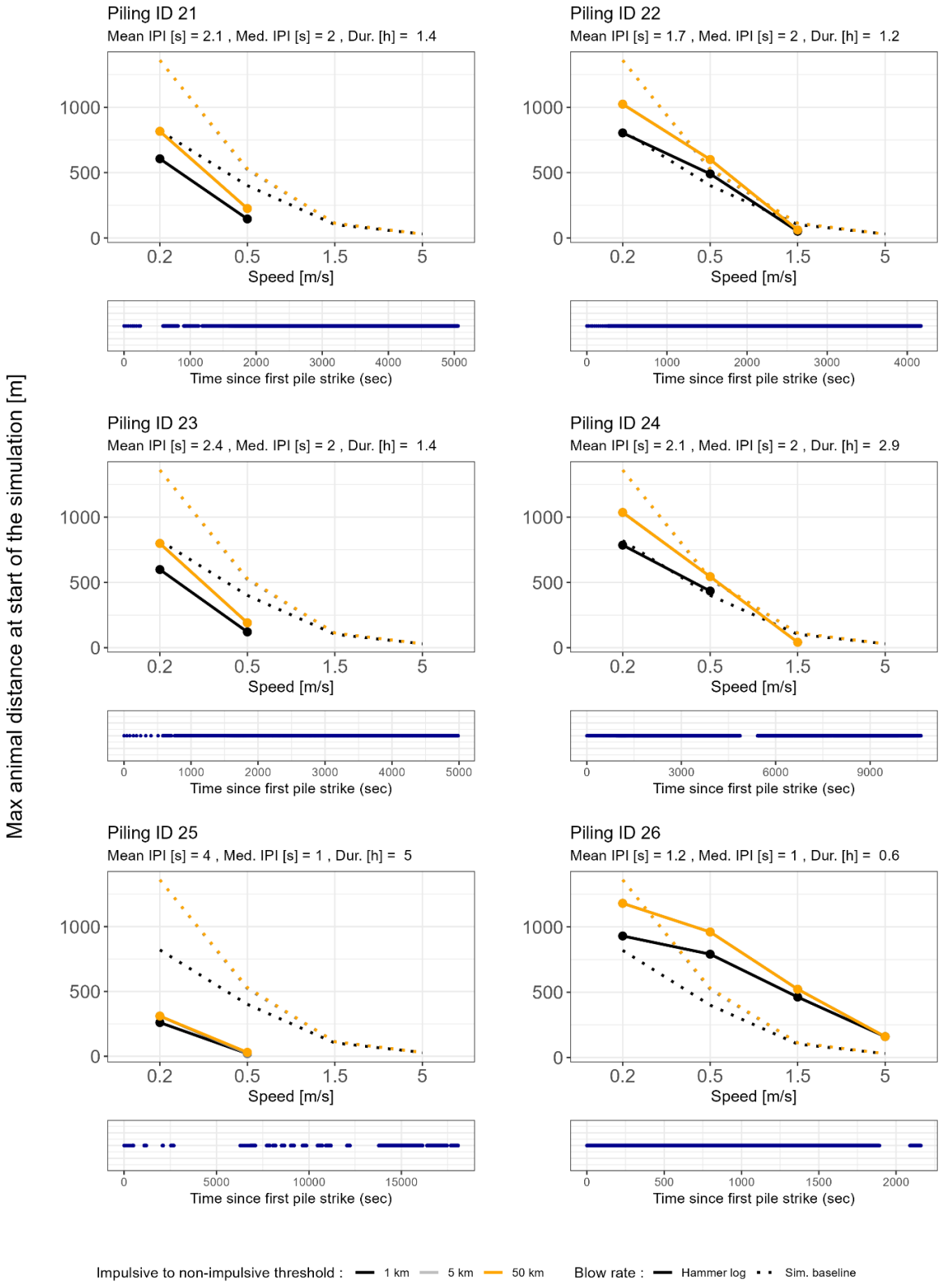

Figure 71. Changes in PTS ranges (expressed as maximum distance at which animals need to be at the start of piling to receive PTS during piling duration) with animal speed on the x-axis for 6 of the 44 real piling schedules (piling IDs 21-26).

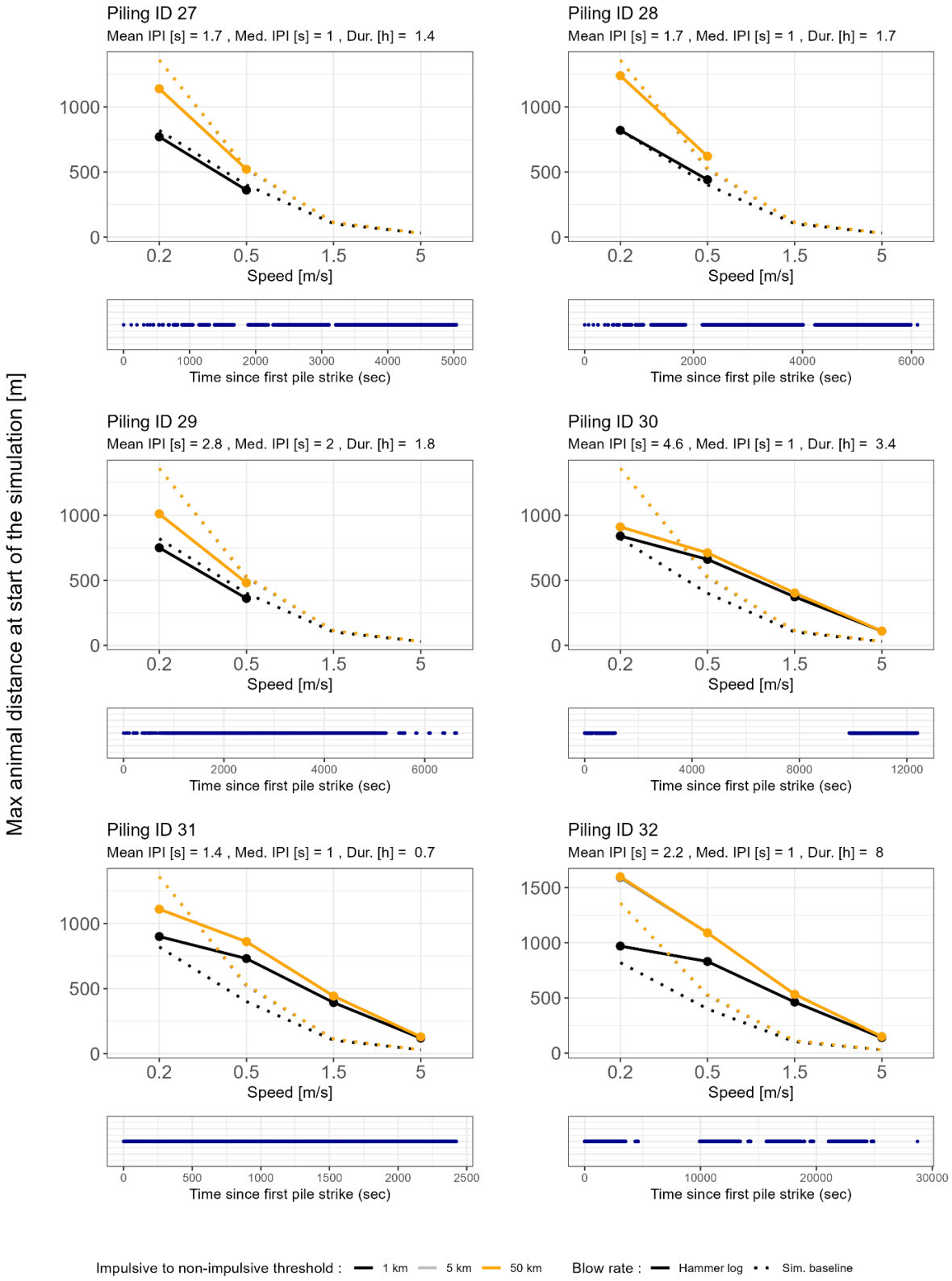

Figure 72. Changes in PTS ranges (expressed as maximum distance at which animals need to be at the start of piling to receive PTS during piling duration) with animal speed on the x-axis for 6 of the 44 real piling schedules (piling IDs 27-32).

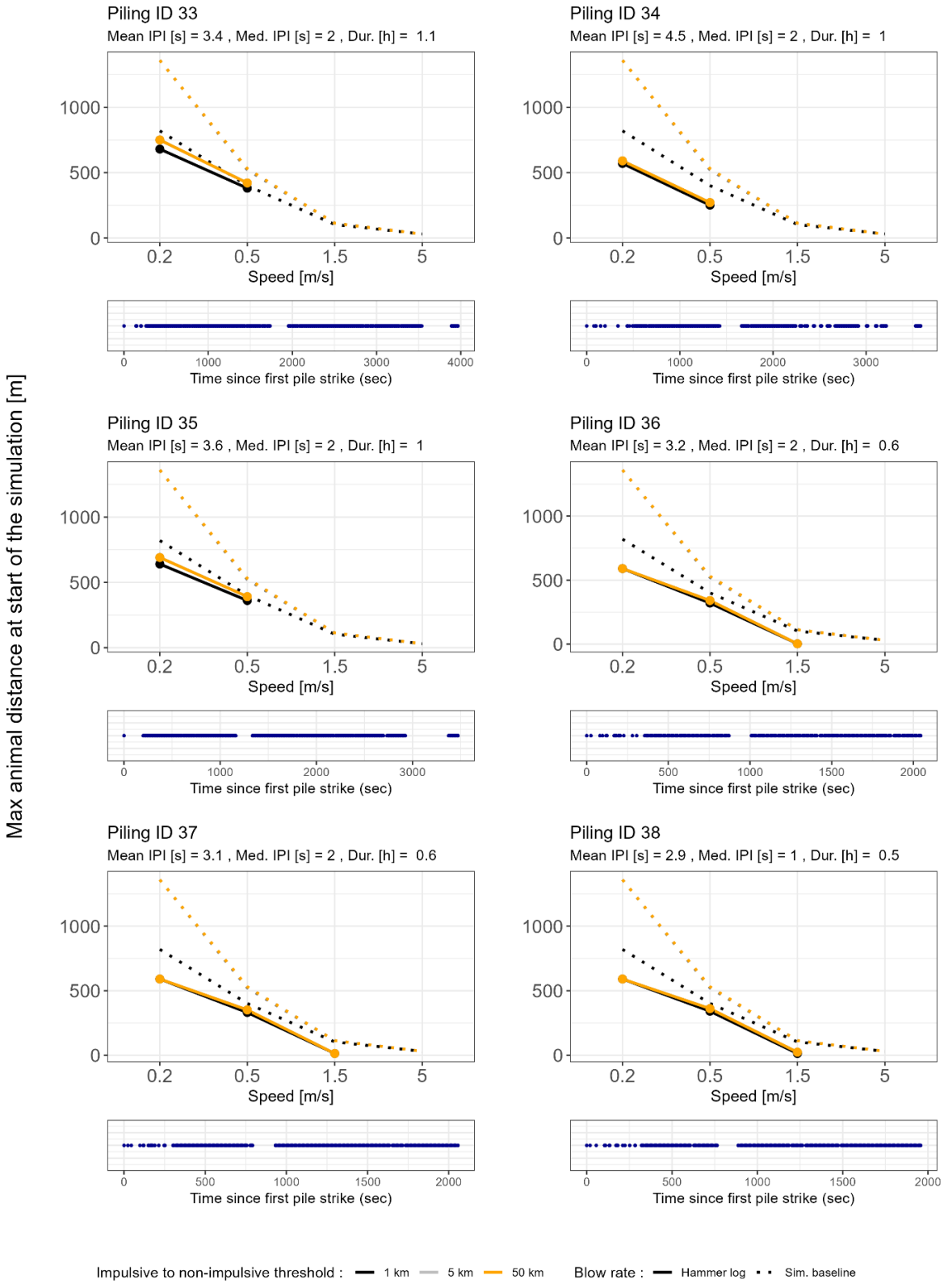

Figure 73. Changes in PTS ranges (expressed as maximum distance at which animals need to be at the start of piling to receive PTS during piling duration) with animal speed on the x-axis for 6 of the 44 real piling schedules (piling IDs 33-38).

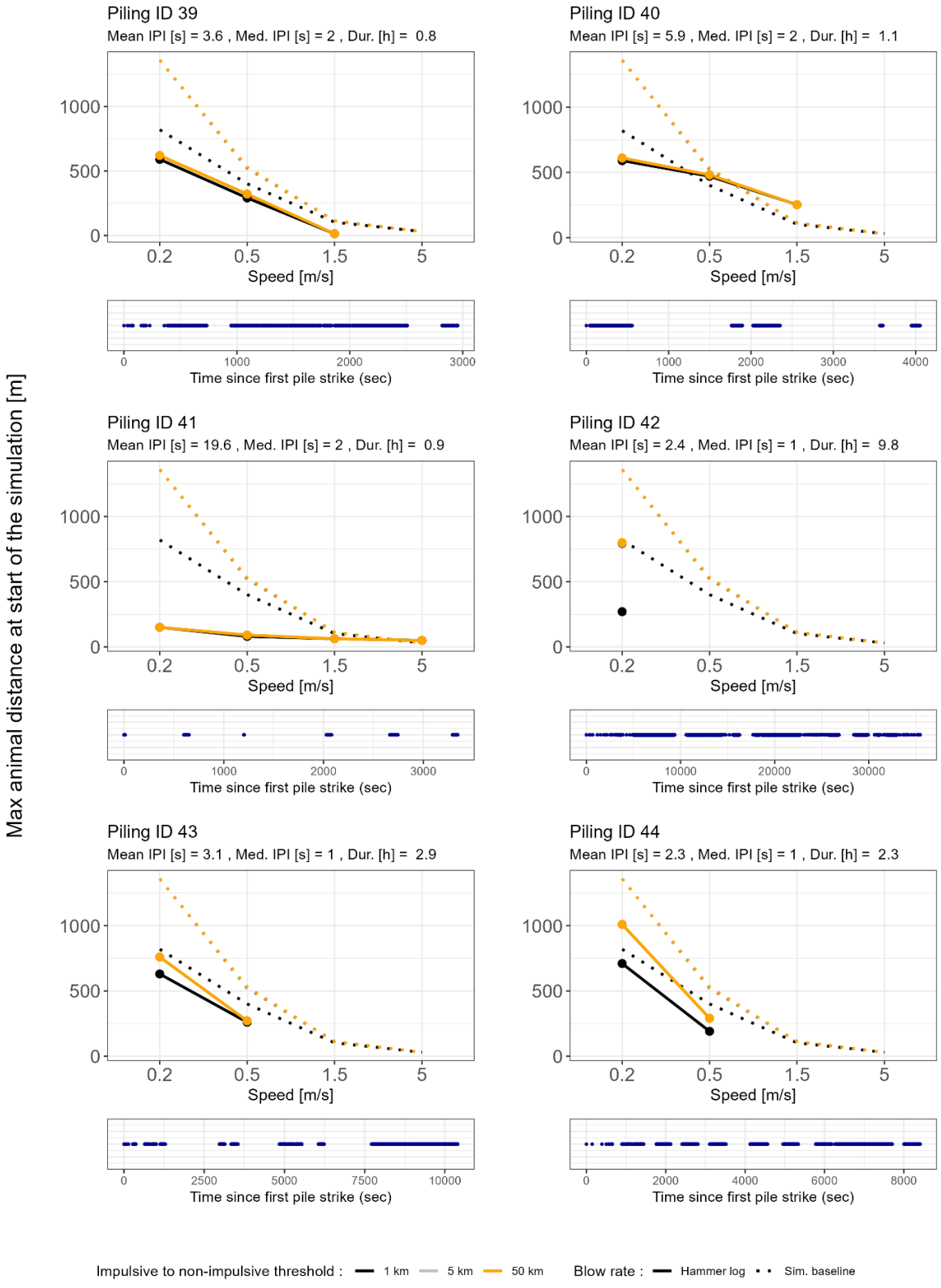

Figure 74. Changes in PTS ranges (expressed as maximum distance at which animals need to be at the start of piling to receive PTS during piling duration) with animal speed on the x-axis for 6 of the 44 real piling schedules (piling IDs 39-44).

carbontrust.com

+44 (0) 20 7170 7000

Published in the UK: 2024